

**UCLA**

**UCLA Electronic Theses and Dissertations**

**Title**

Identification and Characterization of Fusobacterial Adhesins Involved in Interspecies Interactions

**Permalink**

<https://escholarship.org/uc/item/611739qf>

**Author**

Park, Jane

**Publication Date**

2016

Peer reviewed|Thesis/dissertation

UNIVERSITY OF CALIFORNIA

Los Angeles

Identification and Characterization of  
Fusobacterial Adhesins Involved in Interspecies Interactions

A dissertation submitted in partial satisfaction of the  
requirements for the degree Doctor of Philosophy  
in Oral Biology

by

Jane Park

2016

© Copyright by

Jane Park

2016

# ABSTRACT OF THE DISSERTATION

## Identification and Characterization of Fusobacterial Adhesins Involved in Interspecies Interactions

by

Jane Park

Doctor of Philosophy in Oral Biology

University of California, Los Angeles, 2016

Professor Renate Lux, Chair

*Fusobacterium nucleatum* is a Gram-negative opportunistic pathogen that is indigenous to the human oral cavity. It is a prevalent member of the oral microbial community and considered a key organism in biofilm formation due to its ability to adhere to a large variety of microbial species. While present in healthy oral biofilms, *F. nucleatum* is also dominant in periodontal disease and has been implicated in a number of invasive human infections, acute and chronic inflammatory conditions as well as adverse pregnancy outcomes. *F. nucleatum* pathogenicity can be partially attributed to its function as a “bridging organism” that supports the integration of periodontal pathogens into oral biofilms. Despite the extensive exploration of *F. nucleatum* interspecies interactions and the identification of a number of binding partners, only one fusobacterial large outer membrane protein (OMP), RadD, has been extensively

characterized at a molecular level for its role as an adhesin in binding to a variety of Gram-positive species.

The identification and characterization of fusobacterial adhesins involved in interspecies interactions addressed in the following aims:

(1) We have identified an additional fusobacterial OMP, Fap2, a galactose-inhibitable adhesin that mediates attachment with at least two *P. gingivalis* strains. We also demonstrate that RadD is an additional strain-specific fusobacterial adhesin for interaction with *P. gingivalis* and provide evidence that additional adhesins exist that have yet to be identified.

(2) An in-depth investigation of the four-gene operon encoding the RadD adhesin revealed that inactivation of the gene directly upstream of *radD*, named *fad-I*, resulted in increased binding of *F. nucleatum* to both *Streptococcus gordonii* and *Porphyromonas gingivalis* as a result of the overexpression of *radD*. The mutant lacking FAD-I also exhibited the enhanced ability to form robust biofilms with *S. gordonii*. We propose that the protein encoded by *fad-I* is an element acting as a repressor for *radD* expression.

(3) We also took a global approach to examine contact-induced transcriptional changes that occur when *F. nucleatum* is in contact with partner species. We report partner-specific responses, suggesting *F. nucleatum* can differentially regulate its genes based on contact with neighboring species. Furthermore, we report that there are a subset of

genes regulated based on the interacting partner and the adhesin mediating attachment.

In conclusion, this thesis describes a comprehensive study of fusobacterial adhesins involved in interspecies interactions and further highlights the prominence of *F. nucleatum* in the oral microbiome warranting future studies that continue to investigate this organism on molecular and “omic” levels.

The dissertation of Jane Park is approved.

Ann M. Hirsch

Perry Klokkevold

Wenyuan Shi

Renate Lux, Committee Chair

University of California, Los Angeles

2016

*In memory of Dr. Susan Kinder Haake*

## TABLE OF CONTENTS

ABSTRACT OF THE DISSERTATION	ii
LIST OF FIGURES	ix
LIST OF TABLES	xi
ACKNOWLEDGEMENTS	xii
VITA	xiii
CHAPTER 1: Characterization of <i>Fusobacterium nucleatum</i> ATCC 23726 Adhesins Involved in Strain-Specific Attachment to <i>Porphyromonas gingivalis</i>	1
Abstract	2
Introduction	3
Materials and Methods	6
Results	11
Discussion	15
References	28
CHAPTER 2: Characterization of the Fusobacterial <i>radD</i> -Operon	33
Abstract	34
Introduction	35
Materials and Methods	38
Results	44
Discussion	50
References	61
CHAPTER 3: Contact-Dependent Gene Expression Profile of <i>F. nucleatum</i> During Interaction With Partner Species	65

Abstract	66
Introduction	67
Materials and Methods	69
Results	74
Discussion	80
References	99
CONCLUSION	104
References	107

## LIST OF FIGURES

### Chapter 1

- Figure 1. Quantitative autoaggregation levels of bacterial strains and coaggregation levels between *F. nucleatum* ATCC 23726 and seven different *P. gingivalis* strains 20
- Figure 2. Quantitative inhibition of coaggregation assay between *F. nucleatum* ATCC 23726 and *P. gingivalis* strains 21
- Figure 3. Quantitative coaggregation assay between *F. nucleatum* ATCC 23726 and mutant derivatives in outer membrane proteins (OMPs) with *P. gingivalis* strains 23
- Figure 4. *P. gingivalis* integration in dual species biofilms with *F. nucleatum* ATCC 23726  $\Delta$ Fap2,  $\Delta$ RadD and  $\Delta$ Fap2/ $\Delta$ RadD OMP mutant derivatives 25
- Supplemental Figure 1. Quantification of fusobacterial attachment to collagen-coated plates 26

### Chapter 2

- Figure 1. Schematic representation of gene inactivation mutants and controls 55
- Figure 2. Coaggregation of mutants with partner strains 56
- Figure 3. Transcriptional analysis of *radD*-operon genes in wild-type FNN and FNP and mutant derivatives 57
- Figure 4. Coaggregation and transcriptional analysis of FNN  $\Delta$ *fad-I radD*\* 58
- Figure 5. Transcriptional analysis of *radD* levels in the presence of partner strains 59
- Figure 6. Biofilm growth comparison of FNN wild-type, FNN  $\Delta$ *fad-I*, or FNN  $\Delta$ *radD* with *S. gordonii* 60

### Chapter 3

Figure 1. Diagram of the number of <i>F. nucleatum</i> genes regulated in the presence of <i>S. sanguinis</i> and <i>P. gingivalis</i>	85
Figure 2. <i>F. nucleatum</i> metabolic pathway map of all genes regulated in the presence of <i>S. sanguinis</i>	86
Figure 3. <i>F. nucleatum</i> regulatory pathway map of all genes regulated in the presence of <i>S. sanguinis</i>	87
Figure 4. <i>F. nucleatum</i> metabolic pathway map of all genes regulated in the presence of <i>P. gingivalis</i>	88
Figure 5. <i>F. nucleatum</i> regulatory pathway map of all genes regulated in the presence of <i>P. gingivalis</i>	89
Figure 6. <i>F. nucleatum</i> metabolic pathway map of all induced genes regulated in the presence of <i>S. sanguinis</i> and <i>P. gingivalis</i>	90
Figure 7. <i>F. nucleatum</i> regulatory pathway map of all induced genes regulated in the presence of <i>S. sanguinis</i> and <i>P. gingivalis</i>	91
Figure 8. <i>F. nucleatum</i> metabolic pathway map of all repressed genes regulated in the presence of <i>S. sanguinis</i> and <i>P. gingivalis</i>	92
Figure 9. <i>F. nucleatum</i> regulatory pathway map of all repressed genes regulated in the presence of <i>S. sanguinis</i> and <i>P. gingivalis</i>	93
Figure 10. <i>F. nucleatum</i> metabolic pathway map of genes regulated oppositely in the presence of <i>S. sanguinis</i> and <i>P. gingivalis</i>	94
Figure 11. <i>F. nucleatum</i> metabolic pathway map of genes regulated in the presence of <i>S. sanguinis</i> in a RadD-dependent manner	95
Figure 12. <i>F. nucleatum</i> regulatory pathway map of genes regulated in the presence of <i>S. sanguinis</i> in a RadD-dependent manner	96
Figure 13. <i>F. nucleatum</i> metabolic pathway map of gene regulation in the presence of different <i>P. gingivalis</i> strains	97
Figure 14. Gene expression comparison of selected genes relative to wild-type <i>F. nucleatum</i> alone in FnSs or FnPg	98

## LIST OF TABLES

### **Chapter 1**

Supplemental Table 1. Visual scoring of autoaggregation and coaggregation	27
---	----

### **Chapter 2**

Table 1. Primers, plasmids and strains used in this study	53
---	----

## ACKNOWLEDGEMENTS

Chapter 1 is a version of a manuscript that is in press with the International Journal of Oral Science. The authorship is as follows: Park J, Shokeen B, Haake SK, Lux R.

Chapter 2 is a version of a manuscript in preparation for submission with Microbial Ecology. The authorship is as follows: Shokeen B, Park J, Paul MK, Lux R.

This work was supported by NIH T32 and T90 Training Grants 5T32DE007296-15, 5T90DE22734-01, AND 5T90DE22734-02.

I am grateful for my advisor, Dr. Renate Lux, who “adopted” me and was generous with her patience, time and support throughout my training. I would like to thank her for being gentle in her pushes and enthusiastic in her leadership.

I would like to thank, Drs. Ann Hirsch, Perry Klokkevold and Wenyan Shi for their support and interest in my research and for being accommodating throughout the entire process.

I would like to thank my lab mates, both past and present, for wallowing with me, encouraging me, and challenging me intellectually. In particular, I’d like to thank Michaela Chang, for keeping me laughing and sane over the years and Dr. Bhumika Shokeen for being a friend, counselor and model both in and out of the lab.

I am grateful to have met and worked with Dr. Susan Kinder Haake, who believed in me before I did. She is greatly missed.

I would also like to thank my loving friends and family for constantly cheering me on, feeding me and being proud of me without knowing exactly what I do.

And lastly, I’d like to express my greatest thanks to my best friend and husband, Glenn Kam, who has been constant in his warmth and loving support through the immense challenges in graduate school and research.

## VITA

2005	B.S., Microbiology, Immunology and Molecular Genetics University of California, Los Angeles
2011	M.S., Oral Biology University of California, Los Angeles
2011	T32 Pre-doctoral Training Grant National Institute of Dental & Craniofacial Research, NIH
2012	T90 Pre-doctoral Training Grant National Institute of Dental & Craniofacial Research, NIH
2015	Graduate Division Dissertation Year Fellowship University of California, Los Angeles

## PUBLICATIONS AND PRESENTATIONS

**Park, J.**, Sarkar, J., Lux, R., Molecular Characterization of Fusobacterial Interaction with Other Oral Bacteria. *J Dent Res* 93 (A): 1225, 2014. International Association for Dental Research General Meeting, March 2014, Charlotte, NC. Poster Presentation

**Park, J.**, Kaplan, A., Lux, R., Haake, S.K., Characterization of Fusobacterial Adhesins Involved in Coaggregation with *Porphyromonas gingivalis*. *J Dent Res* 92 (A): 2133, 2013. Poster presentation at the International Association for Dental Research General Meeting, March 2013, Seattle, WA.

**Park, J.**, Kaplan, A., Lux, R., Haake, S.K., Identification and characterization of fusobacterial adhesins involved in coaggregation with *Porphyromonas gingivalis*. February 2012. UCLA School of Dentistry Poster Competition. Poster Presentation

**Park, J.**, Chang, M., Haake, S.K., Molecular Analyses in *Fusobacterium nucleatum*. *J*

Dent Res 90 (A): 3516, 2011. International Association for Dental Research General Meeting, March 2011, San Diego, CA. Poster Presentation

**Park, J.** and Haake, S.K., Molecular Analyses in Fusobacterium nucleatum. February 2010. UCLA School of Dentistry Poster Competition (Third place award). Poster Presentation

Chang, M., Shi, B., Sodergren, E., Mitreva, M., **Park, J.**, Weinstock, G., Li, H., Haake, S.K., Community Analyses of the Periodontal Microbiome. J Dent Res 92 (A): 1395, 2013. Poster Presentation

Chang, M., Fitz-Gibbon, S., Tomida, S., **Park, J.**, Li, H., Haake, S.K., The Subgingival Microbiome of Chronic Periodontitis. J Dent Res 90 (A): 3520, 2011. Poster Presentation

**Chapter 1: Characterization of *Fusobacterium nucleatum* ATCC 23726 Adhesins  
Involved in Strain-Specific Attachment to *Porphyromonas gingivalis***

## Abstract

Bacterial adherence is an essential virulence factor in pathogenesis and infection. *Fusobacterium nucleatum* plays a central role in oral biofilm architecture by acting as a bridge between early Gram-positive and late Gram-negative colonizers that do not otherwise adhere to each other. In this study, we survey a key adherence interaction of *F. nucleatum* with *Porphyromonas gingivalis*, and present evidence that multiple fusobacterial adhesins play a role in the attachment of *F. nucleatum* ATCC 23726 to *P. gingivalis* in a highly strain-dependent manner. Interaction between these species displayed varying sensitivities to arginine, galactose and lactose. Arginine was found to hamper coaggregation by at least 62% and up to 89% with several *P. gingivalis* strains and galactose inhibition ranged from no inhibition up to 58% with the same *P. gingivalis* strains. Lactose consistently inhibited *F. nucleatum* interaction with these *P. gingivalis* strains ranging from 40-56% decrease in coaggregation. Among the adhesins involved are the previously described Fap2 and surprisingly, RadD, which was described in an earlier study for its function in attachment of *F. nucleatum* to Gram-positive species. We also provide evidence for the presence of at least one additional adhesin that is sensitive to arginine but unlike Fap2 and RadD, is not a member of the autotransporter family type of fusobacterial large outer membrane proteins. The strain-specific binding profile of multiple fusobacterial adhesins to *P. gingivalis* highlights the heterogeneity and complexity of interspecies interactions in the oral cavity.

## Introduction

*Fusobacterium nucleatum* is a prevalent member of the oral microbial community and considered a key organism in biofilm formation due to its ability to adhere to a large variety of microbial species.<sup>1,2,3</sup> While present in healthy oral biofilms, this Gram-negative opportunistic pathogen is dominant in periodontal disease<sup>4</sup> and has been implicated in a number of invasive human infections<sup>5,6</sup>, acute and chronic inflammatory conditions<sup>7,8</sup> as well as adverse pregnancy outcomes<sup>9,10</sup>. *F. nucleatum* pathogenicity is, in part, attributed to its function as a “bridging organism” that supports the integration of periodontal pathogens into oral biofilms.<sup>2,11</sup> With this unique ability to attach to both early and late colonizers, *F. nucleatum* is thought to play a central role in the ecological shift from a mostly Gram-positive to a predominately Gram-negative and thus, pathogenic, biofilm community in periodontal disease.<sup>2</sup>

Despite the extensive exploration of *F. nucleatum* interspecies interactions and the identification of a number of binding partners, to date, only two fusobacterial large outer membrane proteins (OMPs), RadD and Fap2, have been characterized at a molecular level for their role as adhesins in binding to a variety of Gram-positive species<sup>12,13</sup> and *Porphyromonas gingivalis*, respectively.<sup>14</sup> Both, RadD and Fap2 are members of the autotransporter family of proteins<sup>13</sup>, which are the largest known family of virulence factors expressed by Gram-negative bacteria.<sup>15</sup> Autotransporters account for numerous biological functions including adhesion<sup>16,17</sup> cell-to-cell aggregation<sup>18,19</sup>, biofilm formation<sup>20,21</sup>, and invasion<sup>22</sup>. It is therefore not surprising that in addition to their role in interspecies binding, fusobacterial autotransporters are multifunctionally involved in the

induction of apoptosis in lymphocytes<sup>23,24</sup> and adherence to murine placental cells<sup>14</sup>.

Historically, studies have shown that interbacterial binding measured by the classical coaggregation assay often involves highly serotype or strain-specific cell-to-cell recognition.<sup>25</sup> For example, a panel of different *F. nucleatum* strains and several species of *Selenomonas* were found to bind only to certain subsets of oral partner species tested but no distinct group-specific pattern was observed.<sup>2</sup> In particular, adhesion of different *F. nucleatum* isolates to a selection of *P. gingivalis* strains varied from no interaction to very strong co-aggregation phenotypes, some of which were sensitive to lactose or heat treatment, while others were not.<sup>26</sup> This interspecies binding variation is not limited to fusobacterial interactions but appears to be a common theme among oral bacterial species. Previous studies of different oral bacterial interactions have demonstrated that coaggregation involves highly specific cell-to-cell recognition of distinct isolates of a certain species and that this pattern is not generalizable to all strains of a single species or all species of a genus. Other examples of these differential binding specificities include *Actinomyces naeslundii* with different strains of *Streptococcus sanguinis* and *Streptococcus gordonii*<sup>25,27,28,29</sup>, *P. gingivalis* binding with *Veillonella*, *Capnocytophaga*, and *Actinomyces* but not with *Streptococcus*<sup>30</sup>, intra- and intergeneric coaggregations between *Streptococcus* and *Actinomyces*<sup>31</sup> among others.

Interactions between *F. nucleatum* and *P. gingivalis* are of key interest because they are frequently isolated together from several chronic immunoinflammatory diseases of the oral cavity.<sup>32,33</sup> While identification of Fap2 as the galactose-inhibitable adhesin of *F.*

*nucleatum* strains ATCC 23726 for binding to *P. gingivalis* strain PK1924 provided the first molecular identification of a fusobacterial adhesin involved in this interaction<sup>14</sup>, previous reports of differential binding between various strains of these species<sup>26</sup> as well as the finding that their coaggregation can be inhibited by carbohydrates other than galactose indicated the presence of additional adhesins. In this study, we tested the coaggregation between *F. nucleatum* strain ATCC 23726 and five strains of *P. gingivalis*, characterized the carbohydrate-sensitivity of the interaction and screened the existing panel of autotransporter mutants in ATCC 23726<sup>13</sup> for possible binding defects. This led to the identification of RadD as an additional strain-specific fusobacterial adhesin for interaction with *P. gingivalis* as well as the finding that further adhesins exist that do not belong to the autotransporter family of proteins despite being inhibited by the addition of arginine similar to RadD.

## Materials and Methods

### Bacterial Strains and Culture Conditions

*F. nucleatum* strain ATCC 23726 and its mutant derivatives defective in large outer membrane autotransporter proteins<sup>13,24</sup> as well as seven different *P. gingivalis* strains 4612, T22<sup>35</sup>, MP4-504<sup>34</sup>, ATCC 33277<sup>35</sup>, 381<sup>36</sup>, W50 and W83<sup>37</sup>, were maintained on Columbia agar supplemented with 5% sheep blood or in Columbia broth (Difco, Detroit, MI) under anaerobic conditions (10% H<sub>2</sub>, 10% CO<sub>2</sub>, 80% N<sub>2</sub>) at 37°C. All media for *P. gingivalis* were also supplemented with hemin at 5 µg ml<sup>-1</sup> and menadione at 1 µg ml<sup>-1</sup>. Thiamphenicol at 5 µg ml<sup>-1</sup> and clindamycin at 1 µg ml<sup>-1</sup> (MP Biomedicals, Irvine, CA) were used for the selection and maintenance of strains possessing the *catP* and *ermB* determinants, respectively.

### Coaggregation Assay

*Visual.* Coaggregation assays were performed in coaggregation buffer (CAB; 150mM NaCl, 1mM Tris, 0.1 mM CaCl<sub>2</sub>, 0.1 mM MgCl<sub>2</sub> • H<sub>2</sub>O [pH 7.5]) as previously described<sup>13</sup>. In brief, cells were pelleted and re-suspended in CAB to a final concentration of 2 x 10<sup>9</sup> cells (OD<sub>600</sub> of 2). Suspensions of strains to be examined for coaggregation were combined with an equal volume of a test strain adjusted to the same cellular concentration in CAB to a total volume of 400 µl in a reaction tube. Once the second partner strain was added, reaction mixtures were immediately vortexed for 5 s and incubated for at least 10 min prior to evaluation using a visual scoring system ranging from 0 to 4.<sup>3</sup> A score of 0 was assigned for no visible co-aggregation and a

score of 4 described complete sedimentation of strains with a clear supernatant (Table S1).

*Quantitative.* Coaggregation assays were performed identical to the visual assay except that optical densities of reaction mixtures were obtained spectrophotometrically immediately after addition of the second partner strain and vortexing ( $OD_{t=0 \text{ min}}$ ). After 10 min of incubation, reaction mixtures were centrifuged at low speed ( $100\times g$  for 1 min) to pellet coaggregated cells while leaving non-aggregated bacteria in suspension. Optical densities of the supernatants were measured after the 10 min incubation ( $OD_{t=10 \text{ min}}$ ) in order to quantitate coaggregation. Coaggregation test reactions were calculated as  $(OD_{t=0 \text{ min}} - OD_{t=10 \text{ min}})/(OD_{t=0 \text{ min}})$ . These values were averaged across at least three independent experiments and represented as percentages calculated relative to control reactions (reactions without the addition of a partner strain) as  $(\text{Avg}_{\text{test reaction}} / \text{Avg}_{\text{control reaction}}) \times 100$ .

*Inhibition.* For both visual and quantitative inhibition assays, either L-arginine, D-galactose, L-glutamic acid, D-glucose or lactose was added to the reaction tube containing only *F. nucleatum* cells to a final concentration of 100 mM. The suspension was then vortexed and incubated for 5 min prior to the addition of the coaggregation test partner. Once the partner strain was added, the reaction mixture was vortexed again and the assay was evaluated via the quantitative coaggregation assay as described above. The final concentration of each inhibitor per coaggregation reaction was 50 mM.

## Biofilm Growth

*Dual Species Biofilms.* The *F. nucleatum* and *P. gingivalis* biofilm growth protocol was modified from a previous study<sup>39</sup> by using 96-well collagen coated plates (Advanced BioMatrix, San Diego, CA) that were UV sterilized for 1 h prior to inoculation. For dual-species biofilms 100  $\mu\text{l}$  of CB supplemented with hemin at  $5 \mu\text{g ml}^{-1}$  and menadione at  $1 \mu\text{g ml}^{-1}$  (CBHM) were added into each well. *F. nucleatum* cells (50  $\mu\text{l}$  containing  $\sim 5 \times 10^7$  cells) were seeded into each well and allowed to grow under anaerobic conditions (10%  $\text{H}_2$ , 10%  $\text{CO}_2$ , 80%  $\text{N}_2$ ) at  $37^\circ\text{C}$  for 3 h prior to the addition of *P. gingivalis* (50  $\mu\text{l}$  containing  $\sim 5 \times 10^7$  cells) to allow *F. nucleatum* cells time to bind to and saturate the collagen-coated surfaces. Plates were incubated overnight under anaerobic conditions (10%  $\text{H}_2$ , 10%  $\text{CO}_2$ , 80%  $\text{N}_2$ ) at  $37^\circ\text{C}$ . Triplicate wells were inoculated for each experiment, which were combined for DNA extraction. At least three biological replicates were performed per condition.

*Fusobacterial Attachment.* To ensure that each of the fusobacterial strains attached to collagen-coated wells over 3 h, after of growth under anaerobic conditions (10%  $\text{H}_2$ , 10%  $\text{CO}_2$ , 80%  $\text{N}_2$ ) at  $37^\circ\text{C}$ , contents were removed from each well and rinsed once with 250  $\mu\text{l}$  of sterile phosphate-buffered saline (PBS). Plates were inverted and dried. Afterwards, attached bacteria were fixed at room temperature for 15 min by adding 200  $\mu\text{l}$  of methanol into each well. The plates were stained with a 100  $\mu\text{l}$  aqueous solution of 0.5% crystal violet (Thermo Fisher Scientific, Waltham, MA) for 15 min at room temperature. The plates were then carefully rinsed with Millipore water until there was no visible trace of the stain. Bound stain was dissolved by adding 160  $\mu\text{l}$  of 95% ethanol. The optical density (OD) of each well was measured at 570 nm and was

represented as relative to a negative control wells that only contained CB (Supplemental Figure S1). At least three biological replicates were performed per *F. nucleatum* strain.

### **Extraction of DNA from Biofilms**

Prior to DNA isolation, the medium was carefully removed from the wells. Genomic DNA was isolated directly from the wells using GenElute Bacterial Genomic DNA Kit (Sigma-Aldrich, St. Louis, MO) according to manufacture's instructions with modification of final elution to 30  $\mu$ l. Buffers, enzymes and precipitating DNA were directly added into the wells prior to combining replicate samples and transferring the solution to the columns.

### **Quantitative (Real-Time) Polymerase Chain Reaction**

To quantify the relative proportions of each species in the respective dual-species biofilms, species-specific primer pairs were used. For *F. nucleatum* ATCC 23726 and its mutant derivatives a portion of the *Fusobacterium*-specific *fomA* gene was amplified with Fn-F (forward) 5'AGTTGCTCCAGCTTGGAGACCAAAT3' and Fn-R (reverse) 5' AAGTTTACTTTTGTAAAGTTTGTAAATCTTCC3' primers. For *P. gingivalis* Pg-F (forward) 5'AGGCAGCTTGCCATACTGCG3' and Pg-R (reverse) 5'ACTGTTAGCAACTACCGATGT3' were chosen to amplify a portion of the *P. gingivalis* 16S rRNA gene. Primer pairs were tested for possible cross-reactivity with the other species. Real-time qPCR was performed using an iCycler Thermal Cycler (Bio-Rad, Hercules, CA) in a total volume of 20  $\mu$ l containing 2  $\mu$ l of 10x iQ SYBR Green Supermix (Bio-Rad, Hercules, CA), 0.5  $\mu$ M each of forward and reverse primers, 7  $\mu$ l of

Millipore water and 1  $\mu$ l (10 ng) of template DNA. Amplification and detection were carried out in 96-well optical plates (Thermo Fisher Scientific, Waltham, MA). Each PCR run was carried out with an initial incubation of 10 min at 95°C followed by 40 cycles of denaturing at 95°C for 15 sec; annealing and elongation at 60°C for 1 min. After the 40 cycles of amplification, an additional denaturing step was performed at 95°C for 1 min followed by annealing and elongation at 60°C for 1 min. A melting curve analysis was completed after each run. The DNA concentrations ( $\text{ng ml}^{-1}$ ) were calculated with standard curves obtained by tenfold serial dilutions of bacterial genomic DNA. Three independent qPCR runs were performed with three technical replicates for each sample to assess reproducibility and inter-run variability.

### **Statistical Analysis**

Student's *t*-test was performed to determine statistical significance using Excel 2011 (Microsoft, Seattle, WA).

## Results

### Autoaggregation of Bacteria and Coaggregation of *F. nucleatum* ATCC 23726 with *P. gingivalis* Displays a Strain-Specific Profile

Qualitative and quantitative autoaggregation and coaggregation assays revealed a strain-dependent binding profile of *F. nucleatum* ATCC 23726 with the seven different strains of *P. gingivalis* tested in this study. Robust interactions were observed with *P. gingivalis* strains 4612 (62±8% coaggregation), T22 (54±8 % coaggregation) binding and ATCC 33277 (65±17% coaggregation) (Figure 1). Binding of *P. gingivalis* strains W50 and W83 to *F. nucleatum* ATCC 23726 was notably weaker, showing only 23±10% and 30±22% coaggregation, respectively. *P. gingivalis* strains 381 and the clinical isolate MP-504 revealed 54±2% and 73±4% coaggregation, respectively but were not chosen for further interaction studies with *F. nucleatum* due to notable autoaggregation levels. Interactions of fusobacteria with other species can be disrupted by a number of small molecules including arginine, galactose and lactose.<sup>26</sup> Attachment to early colonizers was described to be largely inhibitable by arginine<sup>40</sup> with identification of RadD as the arginine-inhibitable adhesin for *streptococci*<sup>13</sup> whereas adhesion between *F. nucleatum* and Gram-negative late colonizers including *P. gingivalis* was found to be generally sensitive to galactose<sup>26,41</sup>. Fap2 was recently identified as the galactose-inhibitable adhesin for this interaction.<sup>14</sup> Interestingly, the binding profile of *F. nucleatum* strain ATCC 23726 with the different *P. gingivalis* strains tested in this study exhibited a diverse inhibition profile that involved strain-dependent sensitivities to the inhibitors tested (Figure 2). Attachment to *P. gingivalis* strains 4612 and T22 was partially sensitive to arginine, galactose and lactose, whereas coaggregation with ATCC 33277

was almost completely abolished by the addition of arginine alone and partially sensitive to lactose. Coaggregation reactions in the presence of 50 mM arginine resulted in a relative decrease in coaggregation by  $62\pm 2\%$  with 4612,  $70\pm 6\%$  with T22, and  $89\pm 3\%$  with ATCC 33277 compared to the corresponding reactions with ATCC 23726 in the absence of inhibitor. Reactions between *F. nucleatum* ATCC 23726 and *P. gingivalis* strains in the presence of galactose revealed, a  $58\pm 16\%$  decrease in coaggregation with 4612 and  $36\pm 18\%$  reduction of binding with T22 compared to control reactions without inhibitor. Coaggregation in the presence of 50 mM lactose resulted in a relative decrease in coaggregation by  $46\pm 13\%$  with 4612,  $56\pm 7\%$  with T22, and  $40\pm 8\%$  with ATCC 33277 compared to the corresponding reactions with ATCC 23726 in the absence of inhibitor. Interactions between ATCC 23726 and ATCC 33277 were not affected by galactose, with coaggregation being reduced by only  $12\pm 6\%$  compared to the strains reacting in CAB. Addition of glucose or glutamic acid did not affect adhesion of any of the strain combinations tested.

### **Fusobacterial Outer Membrane Proteins Function as Adhesins for Interaction with *P. gingivalis***

In a previous study, we created gene inactivation mutants in large outer membrane autotransporter proteins (OMPs) of *F. nucleatum* ATCC 23726 and identified one of them, RadD, as an adhesin for interaction with Gram-positive streptococci and actinomyces.<sup>13</sup> Recently, an additional one of these large outer membrane proteins, Fap2 was characterized as the adhesin for galactose-inhibitable binding of *P. gingivalis* PK 1924 to the same strain, ATCC23726, of *F. nucleatum* used here.<sup>14</sup> Since we

observed strain-dependent coaggregation profiles in our inhibition experiments, we examined the binding of the previously generated OMP mutant panel, including the arginine-inhibitable RadD and galactose-inhibitable Fap2 to the three different *P. gingivalis* strains (4612, T22 and ATCC 33277) that exhibited significant binding in this study to the parent strain ATCC 23726 (Figure 3). Similar to the inhibition results, coaggregation between the *F. nucleatum* ATCC 23726 OMP mutant derivatives and the *P. gingivalis* strains varied depending on the interacting pairs. Fusobacterial interaction with *P. gingivalis* strain 4612 appears to be mediated by both Fap2 and RadD, with the average relative decrease for the individual mutants (Fap2 mutant, 53±6% and RadD mutant, 29±6%) adding up to the decrease seen for the Fap2/RadD double mutant (82±5%). Among the OMP mutants tested here, only lack of Fap2 resulted in a reduction of the interaction between *F. nucleatum* ATCC 23726 and *P. gingivalis* T22 with a decrease of 55±27% relative to coaggregation with the wildtype parent strain. Binding to *P. gingivalis* 33277 displayed only a slight decrease with several of the OMP mutants tested. However, with the exception of the decrease (34±4%) observed with the Fap2/RadD double mutant none of the apparent reductions were significant.

### **Biofilm Integration**

Previous studies have shown that the same strains of bacteria grown under biofilms conditions reveal different gene expression and transcriptomic patterns when compared to their planktonically grown counterparts.<sup>42,43,44</sup> Since our coaggregation experiments are typically performed with planktonically grown cells, we wanted to confirm that the differences seen in coaggregation patterns with the *F. nucleatum* OMP mutants is

relevant for the integration of *P. gingivalis* strains 4612 and T22 into pre-existing fusobacterial biofilms. *P. gingivalis* strain 33277 was not included in the biofilm studies because coaggregation reactions with *F. nucleatum* OMP mutants did not show significant involvement of these adhesins in this interaction.

Our dual species biofilm studies were conducted with *P. gingivalis* 4612 and T22 and revealed significant reduction in *P. gingivalis* 4612 integration into a biofilm when grown with *F. nucleatum* derivatives lacking Fap2 (24±14% integration), RadD (41±17% integration), or the Fap2/RadD double mutant (35±29% integration) when compared to biofilms containing wildtype *F. nucleatum*. *P. gingivalis* T22 exhibited a similar pattern of biofilm integration as 4612 with significantly decreased integration when grown with Fap2 (22±2% integration), RadD (49±20% integration) or the Fap2/RadD double mutant (19±11% integration) (Figure 4). Biofilm growth with the *F. nucleatum* ATCC 23726 mutant derivative carrying a deletion in OMP FN1893 served as a control to ensure that decreased *P. gingivalis* integration in the dual species biofilms were mutation specific and not the result of a general biofilm phenotype effect caused by lack of an OMP.

## Discussion

In this study we provide evidence that in addition to the previously described Fap2-mediated interaction between *F. nucleatum* ATCC 23726 and *P. gingivalis* strain PK 1924<sup>14</sup>, multiple adhesins play a role in the attachment of this fusobacterial strain with *P. gingivalis* in a highly strain-dependent manner. The notion of isolate-specific interaction is not new and has been observed for a number of different species pairs including *F. nucleatum* with a variety of *Selemonas*, *Streptococcus*, and *Actinomyces* species as well as different isolates of *P. gingivalis* and other oral bacteria.<sup>2,26,45</sup> Other studies describe similar phenomena of strain-specific interactions for *Actinomyces* species with different streptococci<sup>25,28</sup> as well as a number of additional oral bacterial species<sup>29,30,46</sup>. In addition to Fap2, several adhesins involved in some of these interactions have been identified including SspA/B in the binding of *S. gordonii* with *P. gingivalis*<sup>47</sup> and the fusobacterial RadD in the interaction between *F. nucleatum* and streptococcal species as well as actinomyces<sup>13</sup>. However most studies have only investigated individual strains for each of the species involved and comprehensive studies including multiple isolates are still lacking. Considering the previously observed strain-dependent variations as well as the observation that the inhibition profiles of interactions between species can depend on isolates or serotypes tested, the presence of additional adhesins would be expected.

Quantitative coaggregation studies between *F. nucleatum* ATCC 23726 and different strains of *P. gingivalis* revealed robust coaggregation with strains, 4612, T22 and ATCC

33277, but a relatively weak interaction with strains W50 and W83 (Figure 1). This differential affinity between *F. nucleatum* and the periodontal pathogen *P. gingivalis* could play a role in virulence of oral biofilms. W50 and W83 are highly pathogenic strains of *P. gingivalis*<sup>48,49</sup> and the type of *F. nucleatum* strain already present in the oral biofilm could determine if more or less virulent variants of *P. gingivalis* integrate into the biofilm. For example, W83 has been shown to associate with *F. nucleatum* in oral epithelial cell invasion<sup>50</sup> and *F. nucleatum* clinical isolate TDC100 enhanced invasion significantly more than *F. nucleatum* ATCC 25586. Thus understanding which adhesins are involved in interactions with more virulent pathogens could shed light on the molecular mechanisms of pathogenic biofilm formation.

Similar to previous observations for binding of *F. nucleatum* to streptococci<sup>51</sup>, the interactions between *F. nucleatum* ATCC 23726 and at least two of the three strongly binding strains of *P. gingivalis* is multi-modal, since substantial levels of coaggregation remained even in the presence of inhibitors (Figure 2). Consistent with a strain-dependent multi-modal interaction, binding of *F. nucleatum* to *P. gingivalis* was mediated through adhesins sensitive to arginine, galactose, and lactose at varying degrees. This was especially interesting because historically, fusobacterial adherence to the predominantly Gram-negative late oral colonizers, including *P. gingivalis*, has largely been associated with galactose-inhibitable interactions, while coaggregation with Gram-positive early colonizing species are suggested to be mediated by arginine-inhibitable interactions.<sup>26</sup> In contrast to the binding characterized between *F. nucleatum* ATCC 23726 and *P. gingivalis* strain PK 1924<sup>14</sup>, which followed this paradigm, the

attachment of the same fusobacterial strain to the *P. gingivalis* derivatives tested in this study was only partially sensitive to the addition of galactose (4612 and T22) or not at all (ATCC 33277). Surprisingly, arginine had a stronger effect on the coaggregation with all three *P. gingivalis* strains with the binding to ATCC 33277 being almost completely abolished by addition of this amino acid (Figure 2C). Lactose-inhibition was observable in coaggregation with all three *P. gingivalis* strains used in this study and were consistent with previous findings that suggest lactose-inhibitable coaggregations may be a common form of interaction among changing populations of bacteria in the shift from health to a state of severe periodontal disease.<sup>2,26</sup>

Screening of the autotransporter large outer membrane protein (OMP) mutant collection from a previous study<sup>13</sup>, revealed that in addition to Fap2, RadD functions as one of the adhesins mediating the binding between *F. nucleatum* ATCC 23726 and *P. gingivalis* 4612 (Figure 3A). This was unexpected because RadD was previously identified as a major arginine-inhibitable adhesin for interactions of *F. nucleatum* with several Gram-positive species.<sup>12,13</sup> Among the OMP mutant collection, only lack of Fap2 resulted in a partial reduction (~50%) of coaggregation with *P. gingivalis* strain T22 indicating that the additional adhesin that contributes to the interaction between these strains constitutes a different type of cell surface feature. This unidentified adhesin is likely to provide the arginine-inhibitable feature of the interaction, since Fap2-mediated adhesion to *P. gingivalis* has been described previously as galactose-inhibitable.<sup>14</sup> Both RadD and Fap2 are multifunctional OMPs that were previously characterized for their role in induction of cell death in human lymphocytes.<sup>24</sup> RadD has additional functions as the

above-mentioned arginine-inhibitable adhesin for attachment to gram-positive early colonizers<sup>12,13</sup> and the newly discovered role as one of the adhesins for attachment to *P. gingivalis* strain T22. Multi-functionality has been described for other large outer membrane proteins including TolC of *Escherichia coli*<sup>52</sup>, OprF for *Pseudomonas*<sup>53</sup> and the major outer membrane protein of *Campylobacter jejuni*<sup>54</sup>. The arginine-inhibitable adhesin that largely mediates the coaggregation of *F. nucleatum* ATCC 23726 with *P. gingivalis* ATCC 33277, which could also contribute the arginine-sensitive attachment to T22 has yet to be identified in *F. nucleatum*.

Our results for integration of *P. gingivalis* 4612 and T22 into fusobacterial biofilms formed by *F. nucleatum* ATCC 23726 wildtype and its mutant derivative lacking Fap2, RadD or both as well as FN1893 confirmed the importance of Fap2 and RadD for attachment of 4612 to ATCC 23726 (Figure 4). Under biofilm growth conditions RadD may also play a role in binding between *F. nucleatum* ATCC 23726 and *P. gingivalis* T22. This additional function of RadD was not apparent in the interaction with T22 and could be due to differential expression of adhesins in this strain of *P. gingivalis* under biofilm growth conditions. Adhesins are critical virulence factors whose expression are regulated and coordinated to ensure that the necessary adhesin is expressed at the right time.<sup>55,56</sup> When bacterial species have integrated into existing biofilms, significant changes come about compared to their planktonic counterparts including gene expression patterns and physiological properties.<sup>44,57</sup>

In summary, we report that interspecies interactions between *F. nucleatum* and *P. gingivalis* involve a number of different fusobacterial adhesins. The previously characterized<sup>14</sup> Fap2 appears to be a more prominent adhesin that takes part in the attachment to three of the four *P. gingivalis* strains investigated so far for their attachment to *F. nucleatum* on a molecular level. The arginine-inhibitable adhesin RadD, which we originally identified as a major adhesin for interaction with streptococci and other early colonizers<sup>12,13</sup> contributes to the attachment to at least one strain of *P. gingivalis* and possibly a second one under biofilm growth conditions. Additionally, we provide evidence for the presence of at least one additional adhesin that is sensitive to arginine and is not a member of the autotransporter family type of fusobacterial large outer membrane proteins. These findings are consistent with earlier observations of different coaggregation groups for *F. nucleatum* with *P. gingivalis* that vary in their sensitivity to a variety of inhibitors.<sup>26,58</sup> Because certain strain-strain interactions could be more pathogenic than others, we believe that an improved understanding of the array of adhesins involved in interspecies attachment will continue to clarify the role of *F. nucleatum* in health and disease.

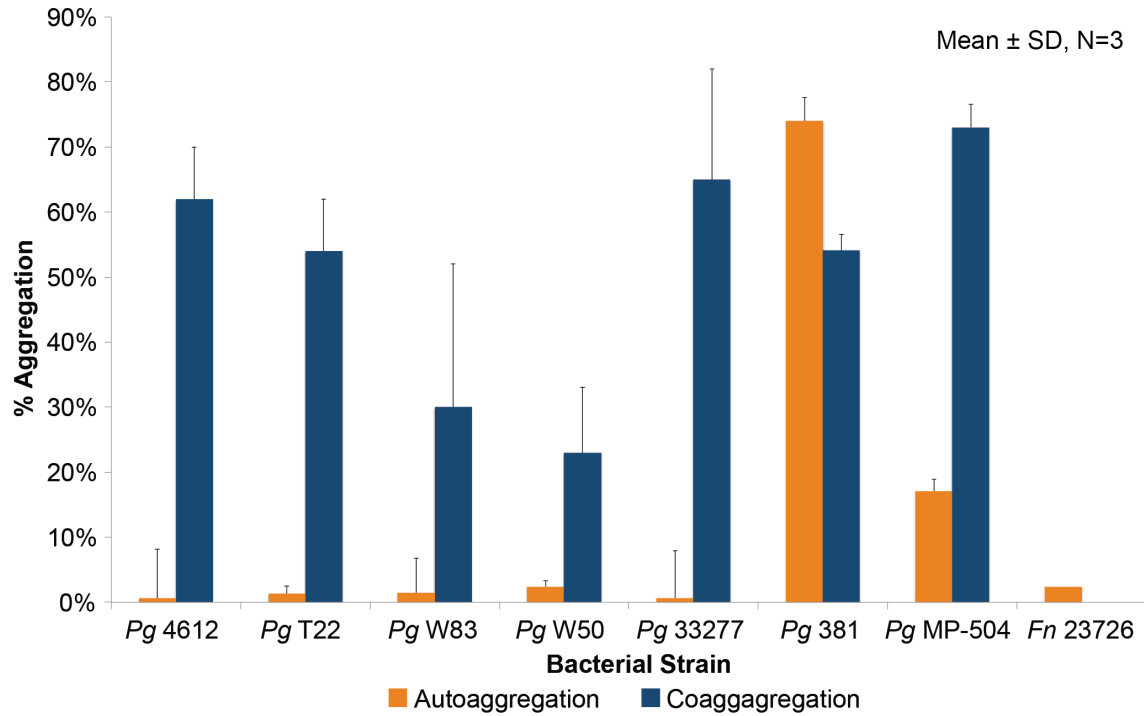


**Figure 1.** Quantitative autoaggregation levels of bacterial strains and coaggregation levels between *F. nucleatum* ATCC 23726 and seven different *P. gingivalis* strains. Data are expressed as % aggregation and represent the means and standard deviation of at least three independent experiments.

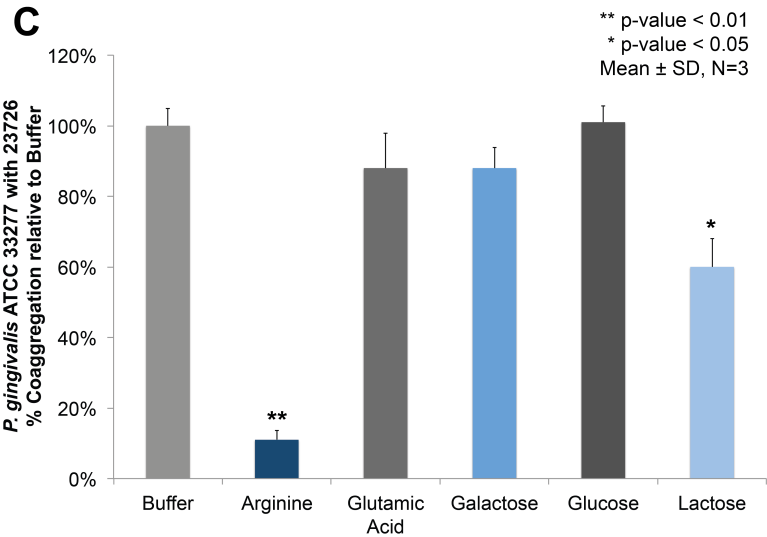
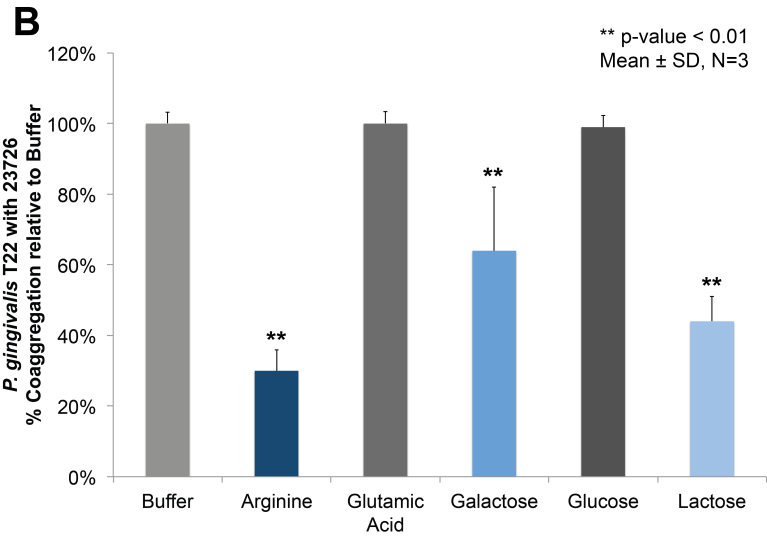
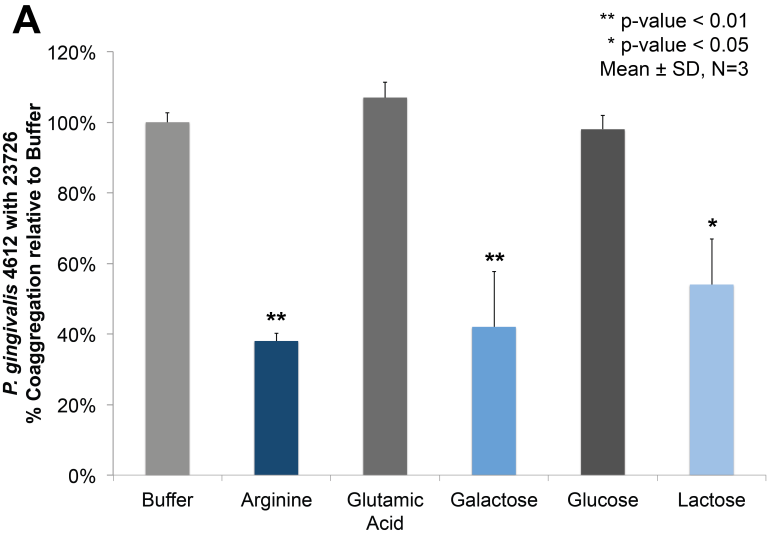


**Figure 2.** Quantitative inhibition of coaggregation assay between *F. nucleatum* ATCC 23726 and *P. gingivalis* strains (A) 4612 (B) T22 and (C) ATCC 33277 in the presence of inhibitors. Data are expressed as relative % coaggregation compared to coaggregation reaction of the partner strains in buffer set as 100% and represent the means and standard deviation of at least three independent experiments.

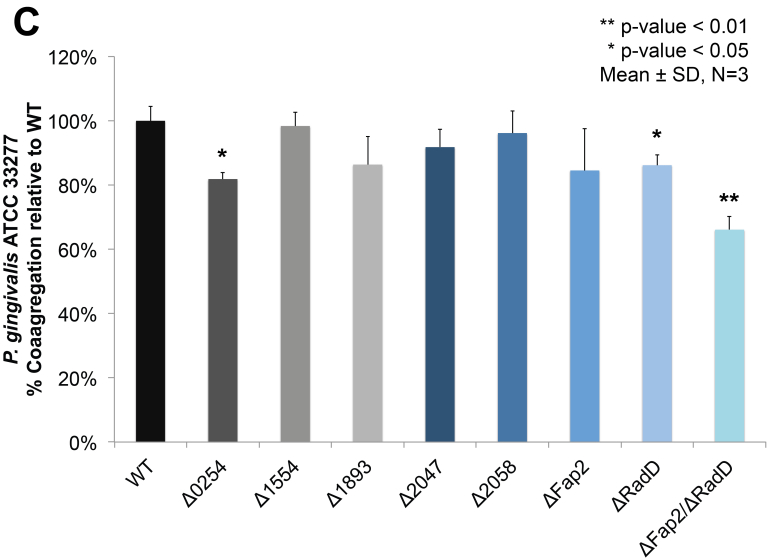
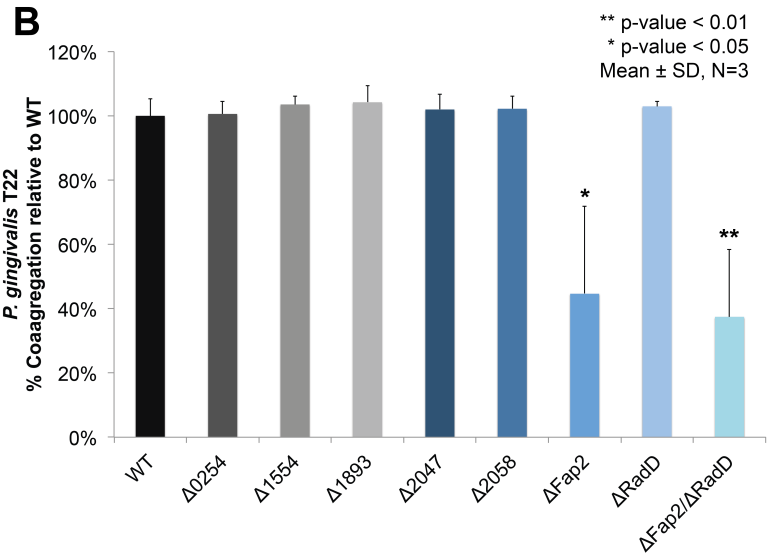
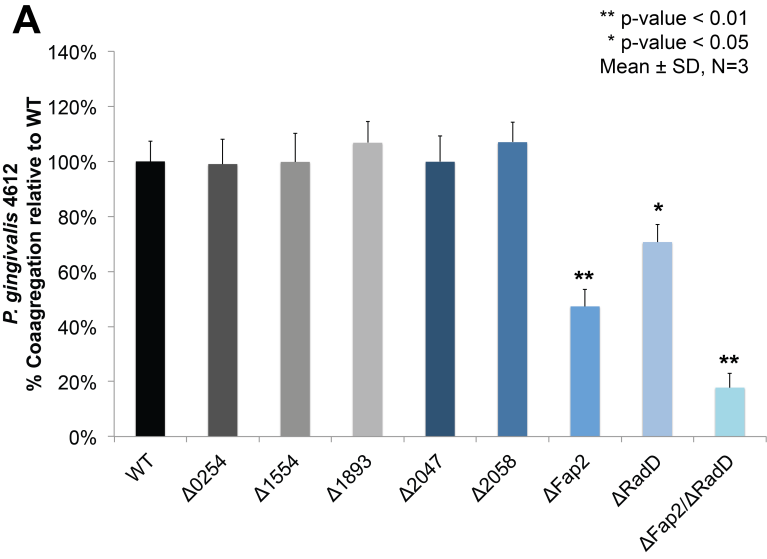


**Figure 3.** Quantitative coaggregation assay between *F. nucleatum* ATCC 23726 and mutant derivatives in outer membrane proteins (OMPs) with *P. gingivalis* strains (A) 4612, (B) T22 and (C) ATCC 33277. Data are expressed as relative % coaggregation compared to coaggregation reaction of the wildtype with the respective *P. gingivalis* partner strains set as 100%. Data represent the means and standard deviation of at least three independent experiments.

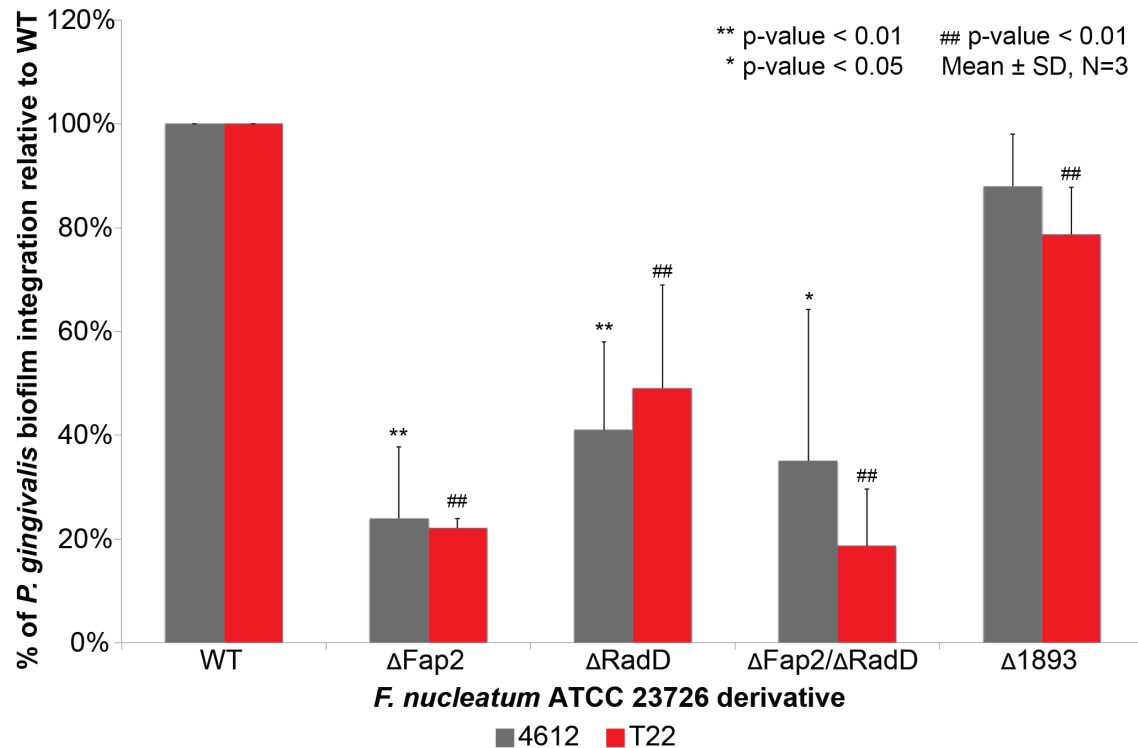
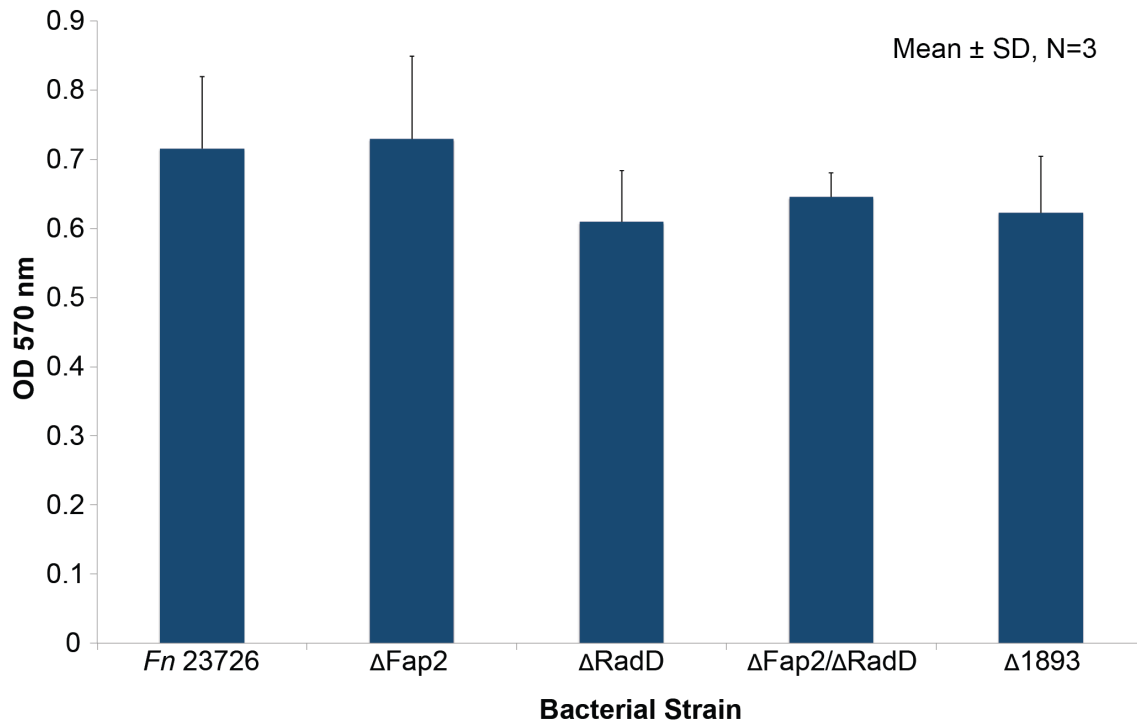


**Figure 4.** *P. gingivalis* integration in dual species biofilms with *F. nucleatum* ATCC 23726 ΔFap2, ΔRadD and ΔFap2/ΔRadD OMP mutant derivatives. Biofilm integration is given as a percentage relative to biofilm integration measured with wildtype *F. nucleatum* ATCC 23726. At least three independent experiments were performed per strain combination. Data represent the means and standard deviation of at least three independent experiments.



**Supplemental Figure 1.** Quantification of fusobacterial attachment to collagen-coated 96-well plates. OD<sub>570nm</sub> measurement of crystal violet-stained biofilms resuspended in 95% ethanol. Averages and SDs of three separate experiments are shown.

	Autoaggregation	<i>F. nucleatum</i> ATCC 23726
Pg 4612	0	4
PgT22	0	4
Pg W83	0	0
Pg W50	0	0
Pg 33277	0	3
Pg 381	4	4
Pg MP-504	1	4

**Supplemental Table 1.** Autoaggregation and coaggregation reactions were visually scored. A score of 0 was assigned for no visible aggregation and a score of 4 described complete sedimentation of strains with a clear supernatant.

## References

1. Andersen RN, Ganeshkumar N, Kolenbrander PE. *Helicobacter pylori* adheres selectively to *Fusobacterium* spp. Oral Microbiol Immunol 1998; 13(1): 51-54.
2. Kolenbrander PE, Andersen RN, Moore LV. Coaggregation of *Fusobacterium nucleatum*, *Selenomonas flueggei*, *Selenomonas infelix*, *Selenomonas noxia*, and *Selenomonas sputigena* with strains from 11 genera of oral bacteria. Infect Immun 1989; 57(10): 3194-203.
3. Kolenbrander PE, Parrish KD, Andersen RN et al. Intergeneric coaggregation of oral *Treponema* spp. with *Fusobacterium* spp. and intrageneric coaggregation among *Fusobacterium* spp. Infect Immun 1995; 63(12): 4584-8.
4. Berezow AB, Darveau RP. Microbial shift and periodontitis. Periodontol 2000 2001; 55(1): 36-47.
5. Han YW, Wang X. Mobile microbiome: oral bacteria in extra-oral infections and inflammation. J Dent Res 2013; 92(6): 485-91.
6. Han YW. *Fusobacterium nucleatum*: a commensal-turned pathogen. Curr Opin Microbiol 2015; 23: 141-7.
7. Swidsinski A, Dorffel Y, Loening-Baucke V et al. Acute appendicitis is characterised by local invasion with *Fusobacterium nucleatum/necrophorum*. Gut 2011; 60(1): 34-40.
8. Temoin S, Chakaki A, Askari A et al. Identification of oral bacterial DNA in synovial fluid of patients with arthritis with native and failed prosthetic joints. J Clin Rheumatol 2012; 18(3): 117-21.
9. Chaim W, Mazor M. Intraamniotic infection with fusobacteria. Arch Gynecol Obstet 1992; 251(1): 1-7.
10. Han YW, Fardini Y, Chen C et al. Term stillbirth caused by oral *Fusobacterium nucleatum*. Obstet Gynecol 2010; 115(2 Pt 2): 442-5.
11. Bradshaw DJ, Marsh PD, Watson GK et al. Role of *Fusobacterium nucleatum* and coaggregation in anaerobe survival in planktonic and biofilm oral microbial communities during aeration. Infect Immun 1998; 66(10): 4729-4732.
12. Kaplan A, Kaplan CW, He X et al. Characterization of aid1, a novel gene involved in *Fusobacterium nucleatum* interspecies interactions. Microb Ecol 2014; 68(2): 379-87.

13. Kaplan CW, Lux R, Haake SK et al. The *Fusobacterium nucleatum* outer membrane protein RadD is an arginine-inhibitable adhesin required for inter-species adherence and the structured architecture of multispecies biofilm. *Mol Microbiol* 2009; 71(1): 35-47.
14. Copenhagen-Glazer S, Sol A, Abed J et al. Fap2 of *Fusobacterium nucleatum* is a galactose-inhibitable adhesin involved in coaggregation, cell adhesion, and preterm birth. *Infect Immun* 2015; 83(3): 1104-13.
15. Henderson IR, Navarro-Garcia F, Desvaux M et al. Type V protein secretion pathway: the autotransporter story. *Microbiol Mol Biol Rev* 2004; 68(4): 692-744.
16. Bullard B, Lipski S, Lafontaine ER. Regions important for the adhesin activity of *Moraxella catarrhalis* Hag. *BMC Microbiol* 2007; 7: 65.
17. Lipski SL, Akimana C, Timpe JM et al. The *Moraxella catarrhalis* autotransporter McaP is a conserved surface protein that mediates adherence to human epithelial cells through its N-terminal passenger domain. *Infect Immun* 2007; 75(1): 314-24.
18. Heras B, Totsika M, Peters KM et al. The antigen 43 structure reveals a molecular Velcro-like mechanism of autotransporter-mediated bacterial clumping. *Proc Natl Acad Sci U S A* 2014; 111(1): 457-62.
19. Klemm P, Hjerrild L, Gjermansen M et al. Structure-function analysis of the self-recognizing Antigen 43 autotransporter protein from *Escherichia coli*. *Mol Microbiol* 2004; 51(1): 283-96.
20. Sherlock O, Schembri MA, Reisner A et al. Novel roles for the AIDA adhesin from diarrheagenic *Escherichia coli*: cell aggregation and biofilm formation. *J Bacteriol* 2004; 186(23): 8058-65.
21. Valle J, Mabbett AN, Ulett GC et al. UpaG, a new member of the trimeric autotransporter family of adhesins in uropathogenic *Escherichia coli*. *J Bacteriol* 2008; 190(12): 4147-61.
22. Capecchi B, Adu-Bobie J, Di Marcello F et al. *Neisseria meningitidis* NadA is a new invasin which promotes bacterial adhesion to and penetration into human epithelial cells. *Mol Microbiol* 2005; 55(3): 687-698.
23. Kaplan CW, Lux R, Huynh T et al. *Fusobacterium nucleatum* apoptosis-inducing outer membrane protein. *J Dent Res* 2005; 84(8): 700-4.
24. Kaplan CW, Ma X, Paranjpe A et al. *Fusobacterium nucleatum* outer membrane proteins Fap2 and RadD induce cell death in human lymphocytes. *Infect Immun* 2010; 78(11): 4773-8.

25. Cisar JO, Kolenbrander PE, McIntire FC. Specificity of coaggregation reactions between human oral streptococci and strains of *Actinomyces viscosus* or *Actinomyces naeslundii*. *Infect Immun* 1979; 24(3): 742-52.
26. Kolenbrander PE, Andersen RN. Inhibition of coaggregation between *Fusobacterium nucleatum* and *Porphyromonas (Bacteroides) gingivalis* by lactose and related sugars. *Infect Immun*. 1989; 57(10): 3204-9.
27. Crowley PJ, Fischlschweiger W, Coleman SE et al. Intergeneric bacterial coaggregations involving mutans streptococci and oral actinomyces. *Infect Immun* 1987; 55(11): 2695-700.
28. Jakubovics NS, Stromberg N, van Dolleweerd CJ et al. Differential binding specificities of oral streptococcal antigen I/II family adhesins for human or bacterial ligands. *Mol Microbiol* 2005; 55(5): 1591-605.
29. Kolenbrander PE, Inouye Y, Holdeman LV. New *Actinomyces* and *Streptococcus* coaggregation groups among human oral isolates from the same site. *Infect Immun* 1983; 41(2): 501-6.
30. Eke PI, Rotimi VO, Laughon BE. Coaggregation of black-pigmented *Bacteroides* species with other oral bacteria. *J Med Microbiol* 1989; 28(1): 1-4.
31. Kolenbrander PE, Andersen RN, Moore LV. Intrageneric coaggregation among strains of human oral bacteria: potential role in primary colonization of the tooth surface. *Appl Environ Microbiol* 1990; 56(12): 3890-4.
32. Noguchi N, Noiri Y, Narimatsu M et al. Identification and localization of extracellular biofilm-forming bacteria associated with refractory endodontic pathogens. *Appl Environ Microbiol* 2005; 71(12): 8738-43.
33. Ximenez-Fyvie LA, Haffajee AD, Socransky SS. Microbial composition of supra- and subgingival plaque in subjects with adult periodontitis. *J Clin Periodontol* 2000; 27(10): 722-32.
34. Lamont RJ, Chan A, Belton CM et al. *Porphyromonas gingivalis* invasion of gingival epithelial cells. *Infect Immun* 1995; 63(10): 3878-85.
35. Kinder SA, Holt SC. Characterization of coaggregation between *Bacteroides gingivalis* T22 and *Fusobacterium nucleatum* T18. *Infect Immun* 1989; 57(11): 3425-33.
36. Ansai T, Yamashita Y, Awano S et al. A murC gene in *Porphyromonas gingivalis* 381. *Microbiology* 1995; 141(9): 2047-2052.

37. Shah HN, Williams RA, Bowden GH et al. Comparison of the biochemical properties of *Bacteroides melaninogenicus* from human dental plaque and other sites. J Appl Bacteriol 1976; 41(3): 473-95.
38. Kinder SA, Holt SC. Coaggregation between bacterial species. Methods Enzymol 1994; 236: 254-70.
39. Saito Y, Fujii R, Nakagawa KI et al. Stimulation of *Fusobacterium nucleatum* biofilm formation by *Porphyromonas gingivalis*. Oral Microbiol Immunol 2008; 23(1): 1-6.
40. Takemoto T, Ozaki M, Shirakawa M et al. Purification of arginine-sensitive hemagglutinin from *Fusobacterium nucleatum* and its role in coaggregation. J Periodontal Res 1993; 28(1): 21-6.
41. Shaniztki B, Hurwitz D, Smorodinsky N et al. Identification of a *Fusobacterium nucleatum* PK1594 galactose-binding adhesin which mediates coaggregation with periopathogenic bacteria and hemagglutination. Infect Immun 1997; 65(12):5231-7.
42. Becker P, Hufnagle W, Peters G et al. Detection of differential gene expression in biofilm-forming versus planktonic populations of *Staphylococcus aureus* using micro-representational-difference analysis. Appl Environ Microbiol 2001; 67(7): 2958-2965.
43. Lo A, Seers C, Dashper S et al. FimR and FimS: biofilm formation and gene expression in *Porphyromonas gingivalis*. J Bacteriol 2010; 192(5): 1332-43.
44. Resch A, Rosenstein R, Nerz C et al. Differential gene expression profiling of *Staphylococcus aureus* cultivated under biofilm and planktonic conditions. Appl Environ Microbiol 2005; 71(5): 2663-76.
45. Biyikoglu B, Ricker A, Diaz PI. Strain-specific colonization patterns and serum modulation of multi-species oral biofilm development. Anaerobe 2012; 18(4): 459-470.
46. Kolenbrander PE, Williams BL. Prevalence of viridans streptococci exhibiting lactose-inhibitable coaggregation with oral actinomycetes. Infect Immun 1983; 41(2): 449-52.
47. Lamont RJ, El-Sabaeny A, Park Y et al. Role of the *Streptococcus gordonii* SspB protein in the development of *Porphyromonas gingivalis* biofilms on streptococcal substrates. Microbiology 2002; 148(6): 1627-36.
48. Grenier D, Mayrand D. Selected characteristics of pathogenic and nonpathogenic strains of *Bacteroides gingivalis*. J Clin Microbiol 1987; 25(4): 738-40.

49. Neiders ME, Chen PB, Suido H et al. Heterogeneity of virulence among strains of *Bacteroides gingivalis*. *J Periodontal Res* 1989; 24(3): 192-8.
50. Saito A, Inagaki S, Kimizuka R et al. *Fusobacterium nucleatum* enhances invasion of human gingival epithelial and aortic endothelial cells by *Porphyromonas gingivalis*. *FEMS Immunol Med Microbiol* 2008; 54(3): 349-55.
51. Takemoto T, Hino T, Yoshida M et al. Characteristics of multimodal co-aggregation between *Fusobacterium nucleatum* and streptococci. *J Periodontal Res* 1995; 30(4): 252-7.
52. Werner J, Augustus AM, Misra R. Assembly of TolC, a structurally unique and multifunctional outer membrane protein of *Escherichia coli* K-12. *J Bacteriol* 2003; 185(22): 6540-7.
53. Bodilis J, Barray S. Molecular evolution of the major outer-membrane protein gene (oprF) of *Pseudomonas*. *Microbiology* 2006; 152(4): 1075-1088.
54. Schroder W, Moser I. Primary structure analysis and adhesion studies on the major outer membrane protein of *Campylobacter jejuni*. *FEMS Microbiol Lett* 1997; 150(1): 141-7.
55. Engstrom MD, Alteri CJ, Mobley HL. A conserved PapB family member, TosR, regulates expression of the uropathogenic *Escherichia coli* RTX nonfimbrial adhesin TosA while conserved LuxR family members TosE and TosF suppress motility. *Infect Immun* 2014; 82(9): 3644-56.
56. Sievers S, Sternkopf Lillebaek EM et al. A multicopy sRNA of *Listeria monocytogenes* regulates expression of the virulence adhesin LapB. *Nucleic Acids Res* 2014; 42(14): 9383-98.
57. Cook GS, Costerton JW, Lamont RJ. Biofilm formation by *Porphyromonas gingivalis* and *Streptococcus gordonii*. *J Periodontal Res* 1998; 33(6): 323-7.
58. Metzger Z, Blasbalg J, Dotan M et al. Characterization of coaggregation of *Fusobacterium nucleatum* PK1594 with six *Porphyromonas gingivalis* strains. *J Endod* 2009; 35(1): 50-4.

## Chapter 2: Characterization of the Fusobacterial *radD*-Operon

## Abstract

The oral Gram-negative bacterium *Fusobacterium nucleatum* has been implicated as an important player in both health and disease. Fusobacteria act as a bridging organism that connect early with late colonizers in oral biofilm formation and can induce apoptosis in lymphocytes. We previously demonstrated that in *F. nucleatum* these functions involve large outer membrane proteins of the autotransporter family such as RadD, which is encoded by the largest and last gene of a four gene operon. The three genes upstream of *radD* (homologue of FN1526) are small genes homologs of FN1529, FN1528 (which we termed *rapA* and *rapB*, respectively) coding for proteins with unknown functions and a homolog of FN1527 (*fad-I*), which was recently reported to induce human  $\beta$ -defensin 2 (hBD-2) in oral epithelial cells. The objective of our study was to confirm *radD* function in *F. nucleatum* ssp. *nucleatum* (FNN) and ssp. *polymorphum* (FNP) and gain insight into the role of the genes in the *radD* operon in interspecies interaction. Here, we report that the gene directly upstream of *radD*, previously identified as *fad-I* encoding a lipoprotein, regulates *radD* expression. Gene inactivation mutants of FNN *rapA*, *rapB*, *fad-I* and FNP *rapA*, *rapB*, *radD*, were generated and all mutants were subjected to coaggregation assays and qPCR analysis. Our studies show that lack of the *fad-I* gene results in increased binding with both *Streptococcus gordonii* and *Porphyromonas gingivalis* as a result of overexpression of *radD*. The FNN and FNP  $\Delta$ *fad-I* mutants also exhibited the enhanced ability to form robust biofilms with *S. gordonii*. These results suggest that the protein encoded by *fad-I* is an element acting as a repressor for *radD* expression.

## Introduction

Bacterial adhesion is an essential process in the development and maturation of multi-species biofilm, mediated by bacterial virulence factors called adhesins. Adhesion has been observed between genetically distinct bacteria isolated from biofilms in a number of human sites including the gut, urogenital tract, and oral cavity<sup>1-7</sup> and is one of the first steps in the cascade of events that lead to the establishment of bacterial infection in a biofilm.

Biofilm development involves the complex and coordinated regulation of adhesin in response to quorum sensing, bacterial stress and host susceptibility.<sup>8-10</sup> The regulation of adhesion expression has been described in two levels.<sup>11</sup> One level involves the sensing changes in the bacterial environment and can be seen as a coordinated response to switch adhesins on or off.<sup>12,13</sup> The other level involves the regulation of bacterial adhesins regardless of environmental factors to allow for a survival advantage in unpredictable environments.<sup>14</sup>

Of interest are the adhesins of the opportunistic pathogen *Fusobacterium nucleatum*, a prominent member of oral biofilms. A key feature of *F. nucleatum* is its remarkable ability to bind using adhesins to bacteria both commensal and pathogenic species alike, in addition to eukaryotic cells. One fusobacterial adhesin in particular, RadD, was identified as the main adhesin to mediate attachment to a number of gram-positive early colonizers,<sup>15</sup> in addition to supporting fusobacterial adherence to certain isolates of *Porphyromonas gingivalis*, a periodontal pathogen.<sup>7</sup> RadD has also been implicated in attachment to and apoptosis induction in human lymphocytes,<sup>16</sup> adding to the

evidence that it is critical in the establishment of fusobacteria and disease.

Sequence analyses using Protein BLAST<sup>17</sup> reveal RadD is encoded by the last gene in a four-gene operon that is conserved across all four subspecies of *F. nucleatum ssp. animalis*: FSDG\_01656, FSDG\_01657, FSDG\_01658 and FSDG\_01659.<sup>15</sup> The gene directly upstream of *radD*, called *fad-I*, was previously described as encoding the lipoprotein FAD-I, which is characterized by its ability to induce human  $\beta$ -defensin 2 (hBD-2) in oral epithelial cells in a subspecies dependent manner.<sup>18,19</sup> FAD-I of *F. nucleatum ssp. nucleatum*, type strains 25586 and 23726, induce expression of hBD-2 effectively, while FAD-I of *F. nucleatum ssp. polymorphum*, type strain 10953 fails to do so, which could have a profound influence on oral community composition. No function has been described for the two other genes encoded by the operon, which we denominated as RapA and RapB (RadD associated proteins).

In the present study, we investigated the role of the genes encoded by the *radD* containing four-gene operon in interspecies interaction of the *F. nucleatum nucleatum* and *polymorphum* subspecies. Our studies revealed that lack of the *fad-I* gene results in increased binding of *Fusobacteria* to both early and late oral colonizers as a result of the overexpression of *radD*, which also conferred the enhanced ability to form robust biofilms with *Streptococcus gordonii*. We also demonstrated that the presence of RadD is not needed for regulating its expression. These results suggest that the protein encoded by *fad-I* is an element acting as a repressor for *radD* expression. Additionally, we report *radD* suppression when *F. nucleatum* is bound to a streptococcal partner species and no change in *radD* expression when bound to *Porphyromonas gingivalis*,

indicating an additional regulatory mechanism that is independent of *fad-I* and *radD*.

## Materials and Methods

### Bacterial Strains and Culture Conditions

*F. nucleatum* ssp *nucleatum* strain ATCC 23726, ssp *polymorphum* strain ATCC 10953 and their respective mutant derivatives generated in this study or described previously<sup>15,19</sup> as well as *P. gingivalis* strain 4612,<sup>20</sup> were maintained on Columbia agar supplemented with 5% sheep blood or in Columbia broth (Difco, Detroit, MI) under anaerobic conditions (10% H<sub>2</sub>, 10% CO<sub>2</sub>, 80% N<sub>2</sub>) at 37°C. All media for *P. gingivalis* were supplemented with hemin at 5 µg ml<sup>-1</sup> and menadione at 1 µg ml<sup>-1</sup>. *S. gordonii* ATCC 10558<sup>21</sup> was maintained on Todd Hewitt agar or Todd Hewitt broth (Difco, Detroit, MI) under anaerobic conditions (10% H<sub>2</sub>, 10% CO<sub>2</sub>, 80% N<sub>2</sub>) at 37°C. Thiamphenicol at 5 µg ml<sup>-1</sup> and clindamycin at 1 µg ml<sup>-1</sup> (MP Biomedicals, Irvine, CA) were used for the selection and maintenance of strains possessing the *catP* cassette. One Shot TOP10 Competent *E.coli* cells (Thermo Fisher Scientific, Waltham, MA) used for DNA manipulation were grown aerobically at 37°C degrees in Luria broth (Difco, Detroit, MI).

### Mutant strain and plasmid construction

#### *Allelic exchange mutagenesis*

Allelic exchange mutagenesis was used to replace target genes with the *catP* resistance cassette that confers thiamphenicol resistance. Internal gene fragments were amplified for each target gene using Phusion HF DNA polymerase (NEB) according to the manufacturer's protocol and primers designed for this study (Table 1). Fusion PCR was carried out as previously described.<sup>22</sup> Fragments were purified and isolated using the QIAquick Gel Extraction Kit (Qiagen, Hilden, Germany). Each construct was

generated by fusing fragments homologous to the upstream and downstream portions of the target gene to flank the *catP* gene along with its promoter. The *catP* gene for each construct was amplified from pHS30.<sup>23</sup> Primers used in fusion PCR were created with overlaps of 25-30 base pairs to allow for fusion in the PCR reactions. The fusion products were cloned into pJET1.2/blunt (Thermo Fisher Scientific, Waltham, MA) and transformed into One Shot TOP10 Competent *E. coli* Cells according to manufacturer's protocols to generate the respective plasmids used for gene replacement (Table 1). After confirmation of the constructs by sequencing and restriction mapping, plasmid DNA was isolated and purified using QIAGEN Plasmid Maxi Kit (Qiagen, Hilden, Germany). Purified plasmids were then transformed into ATCC 23726 or ATCC 10953 to generate respective derivatives lacking target genes as previously described.<sup>24,25</sup> Using internal primers, the genomic DNA obtained colonies was analyzed by PCR for presence of the *catP* gene and absence of the target gene.

#### *Insertional inactivation*

A  $\Delta radD$  mutant derivative of *F. nucleatum* ssp. *polymorphum* ATCC 10953 was constructed by inactivating the *radD* gene (FNP1046) via single homologous recombination as described earlier.<sup>15</sup> Briefly, a 1032 bp gene fragment was amplified using the primer pair BS1000 and BS1001 appended with *EcoR1* and *BamH1*, respectively from genomic DNA of *F. nucleatum* 10953 and sub-cloned into pJET1.2/blunt vector. The resulting plasmid was digested with *EcoR1/BamH1*, ligated into *EcoR1/BamH1* digested pHS31vector and transformed into *E.coli*. After confirmation of the integration plasmid by sequencing, the plasmid DNA was electroporated into *F. nucleatum* ssp. *polymorphum* ATCC 10953 and plated on selective media containing 5 $\mu$ g/ml thiamphenicol. The insertional mutant was

confirmed via PCR and sequencing.

### **Coaggregation Assay**

Quantitative coaggregation assays were performed identical to the visual assay except that optical densities of reaction mixtures were obtained spectrophotometrically immediately after addition of the second partner strain and vortexing ( $OD_{t=0 \text{ min}}$ ). After 10 min of incubation, reaction mixtures were centrifuged at low speed ( $100 \times g$  for 1 min) to pellet coaggregated cells, while leaving non-aggregated bacteria in suspension. Optical densities of the supernatants were measured after the 10 min incubation ( $OD_{t=10 \text{ min}}$ ) in order to quantitate coaggregation. Percent coaggregation was calculated as follows: % coaggregation =  $[(OD_{t=0 \text{ min}} - OD_{t=10 \text{ min}}) / (OD_{t=0 \text{ min}})] \times 100$ . These values were averaged across at least three independent experiments.

### **Co-incubation of *F. nucleatum* with partner species**

Cells were grown to mid-log phase and a total of  $OD_{600} 1$  cells of *F. nucleatum* ATCC 23726 or mutant derivative was added to sterile 15ml conical tubes with either a total  $OD_{600} 1$  of *S. gordonii* ATCC 10558 or *P. gingivalis* 4612 cells. Control tubes contained 1ml ( $OD_{600} 1$ ) of *F. nucleatum* ATCC 23726 or mutant derivative alone. Cells were centrifuged for 5 min at  $4600 \times g$ . supernatant was decanted, and replaced with 1ml of CB for *F. nucleatum* alone tubes, 2ml of CB for tubes with *F. nucleatum* and *S. gordonii*, or 2ml of CB supplemented with hemin ( $5 \mu\text{g ml}^{-1}$ ) and menadione ( $1 \mu\text{g ml}^{-1}$ ) for tubes with *F. nucleatum* and *P. gingivalis*. Tubes were centrifuged again for 3 min followed by anaerobic incubation (10%  $\text{H}_2$ , 10%  $\text{CO}_2$ , 80%  $\text{N}_2$ ) at  $37^\circ\text{C}$  for 30 min or 20 hours. Cells were collected after incubation, pelleted and stored in  $-80^\circ\text{C}$  for at least 24 hours

prior to RNA extraction.

### **Nucleic acid isolation and cDNA generation**

Genomic DNA was isolated from mid-log phase cells using GenElute Bacterial Genomic DNA Kit (Sigma-Aldrich, St. Louis, MO) according to manufacture's instructions with modification of final elution to 30  $\mu$ l. Total RNA was extracted from cells using the PureLink RNA Mini Kit (Thermo Fisher Scientific, Waltham, MA), followed by a TURBO DNA-free DNase Treatment (Thermo Fisher Scientific, Waltham, MA), and finally cleaned and concentrated using RNA Clean & Concentrator (Zymo Research, Irvine, CA). One microgram of total RNA was used for cDNA synthesis using SuperScript III First-Strand Synthesis System (Thermo Fisher Scientific, Waltham, MA) according to the manufacturer's protocol.

### **Quantitative (Real-Time) Polymerase Chain Reaction**

Gene specific primers (Table 1) were used to amplify transcript regions for signal detection by qPCR on iCycler Thermal Cycler (Bio-Rad, Hercules, CA) in a total volume of 20  $\mu$ l containing 2  $\mu$ l of 10x iQ SYBR Green Supermix (Bio-Rad, Hercules, CA), 0.5  $\mu$ M each of forward and reverse primers, 7  $\mu$ l of Millipore water and 1  $\mu$ l of template. Primer sets were designed for each gene of interest in homologous regions of the corresponding open reading frames in *F. nucleatum ssp nucleatum* ATCC 23726 and *F. nucleatum ssp polymorphum* ATCC 10953. Amplification and detection were carried out in 96-well optical plates (Thermo Fisher Scientific, Waltham, MA). Each PCR run was performed with an initial incubation of 10 min at 95°C followed by 40 cycles of denaturing at 95°C for 15 sec; annealing and elongation at 60°C for 1 min. After the

40 cycles of amplification, an additional denaturing step was performed at 95°C for 1 min followed by annealing and elongation at 60°C for 1 min. A melting curve analysis was completed after each run. The DNA concentrations (ng ml<sup>-1</sup>) were calculated with standard curves obtained by tenfold serial dilutions of bacterial genomic DNA. All standards were run in duplicate to generate a standard curve to determine the efficiency of each primer set. Three independent qPCR runs were performed with three technical replicates for each sample to assess reproducibility and inter-run variability. Following amplification, relative expression levels between samples were calculated as fold changes normalized to *rpoB* reference gene amplification.

### **Biofilm Growth**

The *F. nucleatum* and *S. gordonii* biofilms were grown using 8-well chambers on optical plastic slides (Thermo Fisher Scientific, Waltham, MA) that were UV sterilized for 1 h prior to inoculation. For dual-species biofilms 500ul of SHI medium<sup>26</sup> supplemented with 0.5% sucrose and 0.5% mannose<sup>27</sup> were added into each well. *S. gordonii* (10<sup>5</sup> cells) and *F. nucleatum* wild-type or mutant cells (50 µl containing ~10<sup>8</sup> cells) were seeded into each well in a ratio of 1:1000 and allowed to grow under anaerobic conditions (10% H<sub>2</sub>, 10% CO<sub>2</sub>, 80% N<sub>2</sub>) at 37°C for 20 hours. At least three biological replicates were performed per condition.

### **Imaging**

The biofilms were washed with sterile PBS before adding SYTO 9. They were further examined using a LSM-780 confocal laser scanning microscope (Zeiss, Germany) wherein tiled, confocal z-stacks were collected. The signal was summed over

the z-stacks to provide an overall fluorescence signal. 3D rendering and orthogonal sectioning of the z-stacks was performed using the Zeiss Zen software. Zeiss plan-apochromat 20X/0.8 dry and Zeiss plan-neofluar 40x/1.3 oil objectives were used. SYTO9 fluorescence was imaged using a 488 nm laser with a FITC filter set.

### **Statistical Analysis**

Student's *t*-test was performed to determine statistical significance using Excel 2011 (Microsoft, Seattle, WA).

## Results

### Inactivation of genes encoded in the same operon as the RadD adhesin in the *F. nucleatum* subspecies *nucleatum* and *polymorphum*

In oral fusobacteria including the transformable strains of the *F. nucleatum* subspecies *nucleatum* ATCC 23726 (FNN) and the subspecies *polymorphum* ATCC 10953 (FNP) the adhesin RadD is encoded by the last gene of a four gene operon comprised of the respective homologs of FN1529, FN1528, FN1527 (*fad-I*) and FN1526 (*radD*).<sup>15</sup> The genes encoded by homologs of FN1529 and FN1528 were previously unnamed and will be referred to as *rapA* and *rapB*, respectively, (Rap stands for: *radD*-associated proteins). In our previous studies we inactivated *radD* of FNN and *fad-I* of FNP as part of their functional characterization.<sup>15,19</sup> For a comprehensive investigation of all genes encoded by this four-gene operon in the above genetically tractable *F. nucleatum* subspecies, we individually inactivated *rapA*, *rapB* and *fad-I* in FNN, and *rapA* and *rapB* as well as *radD* in FNP (Figure 1). The small genes encoding *rapA*, *rapB* and *fad-I* were inactivated via double-crossover gene inactivation, while FNP *radD* was disrupted via a previously established single-crossover approach.<sup>25</sup> The respective gene inactivation plasmids were created and transformed as described in *Materials and Methods*. The resulting mutant strains were confirmed by PCR and sequencing analysis. We also constructed a strain in which the *catP* resistance cassette was inserted between *fad-I* and *radD* as a control strain named CIC (*catP* Insertion Control) to address possible polar effects of *catP* insertion on gene expression. We employed the same strategy to introduce a mutated version of the *fad-I* gene lacking the start codon into FNP ATCC 10953 (FNP *fad-I*\*) as an additional control strain for possible unspecific effects of the *catP* cassette (Figure 1). The different *fad-I* mutants were further confirmed via

Western blotting using a previously developed anti-FAD-I antibody.

**Mutant derivatives of *F. nucleatum* lacking *rapA*, *rapB*, *fad-I* or *radD* exhibit altered coaggregation with *S. gordonii* and *P. gingivalis*.**

First, we assessed the coaggregation properties of the  $\Delta rapA$ ,  $\Delta rapB$ ,  $\Delta fad-I$  and  $\Delta radD$  mutant derivatives of both *F. nucleatum* subspecies investigated in this study with *S. gordonii* to determine if the Rap and FAD-I proteins play a role in adhesion to Gram-positive early colonizers and confirm RadD as adhesin in interspecies interaction for *F. nucleatum* ssp *polymorphum*. Visual and quantitative coaggregation assays revealed similar patterns of coaggregation between the corresponding mutants of FNN and FNP with *S. gordonii* (Figure 2). Individual inactivation of the genes encoding the Rap proteins (RapA and RapB) of both *F. nucleatum* subspecies exhibited coaggregation levels similar to their respective wild-type parent strains. Specifically, coaggregation of *S. gordonii* with  $\Delta rapA$  mutants of FNN and FNP was  $68\pm 7\%$  and  $68\pm 2\%$ , respectively, and  $59\pm 12\%$  and  $70\pm 5\%$  with the  $\Delta rapB$  derivatives, respectively, compared to  $51\pm 12\%$  and  $62\pm 8\%$  for the corresponding wild-type strains. Interestingly, coaggregation for the  $\Delta fad-I$  mutants in both subspecies showed significantly increased levels of coaggregation ( $85\pm 4\%$  for 23726 and  $96\pm 4\%$  for 10953) (Figure 2), while the *radD* mutants for both strains displayed a coaggregation deficient phenotype in both strains (FNN,  $6\pm 2\%$  coaggregation and FNP,  $15\pm 5\%$  coaggregation), confirming RadD as a major adhesin in the interaction with early gram-positive oral colonizers<sup>15</sup> also for the *F. nucleatum* subspecies *polymorphum*. We further assessed the coaggregation properties of FNN *rap* and *fad-I* mutants with *P. gingivalis* strain 4612, an interaction which was previously determined by our lab to be mediated by two adhesins, RadD and

Fap2.<sup>7</sup> Interactions between *P. gingivalis* and the FNN mutants defective in *rapA*, *rapB* or *fad-I* were significantly enhanced (82±6%, 72±7%, and 73±9% coaggregation, respectively) compared to the coaggregation of wild-type with *P. gingivalis* (37±10%) (Figure 2B). The *radD* mutant displayed a coaggregation deficient phenotype with a 19±2% coaggregation, consistent with the previously observed involvement of RadD in the interaction with *P. gingivalis* 4612.<sup>7</sup>

### **Enhanced coaggregation correlates with increased *radD* expression in *F. nucleatum* and lack of FAD-I**

Next, we determined transcriptional levels of *rapA*, *rapB*, *fad-I* and *radD* in each mutant generated in FNN and FNP via qPCR (Figure 3). Even though some of the differences compared to wild-type gene expression were statistically significant they mostly did not exceed or even come close to two-fold changes in expression levels and will therefore not be considered to be biologically relevant. While the  $\Delta rapA$  derivatives of both strains did not produce any signal confirming lack of the gene, transcriptional levels of *rapA* in most of the mutant strains tested were similar to wild-type levels (fold changes compared to respective wild-type parents: FNN CIC 0.97±0.05; FNP  $\Delta rapB$  1.3±0.14; FNN  $\Delta fad-I$  1.24±0.29; FNP  $\Delta fad-I$  1.30±0.95; FNP *fad-I*\* 0.72±0.09; FNN  $\Delta radD$  0.94±0.06; FNP  $\Delta radD$  1.48±0.60) with the exception of FNN  $\Delta rapB$  (0.41±0.12 fold change) and the CIC derivative of FNP (0.47±0.08 fold change), which exhibited reduced *rapA* transcription (Figure 3A). As expected, both  $\Delta rapB$  mutants did not produce any transcript (Figure 3B). All other strains exhibited less than two-fold differences in *rapB* expression levels (fold changes compared to respective wild-type parents: FNN CIC 0.84±0.09; FNP CIC 0.52±0.11; FNN  $\Delta rapA$  1.92±0.43; FNP

$\Delta rapA$  1.29±0.02; FNN  $\Delta fad-I$  1.27±0.42; FNP  $\Delta fad-I$  1.23±0.13; FNP *fad-I\** 0.66±0.11; FNN  $\Delta radD$  0.90±0.52; FNP  $\Delta radD$  0.95±0.04). Similarly, we did not detect any *fad-I* transcript in both  $\Delta fad-I$  mutants, while *fad-I* expression in most mutant strains was similar to the wild-type parents (fold changes compared to respective wild-type parents: FNN CIC 0.67±0.16; FNN  $\Delta rapA$  1.72±0.49; FNP  $\Delta rapA$  1.38±0.46; FNN  $\Delta rapB$  1.42±0.15; FNP  $\Delta rapB$  1.69±0.58; FNP *fad-I\** 0.55±0.03; FNN  $\Delta radD$  0.80±0.07; FNP  $\Delta radD$  1.21±0.36) with the exception of FNP CIC (0.38±0.08 fold change)(Figure 3C). In contrast to expression levels of *rapA*, *rapB*, and *fad-I*, we found that *radD* expression level were significantly elevated several fold in some mutant derivatives (Figure 3D) and that this increase correlated with the observed increase in coaggregation with *S. gordonii* (Figure 2A). In the CIC controls for each strain *radD* transcript levels were similar to respective wild-type for FNN (1.06±0.20) and FNP (1.22±0.29). While *radD* expression was less than two-fold elevated in the respective  $\Delta rapA$  and  $\Delta rapB$  derivatives of FNN (1.76±0.23 and 1.33±0.26, respectively) the  $\Delta fad-I$  mutant produced 3.49±0.79 fold more *radD*. Lack of *rapA*, *rapB* or *fad-I* resulted in significant more than two-fold increase of *radD* levels compared to wild-type in the ATCC 10953 background with 2.28±0.27 for FNP  $\Delta rapA$ , 3.26±0.23 for FNP  $\Delta rapB$ , 5.95±1.20 for FNP  $\Delta fad-I$  and 4.63±0.52 for FNP *fad-I\**. Additionally, detection of *radD* transcription in the *radD* mutants of both FNN and FNP was possible due to the location of the qPCR primer designed from a region of the sequence upstream of the insertion (Figure 1) and found to be similar to wild-type (0.89±0.13 fold change for FNN *radD* and 0.91±0.09 fold change for FNP *radD*).

**The presence of the RadD adhesin is not required for increased expression**

### **of *radD* in a $\Delta$ *fad-I* mutant**

To further investigate if the role of *radD* in *radD* regulation, we introduced a frameshift mutation in the N-terminal part of the *radD* gene in the FNN  $\Delta$ *fad-I* mutant background to create a derivative in which *radD* would still be expressed but not translated into a functional protein (Figure 1). The resulting FNN  $\Delta$ *fad-I radD\** mutant strain was deficient in coaggregation with *S. gordonii* ( $13\pm 2.6\%$  coaggregation compared to 64% for the wild-type parent control) (Figure 4A). Transcript levels for *radD* in the FNN  $\Delta$ *fad-I radD\** derivative remained elevated relative to wild-type ( $3.26\pm 0.23$  fold increase) (Figure 4B) similar to our findings above for the FNN  $\Delta$ *fad-I* mutant (Figure 3D).

### **Interaction with *S. gordonii* regulates *radD* expression independent of FAD-I**

*F. nucleatum* utilizes RadD as a major adhesin for binding to *S. gordonii* and as an additional adhesin for interaction with certain *P. gingivalis* strains such as 4612. To examine if the presence of binding partners influences regulation of this important adhesin on a transcriptional level, we determined *radD* expression in the presence and absence of *S. gordonii* and *P. gingivalis* as binding partners and found that the presence of *S. gordonii* but not *P. gingivalis* reduced *radD* transcript levels already within the first 30 min of coincubation with *F. nucleatum* ATCC 23726 (Figure 5A) as well as in samples that were coincubated for up to 20 hrs (data not shown). This pattern was maintained in the respective  $\Delta$ *fad-I* and *radD* derivatives, albeit relative to the *radD* expression levels observed in the mutant background without the presence of a partner strain (Figures 5B and C).

**RadD levels are important for dual- species biofilm formation of *F.***

### ***nucleatum* with *S. gordonii***

Next, we investigated if the elevated levels of RadD affect biofilm development with *S. gordonii*. Consistent with our findings for *S. sanguinis*, *S. gordonii* dual-species biofilms formed with *F. nucleatum* wild-type strains but not the corresponding  $\Delta radD$  mutants are significantly thicker compared to the mono-species biofilms formed by *S. gordonii* alone (Figure 6). Addition of the  $\Delta fad-I$  mutant, in contrast, led to a dramatic increase in dual-species biofilm formation with *S. gordonii*. Single-species biofilms of *S. gordonii* were significantly shallower ( $18.4 \pm 4.03 \mu\text{m}$ ) than the height of *F. nucleatum* and *S. gordonii* dual species biofilms ( $38 \pm 16.6 \mu\text{m}$ ), while the  $\Delta radD$  mutant strain largely failed to integrate into the biofilm, which remained similar in height to those formed by *S. gordonii* alone ( $20.8 \pm 3.27 \mu\text{m}$ ). Biofilms developed with the *F. nucleatum*  $\Delta fad-I$  mutant were significantly taller ( $80.4 \pm 3.27 \mu\text{m}$ ) confirming the importance of RadD in biofilm formation and development.

## Discussion

Countless studies have described bacterial adhesion as an essential process in the development of sessile bacterial communities called biofilms that form to promote the survival of the resident bacteria.<sup>1-7</sup> For many organisms, membership in a biofilm community offers important competitive advantages including protection from harmful challenge,<sup>28</sup> nutrient availability,<sup>29</sup> a broader range of habitats available for colonization,<sup>30</sup> and rapid temporal adaptation to the changing microenvironment.<sup>31</sup> Bacterial attachment occurs in two stages, an initial reversible stage that involves transient interactions, and an irreversible, permanent stage that depends on adhesins responsible for mediating attachment.<sup>32-36</sup> These differences in attachment are a result of the regulation of adhesins, reflecting the importance of adhesin regulation for the survival of bacteria in changing environments.<sup>12-14</sup> Examples of this regulation have been shown in *Staphylococcus aureus* where adhesin expression is globally regulated by a switch in phase variation by a regulatory element<sup>11,12,37</sup> and transcriptional regulation of *Streptococcus pyogenes* genes encoding adhesins by a global transcriptional regulator.<sup>38-41</sup> In addition to this, a recent study reported the dual function of *Vibrio parahaemolyticus* adhesin MAM7, as an adhesin mediating attachment to host cell membrane lipids but also as an effector of host signaling.<sup>42</sup>

The major fusobacterial adhesin, RadD, has an important role in biofilm formation supporting the integration of secondary colonizers<sup>7,15</sup> and is also able to induce apoptosis in human lymphocytes.<sup>16</sup> We report that the gene encoding RadD is regulated on several independent levels. Our comprehensive analysis of the additional genes encoded upstream of *radD* revealed that FAD-I, which has previously been found to

differentially induce human  $\beta$ -defensin 2 (hBD-2) in oral epithelial cells,<sup>18,19</sup> plays a role in regulation of *radD* expression. In contrast to its function in hBD-2 induction that is fusobacterial subspecies dependent, we found FAD-I involvement in transcriptional regulation of *radD* and the resulting effect on binding to and biofilm formation with its partner species *S. gordonii* is similar in both *F. nucleatum* subspecies tested in this study (Figure 2A, 3 and 6). Interestingly, this FAD-I mediated regulation of *radD* expression does not require the presence of a functional RadD adhesin, which suggests an independent pathway for FAD-I action. There appears to be involvement of the Rap and FAD-I proteins in the interaction with *P. gingivalis*, as we observed increased coaggregation phenotypes in the absence of these proteins (Figure 2B). This may suggest a possible coordination between the *radD*-operon and *fap2* expression, as *P. gingivalis* was previously shown to interact with FNN via these two adhesins<sup>7</sup> but further studies are needed to confirm this possibility.

Furthermore, *radD* expression is suppressed for wild-type *F. nucleatum* spp. *nucleatum* and mutant derivatives  $\Delta$ *fad-I* and  $\Delta$ *radD* (Figure 5) in the presence of *S. gordonii* but not *P. gingivalis*. This indicates an additional regulatory mechanism independent of FAD-I and RadD and also provides evidence for the partner specific gene regulation of *radD* in *F. nucleatum*. Enhanced expression of *radD* not only led to increased coaggregation of  $\Delta$ *fad-I* *F. nucleatum* derivatives with *S. gordonii*, but also significantly enhanced dual-species biofilms with *S. gordonii* when compared to wild-type, while the  $\Delta$ *radD* mutant failed to effectively integrate into the biofilm consistent with our previous finding for biofilm formation with *Streptococcus sanguinis*.<sup>15</sup> These findings support an important biological role for tight multi-level regulation of RadD production, since

deregulated *radD* expression severely alters interspecies interaction and biofilm architecture.

Adhesins clearly have a central role in coordinating the development of multispecies biofilms. The regulation of adhesins is therefore critical for the versatility of biofilms to respond to both harmful and beneficial factors affecting the polymicrobial community. Previous studies of *F. nucleatum* strains report variation between strains in the adherence properties to host cells and proteins.<sup>43</sup> This difference in adherence capabilities and the complexity of regulatory mechanisms of adhesins likely reflect the importance of specific expression of adhesins for the survival of bacteria in changing environments. The results presented in this study support the role of FAD-I as a repressor of *radD* expression. We believe that further studies in the identification of additional regulatory mechanisms of fusobacterial adhesins is necessary and will continue to clarify the central role of *F. nucleatum* in health and disease.

**Table 1.** Primers, plasmids and strains used in this study

Purpose	Primer	Sequence (5' to 3')
FNP <i>rapA</i> inactivation	BS975	TTACATGGGGTGGAGGAATCTTCTTAGC
	BS976	ATCGATCCCCGCCGAGCGAAACTCACCTCTCCTTTAATTTCAATAAAATATATAGTATAA
	BS990	GAAATTAAGGAGAGGTGAGTTTCGCTCGGCGGGGATCGAT
	BS991	CTTTTATTTTCATTTTCCCCCTCATTATTAACATTTTATCAATTCCTGCAATTCG
	BS978	CGAATTGCAGGAATTGATAAATAGTTAATAATGAGGGGGAAAAATGAAAATAAAGAAAT
	BS979	TTATTTCTGTTCTTAATGGCACTTGTATTGC
FNP <i>rapB</i> inactivation	BS980	CTATGATGCAATATAAGTTCTCCTTTAATAACCTTAAATATAC
	BS981	ATCGATCCCCGCCGAGCGTTTTCCCTCACTATCTTATTTTTGAATTTTC
	BS992	TAAAGATAGTGAGGGGAAAAACGCTCGGCGGGGATCGAT
	BS993	CTTTTTCAAATTTTCCCTCCCTTTATTAACATTTTATCAATTCCTGCAATTCG
	BS982	CGAATTGCAGGAATTGATAAATAGTTAATAAAGGGAGGGGAAAAATTTTGAAAAAG
BS983	GGTGTACCCTTGGTGCTTCTATTATCTTTTG	
FNP <i>radD</i> inactivation	BS1000	GCGGCTGAATTCCTGGAACAGGAATGTATTTAACAGGTAACAGC
	BS1001	GCGGAGGGATCCCATTAGCTGCTTTATTATATCCAGATTTTGTATAAATACC
FNP CIC	BS971	GCAGAATATGAAGATCTAGTAAAAGAAGAAGC
	BS969	TTATTTTATTCCTGCATTATTTAATTCCTCTAATTTTTG
	BS972	CGCTCGGCGGGGATCGAT
	BS936	TAACTATTTATCAATTCCTGCAATTCG
	BS937	TAAAGGGGGGAAAAATATGAAAGACT
	BS938	AATTGAGATATCAATCCATTATTTCCAGTTAC
FNP <i>fad-I*</i>	BS1053	GGAGGGGAAAAATTAATAAAAGATATTACTACTATTATTATC
	BS1054	CTTTATTTTCTTCTGTAATATTTTTTAAAGCTTCTTCAACTTG
FNN $\Delta$ <i>fad-I radD*</i>	BS939	GCGCTGGTACCATAAATTTTATTTTCGAGAGACAAAAGCATT
	BS940	ATCGATCCCCGCCGAGCGCAAATTTTTCCCTCCCTTTATTTTTCT
	BS941	AGAAAAATAAAGGGAGGGAAAAAATTTGCGCTCGGCGGGGATCGAT
	BS942	ACTTTATTATAGTCTTCATATTTTCCCTCTTATTAACATTTTATCAATTCCTGCAATTCG
	BS943	CGAATTGCAGGAATTGATAAATAGTTAATAAAGGGGGAAAAATATGAAGACTATAATAAAGT
	BS944	GGCCGAGCTCGAGTGGTGTA AACCTGCTGGTGTAGCA
qPCR	BS1035	GGCAAGTGATGAAATTTTCAGAGTTAAAAGG
	BS1036	GCTTTTAATTCAGCCAGTTTAAATTTTTGAGCTG
	BS1037	ATTATGAAGAATTAGATAAGAAAAAAGAAAAAGAAC
	BS1038	CATATTATCTATTTTTTCTTTTCTTTTATCTACTTTATATTTAAG
	BS947	TCAAGACTTTTAAAAGAAGCTGATAAGAAAAAAG
	BS948	TTATTTCCCTCTTGTCTTCTTTATGTG
	BS1066	GGATTATCTTTGCTAATTGGGGAATTATAG
	BS1067	ACTATTCCATATTCTCCATAATATTTCCATTAGA
	BS945	CAAAAACCTATTGAAAGACTTGATTTTGA
	BS946	GAATGCTAATTCAAATCCTTTTTCTTCCCT
FNN <i>rapA</i> inactivation	Aup_F	GAGAAAAATAAATTTGAAATA
	Aup_R	ATCCCCGCCGAGCGAAATATTTCCAATAGATAATAAAACAAATAATGTTAAAATAACTTT
	Acat_F	GTTTTATTATCTATTGGAATATTTTCGCTCGGCGGGGATCG
	Acat_R	TAACTATTTATCAATTCCTGCA
	Adown_F	GGAATTGATAAATAGTTAATGAGGGGGAAAAATGAAAATAAAGAAAT
Adown_R	CTTGTCTTTATTTCTGTTCTTAATGGCACTTG	
FNN <i>rapB</i> inactivation	Bup_F	CTGTTGCTATTGATATTGGTTTCCCAGC
	Bup_R	CGATCCCCGCCGAGCGTTTTCCCTCACTATCTTATTTTTGAATT
	Bcat_F	AATTCAAAAATAAGATAGTGAGGGGGAAAAACGCTCGGCGGGGATCG
	Bcat_R	CAAATTTTTCCCTCCCTTAACTATTTATCAATTCCTGCAATTCGTTTAC
	Bdown_F	GAATTGATAAATAGTTAAGGGGAGGGAAAAAATTTGAAAAAATATTATTAC
	Bdown_R	CTGTTTTTCAATTATTGTTTTTCAATTACTGC
FNN <i>fad-I</i> inactivation	Cup_F	CTAAAAATATACTAATAATTTTATATTTTCGAGAGACAAAAGC
	Cup_R	GATCGATCCCCGCCGAGCGATTTTTCCCTCCCTTTATTTTTCTTCTGTG
	Ccat_F	CACAGAAGAAAAATAAAGGGAGGGAAAAATCGCTCGGCGGGGATCGATC
	Ccat_R	CTTTTCATTTTTCCCTCCTTAACTATTTTATCAATTCCTGCAATTCGTTTAC
	Cdown_F	GAATTGATAAATAGTTAAGAGGGGGAAAAATATGAAAGACTATAATAAAGTAGAAA
	Cdown_R	GAGATTTGTGAAATCGCTCCTTTATTTC
FNN CIC	CICup_F	GGCTGAATTAAGCAAGCATTGAAGA
	CICup_R	GATCCCCGCCGAGCGTTATTTTTATTCTGCATTATTTAATTCTTCTAATTTTTG
	CICcat_F	ATAATGCAGGAATAAATAACGCTCGGCGGGGATCG
	Ccat_R	CTTTTCATTTTTCCCTCCTTAACTATTTTATCAATTCCTGCAATTCGTTTAC
	Cdown_F	GAATTGATAAATAGTTAAGAGGGGGAAAAATATGAAAGACTATAATAAAGTAGAAA
	Cdown_R	GAGATTTGTGAAATCGCTCCTTTATTTC

Plasmid	Description	Purpose	Source
pJET1.2	Blunt Cloning Vector, Amp <sup>R</sup>	Cloning	Thermo Scientific
pJP237A	pJET1.2 with 23726 <i>radA</i> ' inserted	Gene Inactivation Plasmid	This study
pJP237B	pJET1.2 with 23726 <i>radB</i> ' inserted	Gene Inactivation Plasmid	This study
pJP237C	pJET1.2 with 23726 <i>radC</i> ' inserted	Gene Inactivation Plasmid	This study
pJP2CIC	pJET1.2 with 23726 <i>radC::catP</i> inserted	Insertion analysis	This study

Bacterial strains	Relevant characteristics	Source
<i>F. nucleatum</i>		
ATCC 23726	<i>ssp. nucleatum</i>	ATCC
$\Delta radA$	ATCC 23726 $\Delta radA::pJP237A$	This study
$\Delta radB$	ATCC 23726 $\Delta radA::pJP237B$	This study
$\Delta radC$	ATCC 23726 $\Delta radA::pJP237C$	This study
$\Delta radD$	ATCC 23726 inactivated <i>radD</i>	Kaplan <i>et al.</i> (2009)
CIC	ATCC 23726 <i>catP</i> inserted after <i>radC</i>	This study
ATCC 10953	<i>ssp. polymorphum</i>	ATCC
$\Delta radA$	ATCC 10953 $\Delta radA::p$	This study
$\Delta radB$	ATCC 10953 $\Delta radB::p$	This study
$\Delta radC$	ATCC 10953 $\Delta radC::p$	This study
$\Delta radD$	ATCC 10953 $\Delta radD::p$	This study
<i>radC</i> *	ATCC 10953 <i>radC</i> with mutated translation start site	This study
CIC	ATCC 10953 <i>catP</i> inserted after <i>radC</i>	This study
<i>E. coli</i>		
OneShot TOP10		Thermo Fisher
Other		
<i>Streptococcus gordonii</i>	ATCC 10558	ATCC
<i>Porphyromonas gingivalis</i>	4612	Lamont <i>et al.</i> (1992)

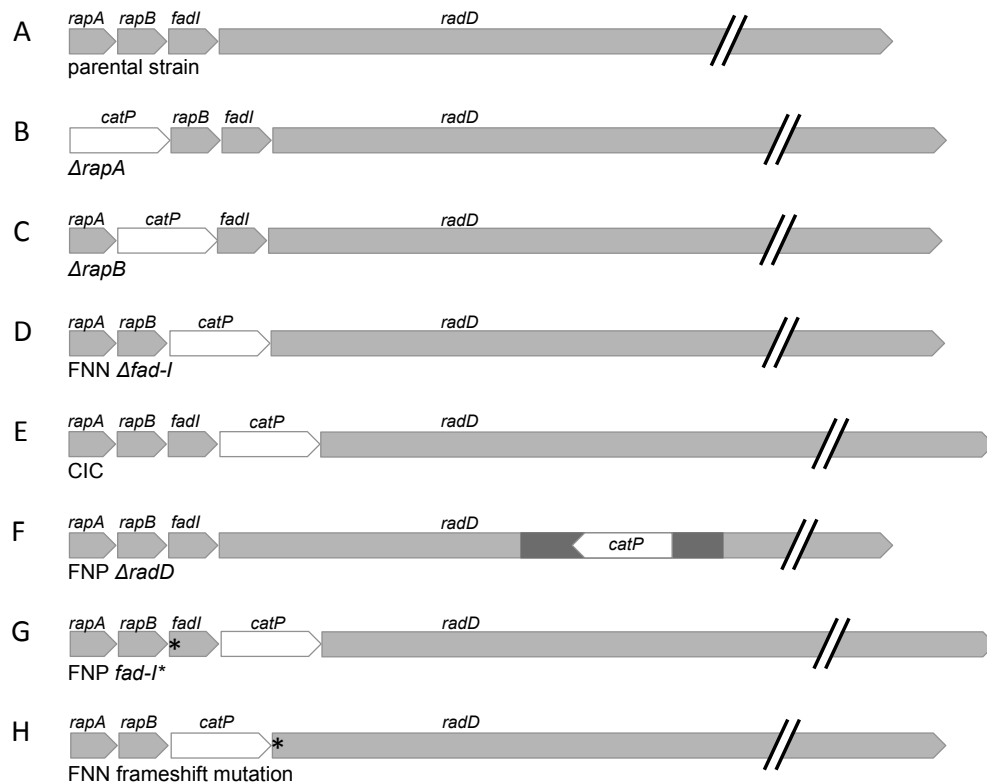


**Figure 1.** Schematic representation of gene inactivation mutants and controls (A) parental strain, (B)  $\Delta rapA$ , (C)  $\Delta rapB$ , (D) FNN  $\Delta fad-I$ , (E) *catP* insertion control (CIC), (F) FNP  $\Delta radD$ , (G) FNP mutated translation start site, *fad-I\**, (H) FNN *radD* frameshift mutation in  $\Delta fad-I$  background,  $\Delta fad-I radD^*$

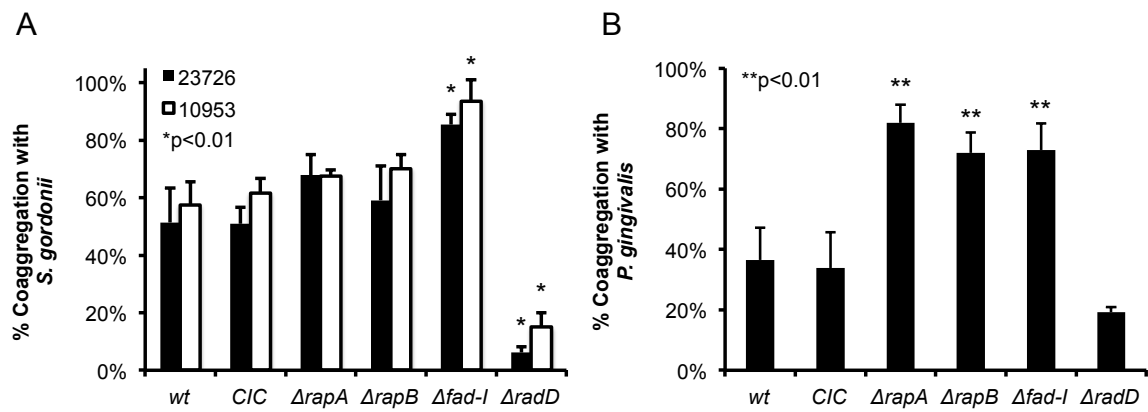


**Figure 2.** Coaggregation of mutants with partner strains

Quantitative coaggregation assay  $\Delta rapA$ ,  $\Delta rapB$ ,  $\Delta fad-I$ , and  $\Delta radD$  (A) in FNN and FNP with *S. gordonii* or (B) FNN with *P. gingivalis*

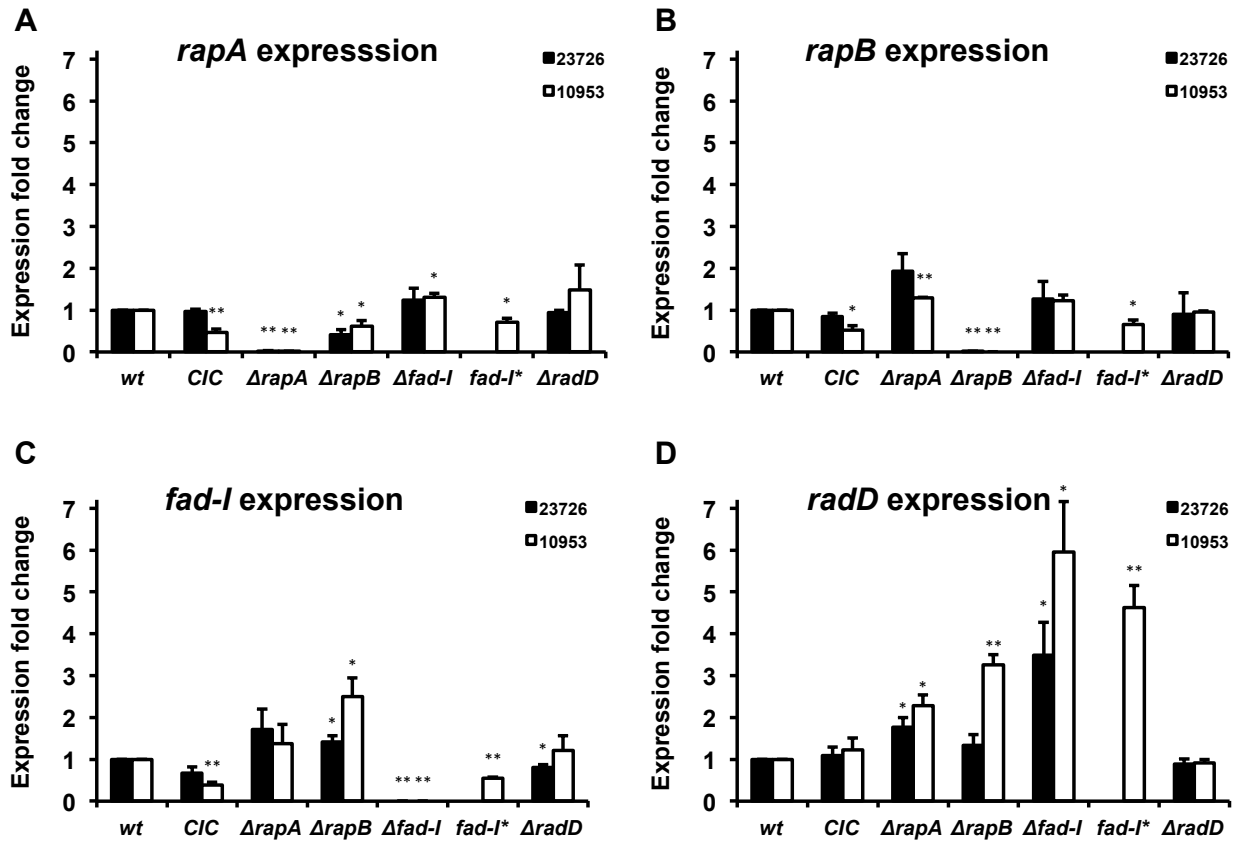


**Figure 3.** Transcriptional analysis of *radD*-operon genes in wild-type FNN and FNP and mutant derivatives. Transcriptional levels of (A) *rapA*, (B) *rapB*, (C) *fad-I*, and (D) *radD* are shown for wild-type and mutant derivatives

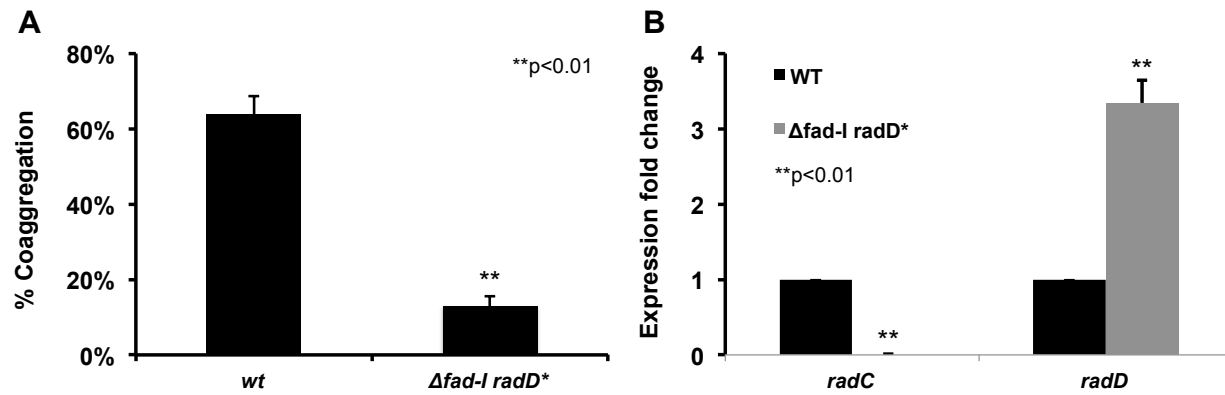


**Figure 4.** Coaggregation and transcriptional analysis of FNN  $\Delta fad-I radD^*$  (A) Coaggregation of FNN wild-type and  $\Delta fad-I radD^*$  with *S. gordonii*. (B) *radD* transcript levels in FNN wild-type and  $\Delta fad-I radD^*$

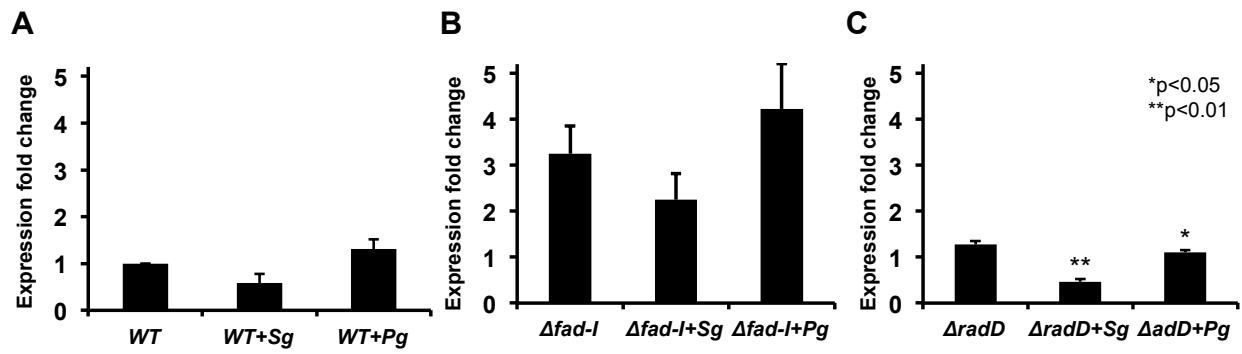


**Figure 5.** Transcriptional analysis of *radD* levels in the presence of partner strains  
 Transcriptional analysis of *radD* levels in (A) wild-type FNN, (B) FNN  $\Delta fad-I$ , or (C)  $\Delta radD$ , alone or in the presence of partner species

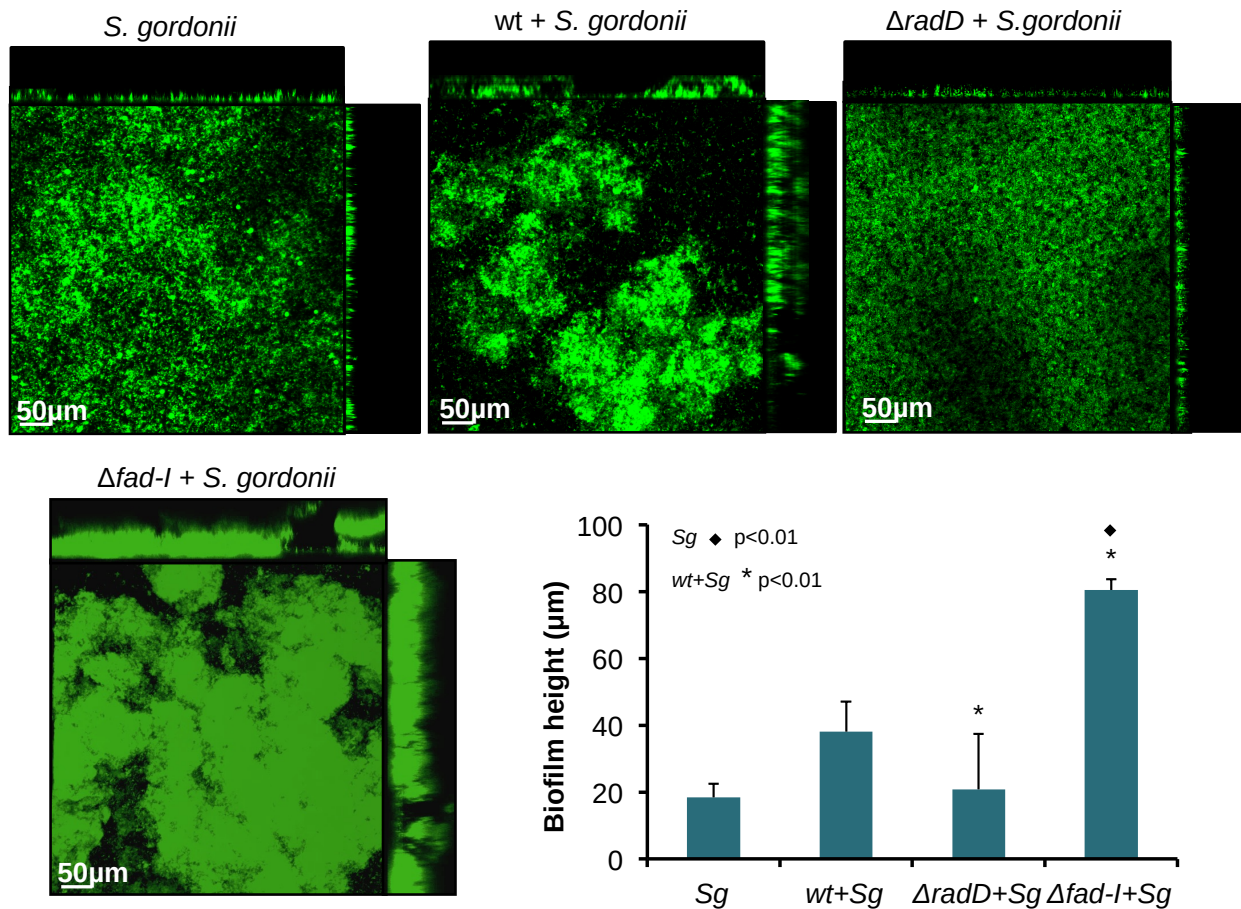


**Figure 6.** Biofilm growth comparison of FNN wild-type, FNN  $\Delta fad-I$ , or FNN  $\Delta radD$  with *S. gordonii*. Representative biofilm images of FNN and mutant derivatives and *S.gordonii* after 20h as visualized by CSLM. Asterisk indicates statistical significance when compared to dual species biofilms of FNN wild-type with *S. gordonii*. Diamond indicates statistical significance when compared to *S. gordonii* single-species biofilm.

## References

1. Drago L, Gismondo MR, Lombardi A, de Haën C, Gozzini L. Inhibition of in vitro growth of enteropathogens by new *Lactobacillus* isolates of human intestinal origin. *FEMS Microbiol Lett.* 1997;153(2):455-463. <http://www.ncbi.nlm.nih.gov/pubmed/9271875>. Accessed July 18, 2016.
2. Soto SM, Soto SM. Importance of Biofilms in Urinary Tract Infections: New Therapeutic Approaches. *Adv Biol.* 2014;2014:1-13. doi:10.1155/2014/543974.
3. Rickard AH, Gilbert P, High NJ, Kolenbrander PE, Handley PS. Bacterial coaggregation: An integral process in the development of multi-species biofilms. *Trends Microbiol.* 2003;11(2):94-100. doi:10.1016/S0966-842X(02)00034-3.
4. Katharios-Lanwermeyer S, Xi C, Jakubovics NS, Rickard a H. Mini-review: Microbial coaggregation: ubiquity and implications for biofilm development. *Biofouling.* 2014;30(10):1235-1251. doi:10.1080/08927014.2014.976206.
5. Foster JS, Kolenbrander PE. Development of a multispecies oral bacterial community in a saliva-conditioned flow cell. *Appl Environ Microbiol.* 2004;70(7):4340-4348. doi:10.1128/AEM.70.7.4340-4348.2004.
6. Rosen G, Sela MN. Coaggregation of *Porphyromonas gingivalis* and *Fusobacterium nucleatum* PK 1594 is mediated by capsular polysaccharide and lipopolysaccharide. *FEMS Microbiol Lett.* 2006;256(2):304-310. doi:10.1111/j.1574-6968.2006.00131.x.
7. Park J, Shokeen B, Haake S, Lux R. Characterization of *Fusobacterium nuclatum* ATCC 23726 Adhesins Involved in Strain-Specific Attachment to *Porphyromonas gingivalis*. *Int J Oral Sci.* 2016;(In Press).
8. Paharik AE, Horswill AR. The Staphylococcal Biofilm: Adhesins, Regulation, and Host Response. *Microbiol Spectr.* 2016;4(2). doi:10.1128/microbiolspec.VMBF-0022-2015.
9. Irie Y, Mattoo S, Yuk MH. The Bvg virulence control system regulates biofilm formation in *Bordetella bronchiseptica*. *J Bacteriol.* 2004;186(17):5692-5698. doi:10.1128/JB.186.17.5692-5698.2004.
10. Arciola CR, Campoccia D, Ravaioli S, Montanaro L. Polysaccharide intercellular adhesin in biofilm: structural and regulatory aspects. *Front Cell Infect Microbiol.* 2015;5(February):7. doi:10.3389/fcimb.2015.00007.
11. Ofek I, Hasty DL, Doyle RJ. Adhesins as Bacterial Cell Surface Structures: General Concepts of Structure, Biogenesis, and Regulation. In: *Bacterial Adhesion to Animal Cells and Tissues*. American Society of Microbiology; 2003:63-96. doi:10.1128/9781555817800.ch4.

12. Arvidson S, Tegmark K. Regulation of virulence determinants in *Staphylococcus aureus*. *Int J Med Microbiol*. 2001;291(2):159-170. doi:10.1078/1438-4221-00112.
13. Cheung AL, Zhang G. Global regulation of virulence determinants in *Staphylococcus aureus* by the SarA protein family. *Front Biosci*. 2002;7:d1825-d1842. <http://www.ncbi.nlm.nih.gov/pubmed/12133812>. Accessed July 18, 2016.
14. Blomfield I, van der Woude M. Regulation and function of phase variation in *Escherichia coli*. In: *Bacterial Adhesion to Host Tissues: Mechanisms and Consequences*. Advances in Molecular and Cellular Microbiology. Cambridge University Press; 2002:89-144. <http://dx.doi.org/10.1017/CBO9780511541575.005>. Accessed July 18, 2016.
15. Kaplan CW, Lux R, Haake SK, Shi W. The *Fusobacterium nucleatum* outer membrane protein RadD is an arginine-inhibitable adhesin required for inter-species adherence and the structured architecture of multispecies biofilm. *Mol Microbiol*. 2009;71(1):35-47. doi:10.1111/j.1365-2958.2008.06503.x.
16. Kaplan CW, Ma X, Paranjpe A, et al. *Fusobacterium nucleatum* outer membrane proteins Fap2 and RadD induce cell death in human lymphocytes. *Infect Immun*. 2010;78(11):4773-4778. doi:10.1128/IAI.00567-10.
17. Altschul SF, Gish W, Miller W, Myers EW, Lipman DJ. Basic local alignment search tool. *J Mol Biol*. 1990;215(3):403-410. doi:10.1016/S0022-2836(05)80360-2.
18. Gupta S, Ghosh SK, Scott ME, et al. *Fusobacterium nucleatum*-associated beta-defensin inducer (FAD-I): identification, isolation, and functional evaluation. *J Biol Chem*. 2010;285(47):36523-36531. doi:10.1074/jbc.M110.133140.
19. Bhattacharyya S, Ghosh SK, Shokeen B, et al. FAD-I, a *Fusobacterium nucleatum* Cell Wall-Associated Diacylated Lipoprotein That Mediates Human Beta Defensin 2 Induction through Toll-Like Receptor-1/2 (TLR-1/2) and TLR-2/6. *Infect Immun*. 2016;84(5):1446-1456. doi:10.1128/IAI.01311-15.
20. Lamont RJ, Hersey SG, Rosan B. Characterization of the adherence of *Porphyromonas gingivalis* to oral streptococci. *Oral Microbiol Immunol*. 1992;7(4):193-197. doi:10.1111/j.1399-302X.1992.tb00024.x.
21. White JC, Niven CF. Streptococcus S.B.E.: A Streptococcus Associated with Subacute Bacterial Endocarditis. *J Bacteriol*. 1946;51(6):717-722. <http://www.ncbi.nlm.nih.gov/pubmed/16561124>. Accessed July 18, 2016.
22. Shevchuk NA, Bryksin A V, Nusinovich YA, Cabello FC, Sutherland M, Ladisch S. Construction of long DNA molecules using long PCR-based fusion of several fragments simultaneously. *Nucleic Acids Res*. 2004;32(2):e19. doi:10.1093/nar/gnh014.

23. Kinder Haake S, Yoder S, Hunt Gerardo S. Efficient gene transfer and targeted mutagenesis in *Fusobacterium nucleatum*. *Plasmid*. 2006;55(1):27-38. doi:10.1016/j.plasmid.2005.06.002.
24. Haake SK, Yoder SC, Attarian G, Podkaminer K. Native plasmids of *Fusobacterium nucleatum*: characterization and use in development of genetic systems. *J Bacteriol*. 2000;182(4):1176-1180. <http://www.ncbi.nlm.nih.gov/pubmed/10648549>. Accessed July 18, 2016.
25. Kaplan CW, Lux R, Huynh T, Jewett A, Shi W, Haake SK. *Fusobacterium nucleatum* apoptosis-inducing outer membrane protein. *J Dent Res*. 2005;84(8):700-704. <http://www.ncbi.nlm.nih.gov/pubmed/16040725>. Accessed July 18, 2016.
26. Tian Y, He X, Torralba M, et al. Using DGGE profiling to develop a novel culture medium suitable for oral microbial communities. *Mol Oral Microbiol*. 2010;25(5):357-367. doi:10.1111/j.2041-1014.2010.00585.x.
27. de Avila ED, Lima BP, Sekiya T, et al. Effect of UV-photofunctionalization on oral bacterial attachment and biofilm formation to titanium implant material. *Biomaterials*. 2015;67:84-92. doi:10.1016/j.biomaterials.2015.07.030.
28. Goldberg J, Drenkard E, Ausubel FM. Biofilms and antibiotic resistance: a genetic linkage. *Trends Microbiol*. 2002;10(6):264. doi:10.1016/S0966-842X(02)02381-8.
29. O'Toole G, Kaplan HB, Kolter R. Biofilm Formation as Microbial Development. <http://dx.doi.org/101146/annurev.micro54149>. 2003.
30. Jefferson KK. What drives bacteria to produce a biofilm? *FEMS Microbiol Lett*. 2004;236(2):163-173. doi:10.1016/j.femsle.2004.06.005.
31. Kjelleberg S, Molin S. Is there a role for quorum sensing signals in bacterial biofilms? *Curr Opin Microbiol*. 2002;5(3):254-258. doi:10.1016/S1369-5274(02)00325-9.
32. van Loosdrecht MCM, Norde W, Lyklema J, Zehnder AJB. Hydrophobic and electrostatic parameters in bacterial adhesion. *Aquat Sci*. 1990;52(1):103-114. doi:10.1007/BF00878244.
33. Van Dellen KL, Houot L, Watnick PI. Genetic analysis of *Vibrio cholerae* monolayer formation reveals a key role for DeltaPsi in the transition to permanent attachment. *J Bacteriol*. 2008;190(24):8185-8196. doi:10.1128/JB.00948-08.
34. Agladze K, Wang X, Romeo T. Spatial periodicity of *Escherichia coli* K-12 biofilm microstructure initiates during a reversible, polar attachment phase of development and requires the polysaccharide adhesin PGA. *J Bacteriol*. 2005;187(24):8237-8246. doi:10.1128/JB.187.24.8237-8246.2005.

35. Beloin C, Houry A, Froment M, Ghigo J-M, Henry N. A short-time scale colloidal system reveals early bacterial adhesion dynamics. *PLoS Biol.* 2008;6(7):e167. doi:10.1371/journal.pbio.0060167.
36. Otto M. Staphylococcal biofilms. *Curr Top Microbiol Immunol.* 2008;322:207-228. <http://www.ncbi.nlm.nih.gov/pubmed/18453278>. Accessed July 18, 2016.
37. Balaban N, Goldkorn T, Gov Y, et al. Regulation of *Staphylococcus aureus* pathogenesis via target of RNAIII-activating Protein (TRAP). *J Biol Chem.* 2001;276(4):2658-2667. <http://www.ncbi.nlm.nih.gov/pubmed/11160124>. Accessed July 18, 2016.
38. McIver KS, Thurman AS, Scott JR. Regulation of *mga* transcription in the group A streptococcus: specific binding of *mga* within its own promoter and evidence for a negative regulator. *J Bacteriol.* 1999;181(17):5373-5383. <http://www.ncbi.nlm.nih.gov/pubmed/10464209>. Accessed July 18, 2016.
39. McIver KS, Scott JR. Role of *mga* in growth phase regulation of virulence genes of the group A streptococcus. *J Bacteriol.* 1997;179(16):5178-5187. <http://www.ncbi.nlm.nih.gov/pubmed/9260962>. Accessed July 18, 2016.
40. Chaussee MS, Watson RO, Smoot JC, Musser JM. Identification of Rgg-regulated exoproteins of *Streptococcus pyogenes*. *Infect Immun.* 2001;69(2):822-831. doi:10.1128/IAI.69.2.822-831.2001.
41. Chaussee MS, Sylva GL, Sturdevant DE, et al. Rgg influences the expression of multiple regulatory loci to coregulate virulence factor expression in *Streptococcus pyogenes*. *Infect Immun.* 2002;70(2):762-770. <http://www.ncbi.nlm.nih.gov/pubmed/11796609>. Accessed July 18, 2016.
42. Stones DH, Krachler AM. Dual function of a bacterial protein as an adhesin and extracellular effector of host GTPase signaling. *Small GTPases.* 2015;6(3):153-156. doi:10.1080/21541248.2015.1028609.
43. Xie H, Gibbons RJ, Hay DI. Adhesive properties of strains of *Fusobacterium nucleatum* of the subspecies *nucleatum*, *vincentii* and *polymorphum*. *Oral Microbiol Immunol.* 1991;6(5):257-263. <http://www.ncbi.nlm.nih.gov/pubmed/1820561>. Accessed July 18, 2016.

**Chapter 3: Contact-Dependent Gene Expression Profile of *F. nucleatum* During  
Interaction With Partner Species**

## Abstract

The oral cavity is home to a plethora of bacterial species mostly residing in biofilm communities, which form as a result of intimate physical contact between bacterial species resulting in spatial organization. One prominent member of the oral microbiota is *Fusobacterium nucleatum*, a Gram-negative opportunistic pathogen that is indigenous to the human oral cavity. Due to its ability to adhere to a wide range of species present in the oral microbial community, *F. nucleatum* has often been described as a “bridging organism” that acts to bring together species that do not otherwise interact with each other and thus is important in oral biofilm architecture.<sup>1,2</sup> While bacterial adhesins are known to mediate physical interaction during coaggregation<sup>3,4</sup>, not much is known with regard to their role in transcriptional regulation. In this study, we provide evidence for adhesin-dependent regulation of *F. nucleatum* when in contact with *Streptococcus sanguinis*, an early oral colonizer and *Porphyromonas gingivalis*, a late colonizer, using RNA-Seq, a powerful tool for transcriptional profiling using deep-sequencing technology. *F. nucleatum* was co-incubated with *S. sanguinis* or *P. gingivalis* and RNA-Seq analysis was performed on extracted RNA. Partner-specific responses were observed suggesting *F. nucleatum* can differentially regulate its genes based on contact with neighboring species. Furthermore, we identified a subset of genes that is regulated based on the adhesin used for attachment and the interacting partner. *F. nucleatum* appears to have overlapping responses between the different partner species we tested however, it is evident that its response is affected by the type of partner species as well as adhesin involved.

## Introduction

The study of multispecies microbial communities has uncovered ecological niches where numerous bacterial species exist and interact functionally. One biofilm community of increasing interest has been the human oral microbiota, home to more than 700 bacterial species. Biofilm growth begins with initial surface attachment of early colonizers that act as a foundation for colonization by other bacteria, intermediate and late colonizers, to develop a microbial community.<sup>5</sup> Polymicrobial oral biofilms mature as a result of intimate physical contact between bacterial species, allowing for communication and adaptation as a community. There have been extensive studies on the mechanism of cell-to-cell binding through in vitro coaggregation assays as well as growth of dual species biofilms to obtain a snapshot view of the interaction of partner species in the process of biofilm maturation.

Given its remarkable ability to attach to both early and late colonizers in the oral biofilm, *Fusobacterium nucleatum* has been commonly referred to as a “bridging organism” regarding its central role in developing and supporting oral biofilm architecture. With such a critical role in oral biofilms, it is an obvious candidate to examine its capacity beyond its structural role. We are interested in determining if and how *F. nucleatum* controls community membership, how it contributes to the overall fitness of the community, if it plays a part in responding to environmental challenges, and importantly, how it aids in biofilm virulence.

We have found that binding capacity and variability in *F. nucleatum* might be a result of

adhesins specificity depending on the partner species and strain.<sup>3,6</sup> Initial studies in *F. nucleatum* contact-dependent gene expression reveal different response patterns to specific partner species identifying numerous genes that may be relevant in interspecies communication and cooperation.<sup>7</sup> Additionally, differential gene expression were observed in *F. nucleatum* when in contact with *Streptococcus sanguinis*, and found to be mediated by the RadD adhesin.<sup>8</sup>

Studies in other pathogenic bacteria have shown that adhesins can act as bacterial mechanosensors to regulate virulence,<sup>9,10</sup> have direct involvement in the induction of signaling pathways,<sup>11</sup> and play major roles in quorum-sensing for biofilm formation and virulence.<sup>6,12</sup> The goal of this study is to provide a more in-depth look into contact-dependent regulation of *F. nucleatum*, specifically how adhesins play a role in the regulation of gene expression.

## Materials and Methods

### Bacterial Strains and Culture Conditions

*F. nucleatum* ssp. *nucleatum* strain ATCC 23726, and respective mutant derivatives described previously<sup>6</sup> as well as *P. gingivalis* strains 4612<sup>13</sup>, T22<sup>14</sup>, ATCC 33277<sup>15</sup> were maintained on Columbia agar supplemented with 5% sheep blood or in Columbia broth (Difco, Detroit, MI) under anaerobic conditions (10% H<sub>2</sub>, 10% CO<sub>2</sub>, 80% N<sub>2</sub>) at 37°C. All media for *P. gingivalis* were supplemented with hemin at 5 µg ml<sup>-1</sup> and menadione at 1 µg ml<sup>-1</sup>. *S. sanguinis* was maintained on Todd Hewitt agar or Todd Hewitt broth (Difco, Detroit, MI) under anaerobic conditions (10% H<sub>2</sub>, 10% CO<sub>2</sub>, 80% N<sub>2</sub>) at 37°C.

### Co-incubation of *F. nucleatum* with partner species

Cells were grown to stationary phase and 1ml of *F. nucleatum* ATCC 23726 or mutant derivative calculated to a concentration of OD<sub>600</sub> 1 was added to sterile 15ml conical tubes with either 1ml (OD<sub>600</sub> 1) of *S. sanguinis* or *P. gingivalis* cells. Control tubes contained 1ml (OD<sub>600</sub> 1) of *F. nucleatum* ATCC 23726 or mutant derivative alone. Cells were centrifuged for 5 min at 4600 x g and supernatant was decanted, and replaced with 1ml of CB for *F. nucleatum* alone tubes, 2ml of CB for tubes with *F. nucleatum* and *S. sanguinis*, or 2ml of CB supplemented with hemin (5 µg ml<sup>-1</sup>) and menadione (1 µg ml<sup>-1</sup>) for tubes with *F. nucleatum* and *P. gingivalis*. Tubes were centrifuged again for 3 min followed by anaerobic incubation (10% H<sub>2</sub>, 10% CO<sub>2</sub>, 80% N<sub>2</sub>) at 37°C for 3 hours. Cells were collected after incubation, pelleted and stored in - 80°C for at least 24 hours prior to RNA extraction.

## **mRNA isolation and sequencing**

Isolation and sequencing was performed using the same protocol from a previously published study.<sup>16</sup> Briefly, total RNA extraction and purification was performed using the mirVana RNA extraction kit (Life Technologies) and the RNA Clean/Concentrator™ kit (Zymo Research, Irvine, CA). DNA was removed from the samples by adding 1µl (2U) Turbo™ DNase (Life Technologies) and incubating samples at 37 °C for 30min. After DNA removal, 16S rDNA PCR was performed using the same protocol and primers as previously described<sup>17</sup> to verify that DNA was removed. To remove rRNA in total RNA extracts the RiboZero™ Magnetic Kit (Epicenter) was used according to manufacturer's instruction. mRNA was purified by using the Zymo RNA Clean and Concentrator™ kit (Zymo Research). RNA concentration and integrity was analyzed before and after rRNA removal by using the Agilent RNA 6000 Nano Kit (Agilent Technologies, Inc. Santa Clara, CA) and the Agilent RNA 6000 Pico Kit (Agilent Technologies), respectively. cDNA library from rRNA-depleted RNA was generated by using random-primed cDNA synthesis methods according to the ScriptSeq™ v2 RNA-Seq Library Preparation Protocol (Epicenter). Prior to second strand cDNA synthesis the di-tagged cDNA was purified using the Agencourt AMPure XP system (Beckman Coulter). Index-reads supplied with the ScriptSeq Kit were added to the libraries that were PCR amplified for 15 cycles. RNA-Seq libraries were purified and quantified by using the Agencourt AMPure XP system (Beckman Coulter) and the Agilent DNA 1000 protocol (Agilent Technologies), respectively. Sequencing of cDNA libraries was performed by using an Illumina HiSeq 2000 platform (100bp paired end reads) which has the capacity of 19GB per lane providing high coverage of reads. Sequencing was carried out at the JCVI

sequencing facility JTC. cDNA sample concentrations were normalized at JTC prior to sequencing. Using each sample's individual barcodes, the Illumina data was deconvolved into the respective samples. After trimming the bar codes, low-quality and short sequences (<100bp) were removed by using the CLC Genomics Workbench Software (CLCbio, Aarhus, Denmark). The following CLC-parameters were applied during paired read sequence trimming and quality control: quality score setting: NCBI/Sanger or Illumina Pipeline 1.8 and later, minimum distance: 180, maximum distance: 250.

### **Read mapping of raw cDNA reads onto *F. nucleatum* ATCC 23726 genome**

Read mapping for *F. nucleatum* 23726 genome was carried out similarly to a protocol used in a previously published study.<sup>16</sup> Expression values for each mRNA sample were generated by BWA mapping<sup>43</sup> of both filtered fragment and paired reads onto the well-annotated reference genome *F. nucleatum* ATCC 23726. Reads were mapped with the default BWA option (96% sequence identity). CLC RNAseq plugin software was used to normalize and determine statistical significance of expression. DESeq, which uses a model based on the negative binomial distribution with variance and mean linked by local regression<sup>18</sup> was also employed to validate the expression observed with good agreement between the methods. Additional investigations of the transcription start sites, co-expressed genes, predicted small RNAs and normalized expression using by upper quartile normalization were performed with Rockhopper<sup>19</sup> and manual curation.

## **Visualization of global metabolic network analysis**

To create visualization using all data sets, iPath2.0: Interactive Pathway Explorer<sup>20</sup> was used to generate metabolic and regulatory pathway maps. Clusters of Orthologous Groups (COG) numbers were used as input.<sup>21</sup>

## **Quantitative (Real-Time) Polymerase Chain Reaction**

Gene specific primers were used to amplify transcript regions for signal detection by qPCR on iCycler Thermal Cycler (Bio-Rad, Hercules, CA) in a total volume of 20  $\mu$ l containing 2  $\mu$ l of 10x iQ SYBR Green Supermix (Bio-Rad, Hercules, CA), 0.5  $\mu$ M each of forward and reverse primers, 7  $\mu$ l of Millipore water and 1  $\mu$ l of template. Primer sets were designed for each gene of interest in homologous regions of the corresponding open reading frames in *F. nucleatum* ssp. *nucleatum* ATCC 23726. Amplification and detection were carried out in 96-well optical plates (Thermo Fisher Scientific, Waltham, MA). Each PCR run was carried out with an initial incubation of 10 min at 95°C followed by 40 cycles of denaturing at 95°C for 15 sec; annealing and elongation at 60°C for 1 min. After the 40 cycles of amplification, an additional denaturing step was performed at 95°C for 1 min followed by annealing and elongation at 60°C for 1 min. A melting curve analysis was completed after each run. The DNA concentrations ( $\text{ng ml}^{-1}$ ) were calculated with standard curves obtained by tenfold serial dilutions of bacterial genomic DNA. All standards were run in duplicate to generate a standard curve to determine the efficiency of each primer set. Three independent qPCR runs were performed with three technical replicates for each sample to assess reproducibility and inter-run variability.

Following amplification, relative expression levels between samples were calculated as fold changes normalized to *rpoB* reference gene amplification.

## Results

Previous studies have shown that *F. nucleatum* adheres well to *S. sanguinis*<sup>6</sup> and *P. gingivalis* in a specific adhesin-dependent manner and that gene regulation occurs in response to the presence of *S. sanguinis* when they are coincubated.<sup>7,8</sup> Our goal was to investigate the involvement of adhesins in the transcriptional changes in *F. nucleatum* in response to partner species. To accomplish this, transcriptome analysis was performed for *F. nucleatum* as well as a RadD adhesin deficient *F. nucleatum* mutant when in contact with the gram-positive health-associated *S. sanguinis* (FnSs and  $\Delta$ DSs, respectively). Furthermore, we evaluated the transcriptional changes of *F. nucleatum* during interaction with different strains of the gram-negative disease-associated *P. gingivalis* (FnPg) that attach via different fusobacterial adhesins.

### Expression profile of *F. nucleatum* with *S. sanguinis*

RNAseq analysis of the *F. nucleatum* transcriptome from the FnSs sample revealed the upregulation of 303 genes that were above a two-fold threshold and the downregulation of 345 genes below negative two-fold (Figure 1). Together, this represents about 31% of the 2067 predicted open reading frames (ORF) in *F. nucleatum*.<sup>22</sup> Pathway mapping of regulated genes revealed a number of metabolic and regulatory pathways that were differentially transcribed in *F. nucleatum* upon contact with *S. sanguinis* (Figures 2 and 3). A general induction was observed in several pathways involved in the metabolism of cofactors and vitamins (ie. thiamine metabolism), nucleotide metabolism (ie. ascorbate and aldarate metabolism, puromycin biosynthesis) and carbohydrate metabolism pathways including inositol phosphate and pyruvate metabolism in *F. nucleatum*.

Downregulated pathways included metabolism of amino acids, including arginine, proline, valine, leucine and isoleucine biosynthesis, and D-glutamine and D-glutamate metabolism. Another pathway that was generally repressed was the glycolysis/gluconeogenesis pathway. Fatty acid biosynthesis and metabolism pathways were also downregulated. We also observed the induction of translation pathways, including ribosome and aminoacyl-tRNA biosynthesis and ABC transporter pathways. Transcription pathways involving RNA polymerase were also generally induced. Membrane transport pathways, namely, the phosphotransferase system (PTS) were generally repressed.

### **Expression profile of *F. nucleatum* with *P. gingivalis***

We also investigated the response of *F. nucleatum* to three different strains of the gram-negative periodontopathogen *P. gingivalis*, since they are known to coaggregate with each other and are frequently isolated together from several chronic immunoinflammatory diseases of the oral cavity.<sup>23-25</sup> RNAseq analysis revealed the upregulation of 405 genes (over two-fold) and the downregulation of 424 genes below negative two-fold (Figure 1), representing about 40% of the 2067 ORFs in *F. nucleatum*. Regulated genes were mapped on metabolic and regulatory pathways maps and revealed regulation of a number of pathways (Figures 4 and 5). In general, lipid metabolism (ie. fatty acid metabolism), carbohydrate metabolism (ie. fructose, mannose, amino sugar, and nucleotide sugar metabolism), amino acid and energy metabolism (ie. alanine, aspartate and glutamate metabolism), and nucleotide metabolism (ie. purine, ascorbate and aldarate metabolism) were upregulated pathways

in FnPg samples. Carbohydrate metabolism pathways including glycolysis/gluconeogenesis and pyruvate metabolism were metabolic pathways that were repressed. Similar to the response to *S. sanguinis*, the *F. nucleatum* transcriptome exhibited a general induction of translation pathways, including ribosome and aminoacyl-tRNA biosynthesis and ABC transporter pathways in FnPg. Transcription pathways involving RNA polymerase were also generally induced. A specific response to *P. gingivalis* that was not observed in the presence of *S. sanguinis* was the repression of the replication and repair regulatory pathway involving nucleotide excision repair. Similar to the *F. nucleatum* transcriptome of the FnSs sample, we observed the repression of the PTS system pathway, which is a membrane transport regulatory pathway.

### **Comparison of *F. nucleatum* expression profiles associated with response to partner species**

Further analyses were conducted to compare the expression profiles of *F. nucleatum* transcriptome in FnSs and FnPg samples to investigate partner-specific gene regulation. Transcriptome analyses revealed 251 genes of *F. nucleatum* that were induced over two-fold in response to both *S. sanguinis* and *P. gingivalis*, and 247 genes that were commonly downregulated negative two-fold in response to the presence of both partner species. Opposite regulation was observed for 16 genes that were upregulated in response to *S. sanguinis* but downregulated in the presence of *P. gingivalis*, and vice versa for 22 genes. All genes induced over two-fold in or reduced below two-fold in FnSs and FnPg samples were mapped and screened or overlap

(Figures 6 - 9). Pathways commonly induced in FnSs and FnPg samples included metabolic pathways: nucleotide and carbohydrate metabolism as well as regulatory pathways (ie. transcription and translation regulation and membrane transport regulation associated with bacterial secretion system pathways). General repression was seen in both FnSs and FnPg samples of the glycolysis/gluconeogenesis pathways (Figure 6) as well as membrane transport regulation associated with the PTS system (Figure 8). Distinct regulation specific to partner strains was also observed when comparing all genes induced (Figure 7) and all genes repressed (Figure 9). As an example, lipid metabolism pathways responded to the different partners being generally induced in FnPg samples and repressed in FnSs samples. Comparison of genes that showed opposite regulation between FnSs and FnPg samples included genes encoding neutrophil activating protein, phosphoenolpyruvate synthase, phosphoserine phosphatase, and a class of ethanolamine utilization proteins, which we comment on in the discussion (Figure 10).

### **Adhesion-mediated gene-expression of *F. nucleatum* in the presence of partner species**

The *F. nucleatum* interaction with early gram-positive species is known to interact through fusobacterial adhesin, RadD.<sup>6</sup> We have also shown that *F. nucleatum* interacts with *P. gingivalis* through RadD, as well as Fap2 and a yet to be identified adhesin in a strain-specific manner.<sup>3</sup> RNAseq analyses revealed that of the genes that are regulated in the  $\Delta$ DSs sample, 107 genes are regulated in adhesin-dependent manner. Of these 107 genes, 75% were upregulated over two-fold, and 25% were downregulated by at

least two-fold in the absence of the RadD adhesin. Metabolic pathways that were induced in an adhesin-dependent manner for  $\Delta$ DSs samples included nucleotide metabolism and biosynthesis of secondary metabolites. Amino acid and energy metabolism pathways were generally repressed in  $\Delta$ DSs samples (Figure 11). Interestingly, regulation of transcription pathways included DNA replication, mismatch repair and homologous recombination pathways (Figure 12). Membrane transport regulatory pathways associated with ABC transporters were shown to be a RadD-dependent response.

Adhesion-mediated gene regulation was also observed in FnPg samples. Previous studies from our group established that *F. nucleatum* interacts with *P. gingivalis* strain T22 via Fap2 and strain 4612 via both RadD and Fap2 adhesins. We observed gene regulation that was specific to each of the individual *P. gingivalis* strains that were used. Specifically, 17 fusobacterial genes were differentially regulated in response to *P. gingivalis* strain 4612. Furthermore, we observed 11 genes that appear to be regulated in the presence of *P. gingivalis* strain T22 that interacts with *F. nucleatum* via the Fap2 adhesin. There were 37 genes regulated when interacting with *P. gingivalis* ATCC 33277 that is shown to interact with *F. nucleatum*, albeit through unknown adhesin(s). Mapping of the genes revealed induction of nucleotide and lipid metabolism pathways (Figure 13). Interestingly, the pyruvate metabolism pathway was seen to be differentially regulated depending on the interacting *P. gingivalis* strain.

#### **qPCR analysis of selected genes that respond to presence of partner species**

As a means of comparison, genes were selected from transcriptome data for confirmation of gene expression via qPCR. A wild-type *F. nucleatum* sample without a partner species served as a comparison to observe relative gene expression in the presence of *S. sanguinis* or *P. gingivalis*. Though some differences compared to wild-type gene expression were statistically significant, changes not exceeding two-fold in expression levels are unlikely to be biologically relevant. Three *F. nucleatum* genes were chosen that were regulated in the transcriptome data in the presence of *S. sanguinis* only, homologs of FN0649, FN1515, and FN0940 (Figure 14A-C). Three additional genes that are regulated in both FnSs and FnPg cocultures were chosen, FN1421, FN0791, FN0214 (Figure 14D-F). Survey of transcriptional levels of FN0649 for each dual-species sample compared to wild-type showed a significant increase in fold change for FnSs samples ( $5.30 \pm 0.09$ ) and FnPg samples ( $1.24 \pm 0.13$ ), though based on the transcriptome data, FnSs levels of FN0649 were expected to be downregulated. No significant differences were observed in transcription of FN1515 between samples. FN0940 levels showed a consistent pattern with transcriptome data with a significant decrease in expression levels in FnSs samples ( $0.40 \pm 0.09$  fold change) and in FnPg samples ( $0.87 \pm 0.07$ ). Expression levels of FN1421 revealed a significant and dramatic increase in FnSs samples ( $13.88 \pm 4.53$ ) and significant increase in FnPg sample ( $2.32 \pm 0.51$ ). Transcription levels of FN0791 and FN0214, both regulated in the presence of *S. sanguinis* and *P. gingivalis* according to transcriptome results, only showed significant increase in FnSs samples ( $1.57 \pm 0.1$  and  $1.38 \pm 0.11$ , respectively).

## Discussion

Bacteria are highly adaptive organisms, with the capability to sense their environment. In this study, we report that *F. nucleatum* is able to distinguish between and respond to different partner species and that part of the fusobacterial transcriptional response to these partners is mediated by adhesins. Studies in other bacteria have shown that adhesins can have functional roles beyond attachment. A study in *Vibrio parahaemolyticus* describes an adhesin that also acts as an extracellular effector of host signaling.<sup>26</sup> A study in *Campylobacter jejuni* reports on a protein that has the dual role of an adhesin and solute-binding protein.<sup>27</sup> Furthermore, studies in other pathogenic bacteria have shown that adhesins can act as bacterial mechanosensors to regulate transcriptional changes promoting virulence,<sup>9,10</sup> are directly involved in the induction of signaling pathways,<sup>11</sup> and play major roles in quorum-sensing for biofilm formation and virulence.<sup>12,28</sup>

From our study, we were able to determine that *F. nucleatum* responds to the presence of partner species on a global transcriptional level. We report that some genes are regulated irrespective of the type of partner species but also observe partner-specific responses. As an example, when *F. nucleatum* interacts with *P. gingivalis*, we observe induction of genes involved in butanoate metabolism. Butanoate, also referred to as butyrate, is considered a virulence factor produced by bacteria, including *F. nucleatum*.<sup>29,30</sup> Butyrate production by *F. nucleatum* has been confirmed in samples from patients with chronic periodontitis when comparing transcriptome profiles of the samples with those from healthy subjects.<sup>31</sup> Our observation of butyrate stimulation in

the presence of *P. gingivalis* could be a possible factor to explain how *P. gingivalis* manipulates the oral commensal community into behaving pathogenically. Furthermore, opposite regulation was observed between FnSs and FnPg samples of genes encoding neutrophil activating protein (NAP) and phosphoenolpyruvate synthase (PEP synthase), which were both induced in FnSs samples and repressed in FnPg samples. Neutrophil activating protein has been previously described in *Helicobacter pylori* to stimulate high production of oxygen radicals and adhesion to endothelial cells, promoting the gastric inflammatory response.<sup>32</sup> Opposite regulation of the gene encoding NAP in FnSs (induced) and FnPg (repressed) might indicate a modulation of the host immune response to maintain health, associated with *S. sanguinis*<sup>33</sup> or progression to disease, associated with *P. gingivalis*, which is known to manipulate the host-immune response.<sup>34,35</sup> This indicates that in addition to interacting directly with the host, *P. gingivalis* may manipulate partner species into altering immune-associated interactions with the host. The gene encoding PEP synthase was found to also be upregulated in FnSs samples while downregulated in FnPg samples. The enzyme is functionally characterized to catalyze the phosphorylation of pyruvate to PEP with the hydrolysis of ATP to AMP, processes which are essential for cell growth.<sup>36,37</sup>

Mixed responses in our study imply both synergistic and competitive interactions between *F. nucleatum* and interacting partner species. Opposite regulation was also observed in genes encoding phosphoserine phosphatase and a class of ethanolamine utilizing proteins in FnSs (repressed) and FnPg (induced). A 2010 report found that *P. gingivalis* phosphoserine phosphatase (SerB) plays a critical role in pathogenesis,

mediating internalization and survival of *P. gingivalis* in epithelial cells.<sup>38</sup> Ethanolamine utilization proteins are involved in the bacterial process of converting ethanolamine as a source of carbon and nitrogen for successful host colonization.<sup>39,40</sup> Upregulation of these genes in *F. nucleatum* in response to contact with *P. gingivalis* may further support synergistic growth enhancement of the two species that have been previously described.<sup>2,41</sup>

Induction of translation regulation pathways for both FnSs and FnPg samples may reflect a response to changes in nutrient availability with the introduction of microbes found in the same ecological niche or that *F. nucleatum* has developed a programmed response to the presence of other organisms realizing the potential for nutrient exchange. Alternatively, the downregulation of the glycolysis/gluconeogenesis pathways in the presence of both partner species may be a way for *F. nucleatum* to reduce energy consumption. This may be due to the sensing of amino acid deprivation or conversely, that amino acids may have become available and do not need to be synthesized due to biosynthesis by *P. gingivalis*. A previous study has shown that *P. gingivalis* and *Treponema denticola* exhibit metabolic symbiosis in *in vitro* growth, with *P. gingivalis* acting as a source of free glycine to *T. denticola* in return for a breakdown of glycine by *T. denticola* into acetate and lactate.<sup>42</sup> These concepts are supported by proteomic studies on *P. gingivalis* and *Streptococcus gordonii*, which indicated increased translation in mixed communities compared to monocultures<sup>43,44</sup> and decreased glycolysis/gluconeogenesis proteins of *F. nucleatum* in mixed cultures.<sup>45</sup> The phosphotransferase system of bacteria is used to transport resources into the cell and

assures optimum utilization of the resources in changing environments.<sup>46</sup> A general repression of genes involved in this system in our studies might be a response by *F. nucleatum* to potential competitors and the need to conserve energy and resources.

Analysis by qPCR revealed varying transcriptional profiles of genes examined with only one out of the six genes profiled matching the pattern seen in transcriptome analyses. Another concern is the housekeeping gene we chose to normalize levels to, *rpoB*, seems to also be regulated in the presence of partner strains. Further studies are warranted to establish an accurate method to observe gene expression in *F. nucleatum* grown in monocultures or with other species and we are currently in the process of evaluating other genes such as the gene encoding for 16S ribosomal RNA for normalization.

Investigation of *F. nucleatum* adhesins in the regulation of genes revealed their involvement in the process. Mapping of pathways show pathways that are dependent on the mediating adhesin and interacting partner, as an example, when *F. nucleatum* interacts via RadD with *S. sanguinis*, we observe induction of transcriptional pathways for DNA replication, mismatch repair, and homologous recombination, not observed in the FnPg interaction, but also a differential response to specific strains of *P. gingivalis* in repressing or inducing the pyruvate metabolism pathway (*P. gingivalis* 4612 and T22, respectively).

Adhesin-dependent signaling has been described in a study where investigators report regulation of a key signaling pathway is dependent on the interaction between *P. gingivalis* Mfa and *S. gordonii* SspA/B adhesins<sup>11</sup>. We report here that *F. nucleatum* is able to differentially respond to partner bacteria and transcriptional changes can be adhesin-dependent. Further studies are warranted to elucidate the mechanisms behind adhesin-dependent regulation. RadD should be given special consideration in future studies as it is the best characterized fusobacterial adhesin and our studies show that it is involved in interaction with both gram-positive and gram-negative species. The extremely complex mechanisms of gene regulation reflect the importance of environmental sensing by bacteria for survival of the bacterium in different environments. *F. nucleatum* is a prime candidate for adhesin-dependent gene expression studies given the abundance of interacting partners and its implication in numerous diseases.

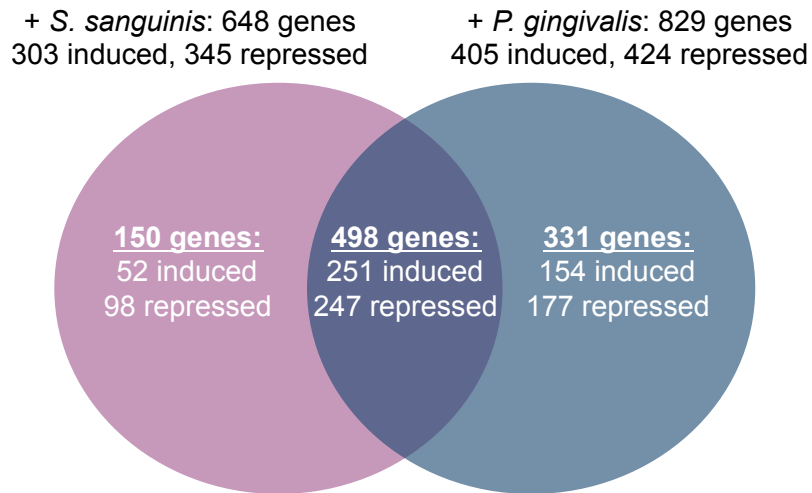


**Figure 1.** Diagram of the number of *F. nucleatum* genes regulated in the presence of *S. sanguinis* (pink) and *P. gingivalis* (blue). Genes commonly induced or repressed by *S. sanguinis* and *P. gingivalis* can be seen in the overlapping region.

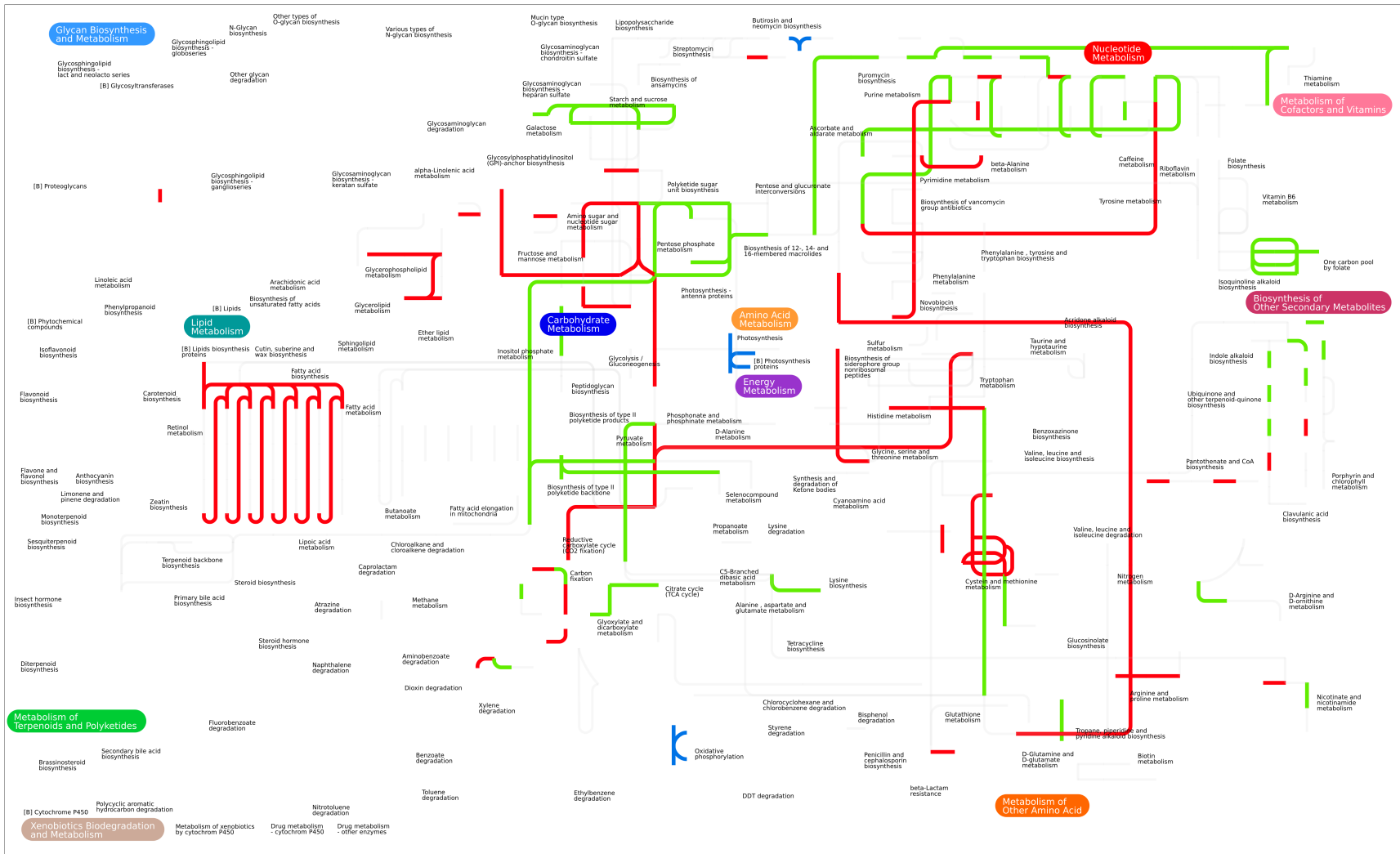


**Figure 2.** *F. nucleatum* metabolic pathway map of all genes regulated in the presence of *S. sanguinis* including induced pathways (green), repressed pathways (red) and pathways containing genes that are both induced and repressed (blue).

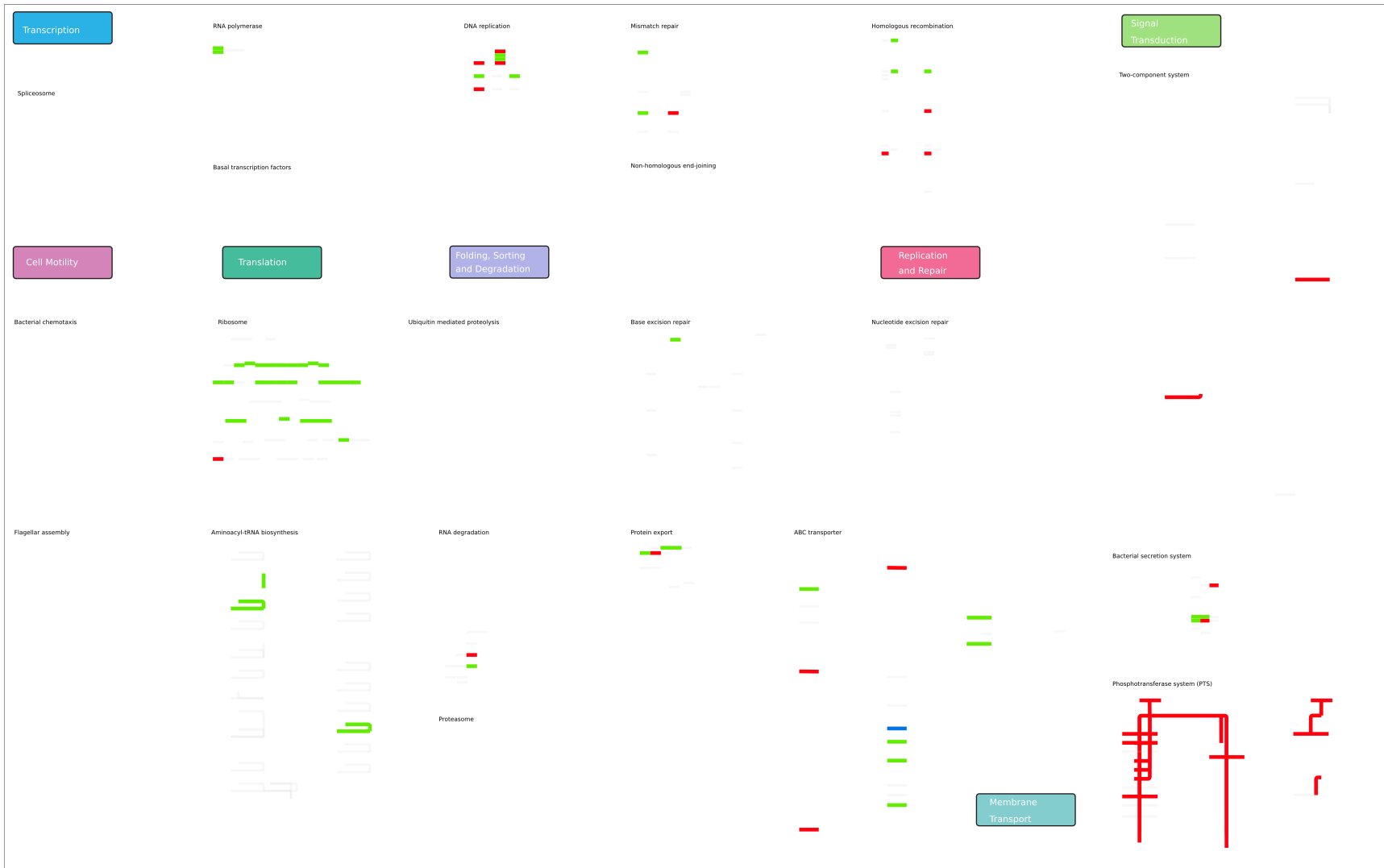


**Figure 3.** *F. nucleatum* regulatory pathway map of all genes regulated in the presence of *S. sanguinis* including induced pathways (green), repressed pathways (red) and pathways containing genes that are both induced and repressed (blue).

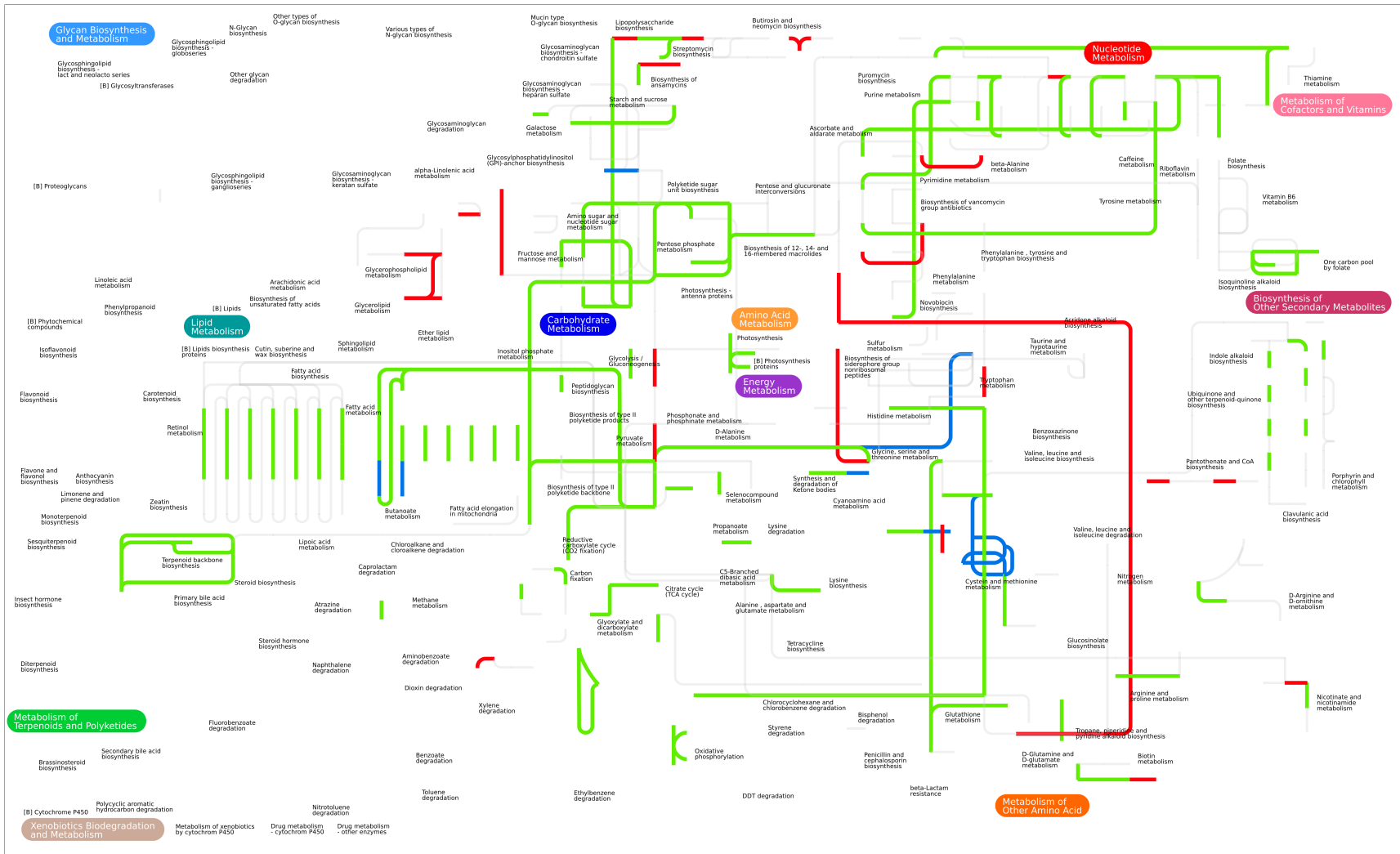


**Figure 4.** *F. nucleatum* metabolic pathway map of all genes regulated in the presence of *P. gingivalis* including induced pathways (green), repressed pathways (red) and pathways containing genes that are both induced and repressed (blue).

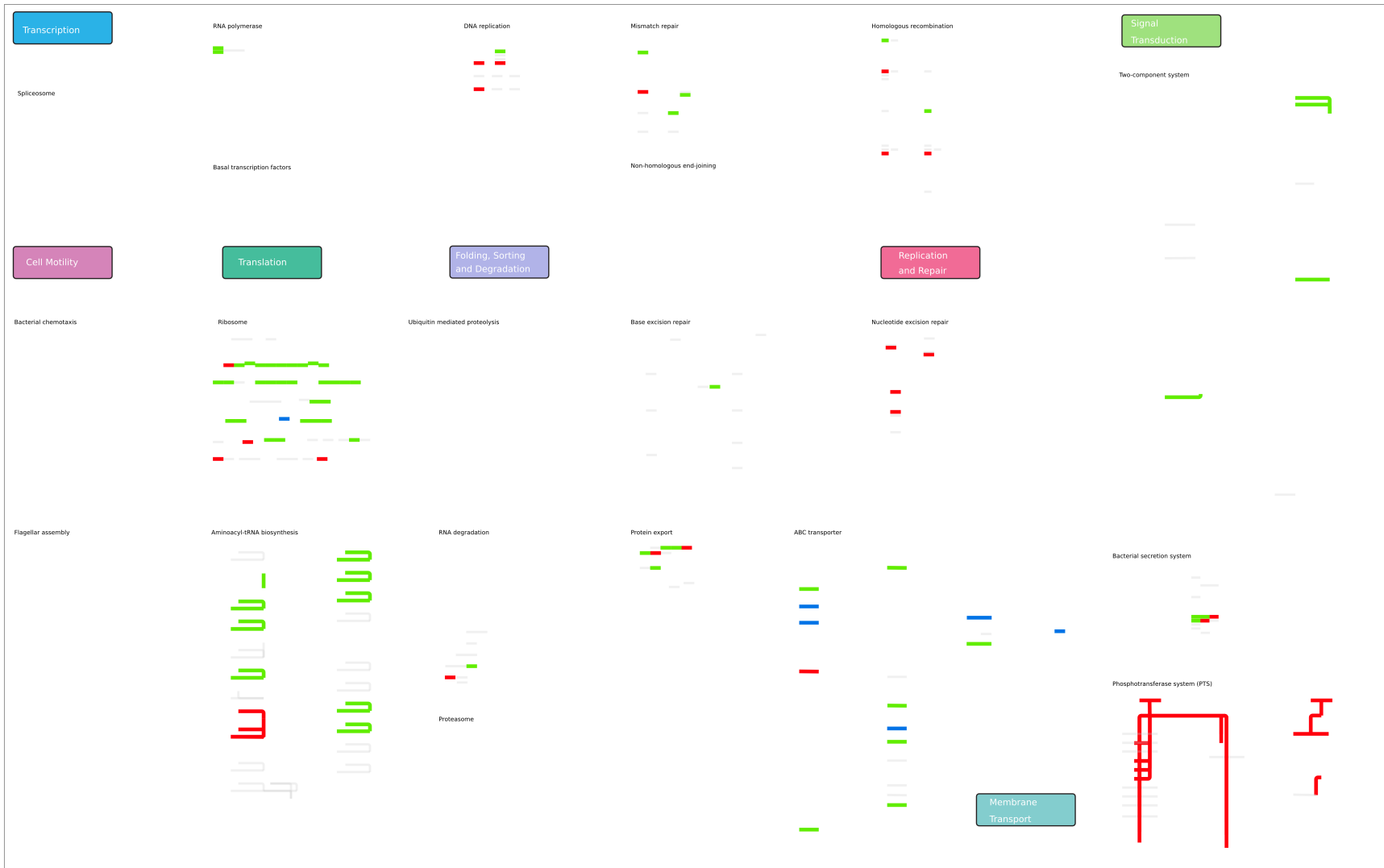


**Figure 5.** *F. nucleatum* regulatory pathway map of all genes regulated in the presence of *P. gingivalis* including induced pathways (green), repressed pathways (red) and pathways containing genes that are both induced and repressed (blue).

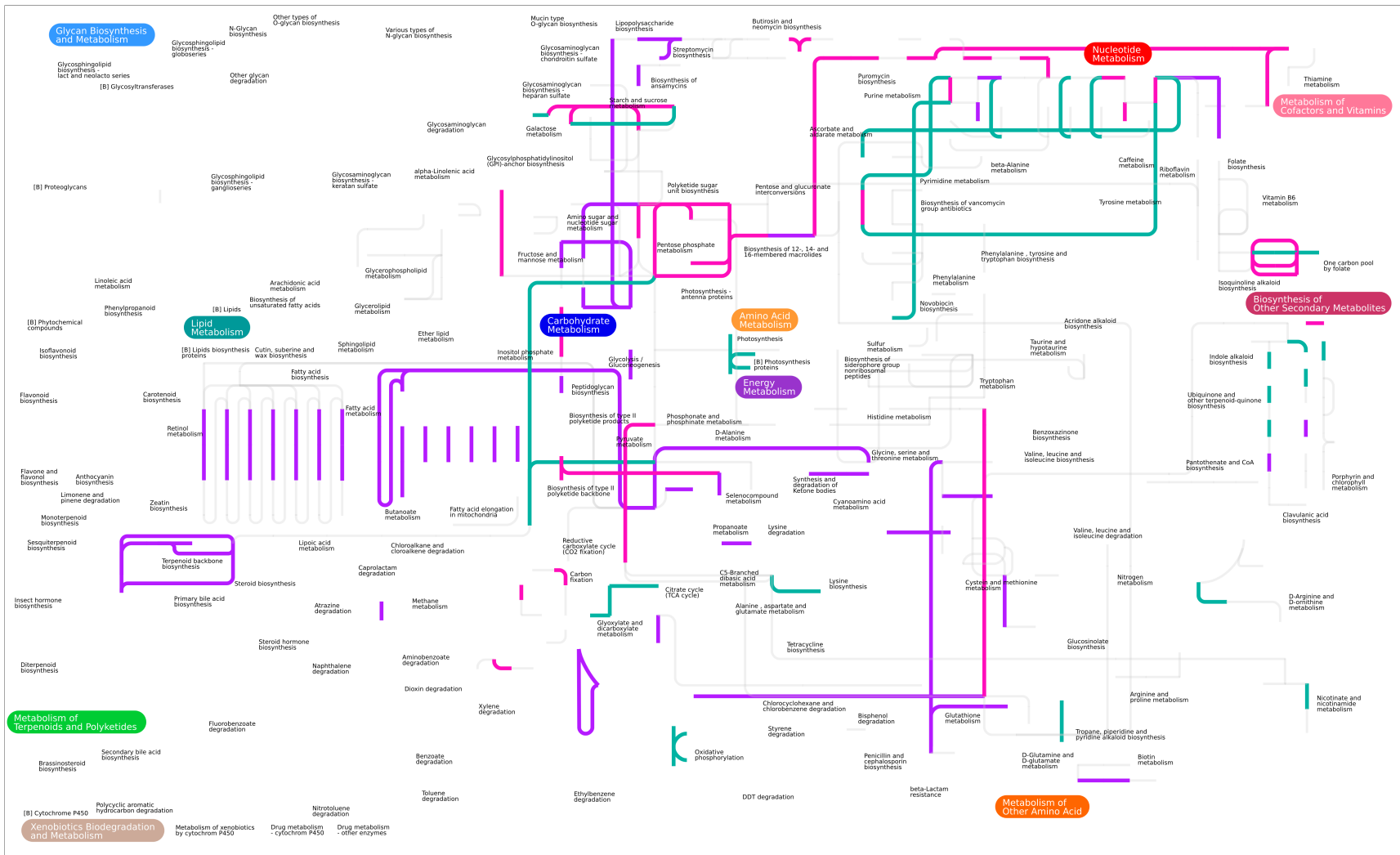


**Figure 6.** *F. nucleatum* metabolic pathway map of all induced genes regulated in the presence of *S. sanguinis* (pink), *P. gingivalis* (purple), or both (teal).

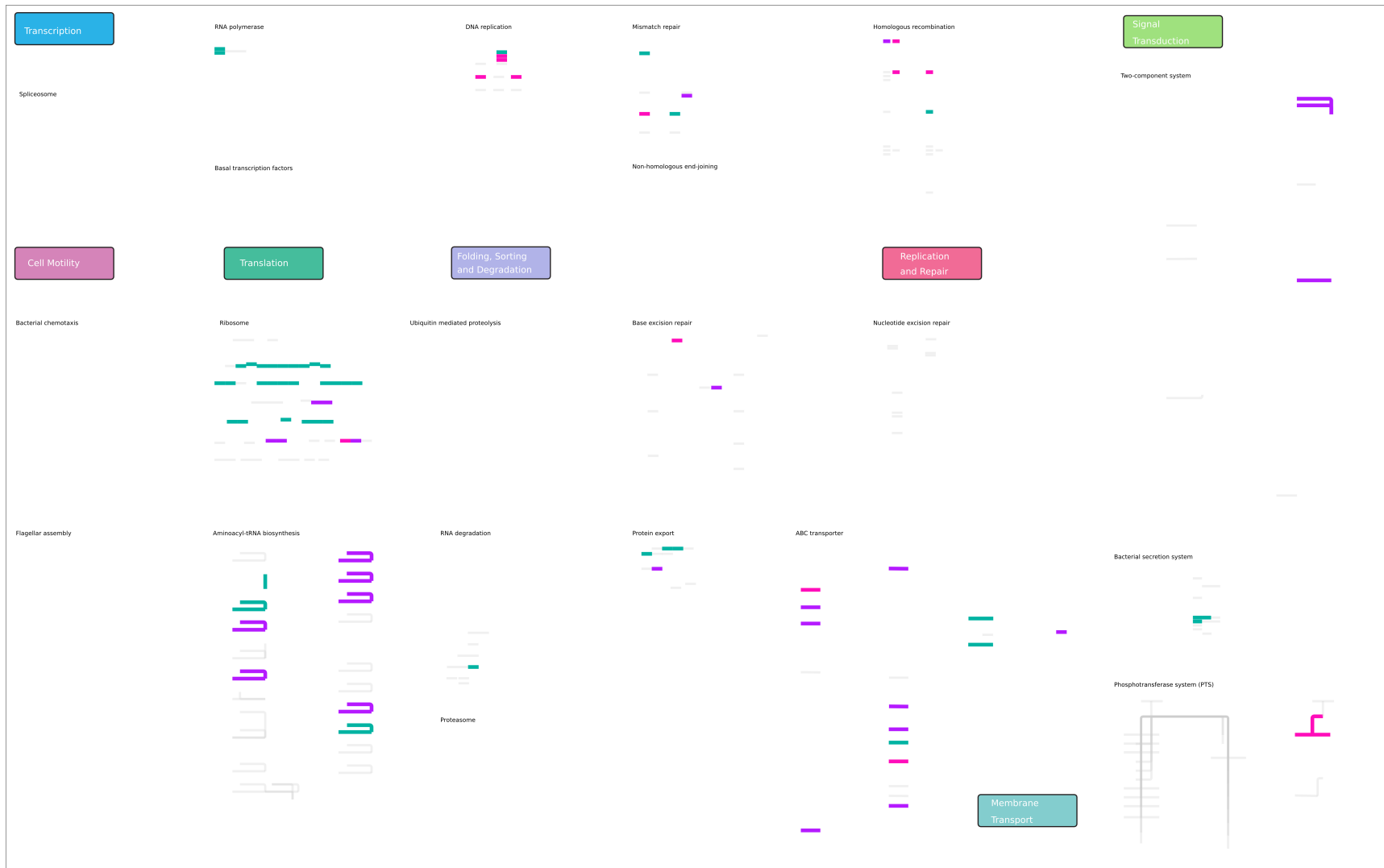


**Figure 7.** *F. nucleatum* regulatory pathway map of all induced genes regulated in the presence of *S. sanguinis* (pink), *P. gingivalis* (purple), or both (teal).

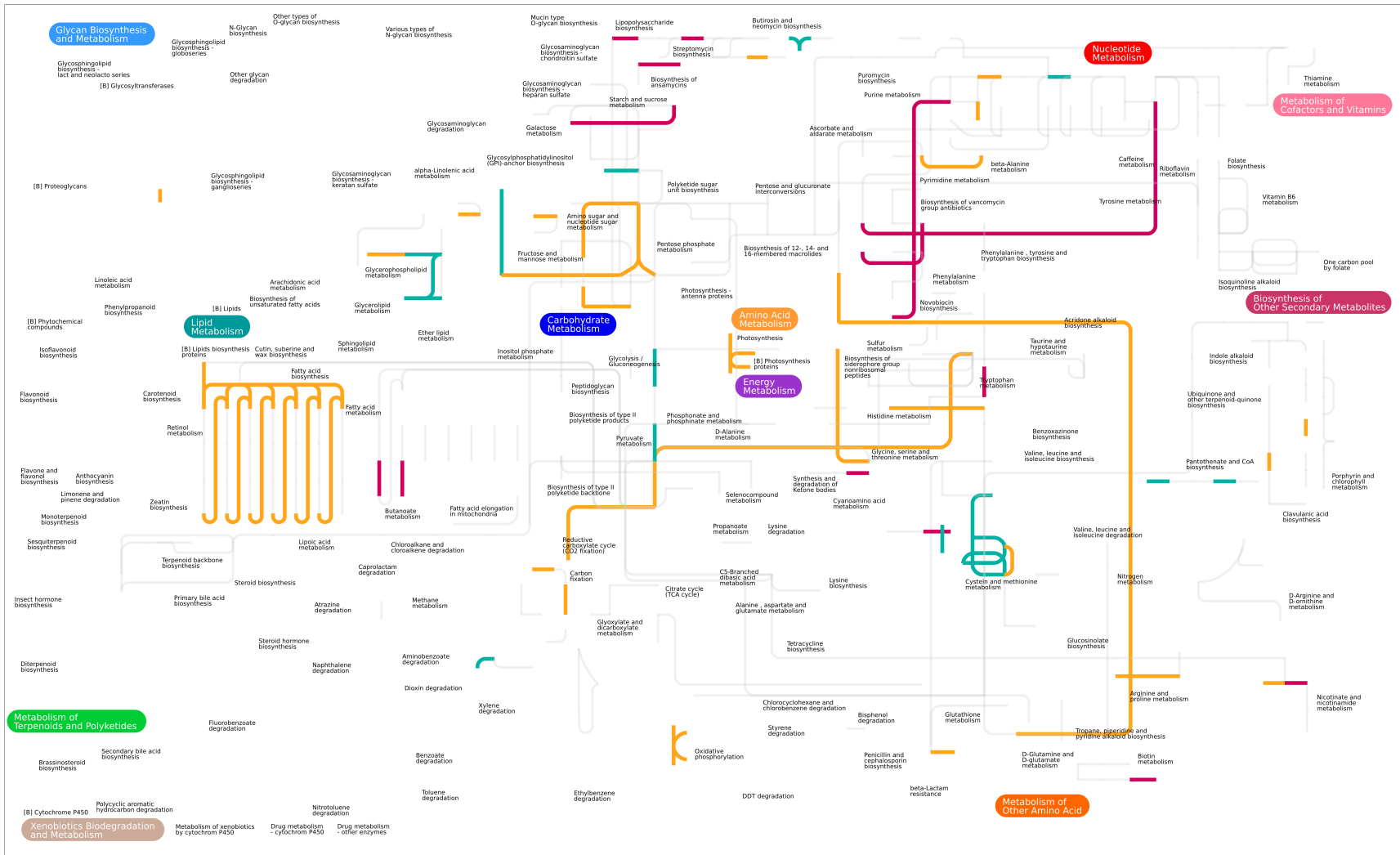


**Figure 8.** *F. nucleatum* metabolic pathway map of all repressed genes regulated in the presence of *S. sanguinis* (orange), *P. gingivalis* (red), or both (teal).

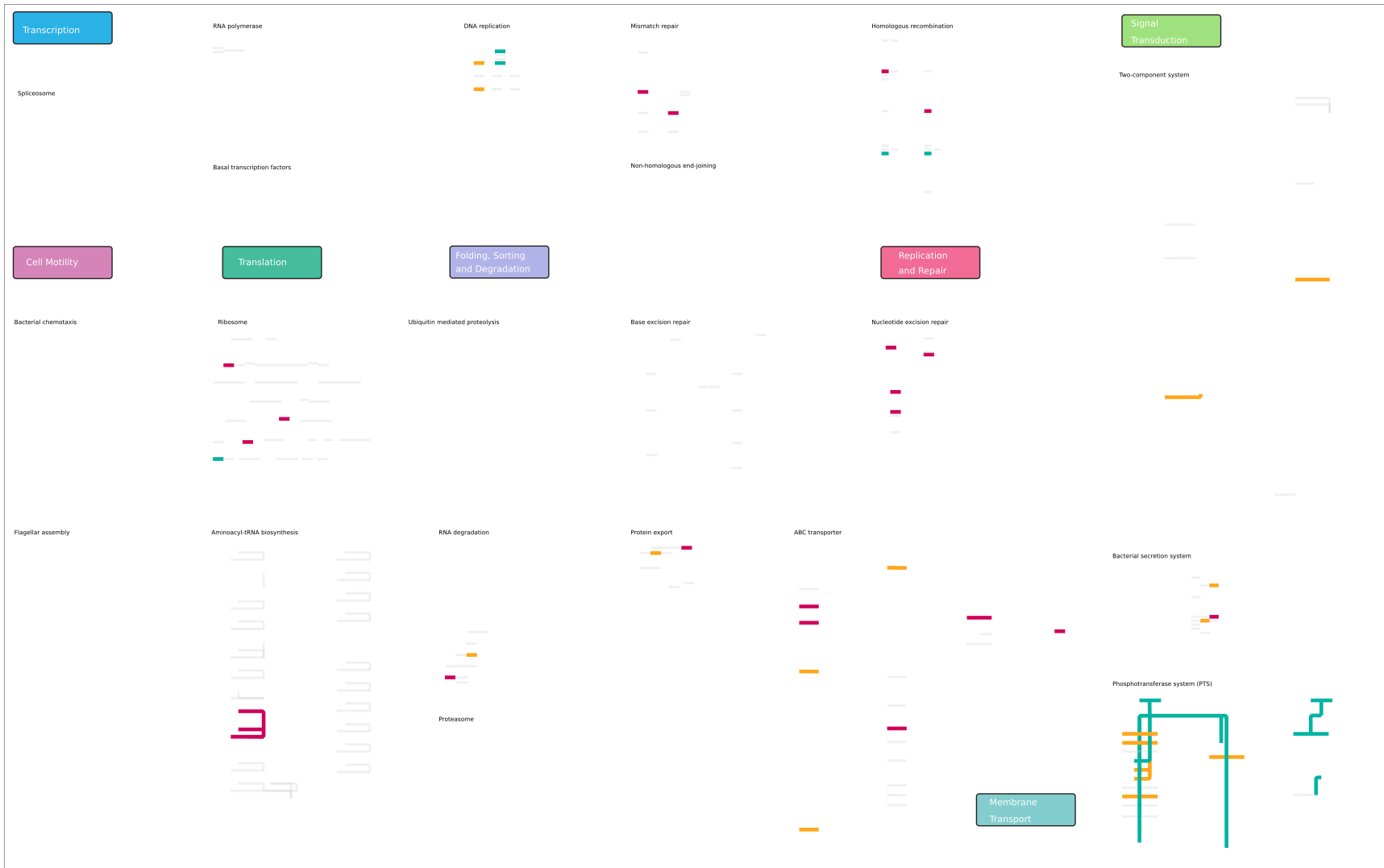


**Figure 9.** *F. nucleatum* regulatory pathway map of all repressed genes regulated in the presence of *S. sanguinis* (orange), *P. gingivalis* (red), or both (teal).

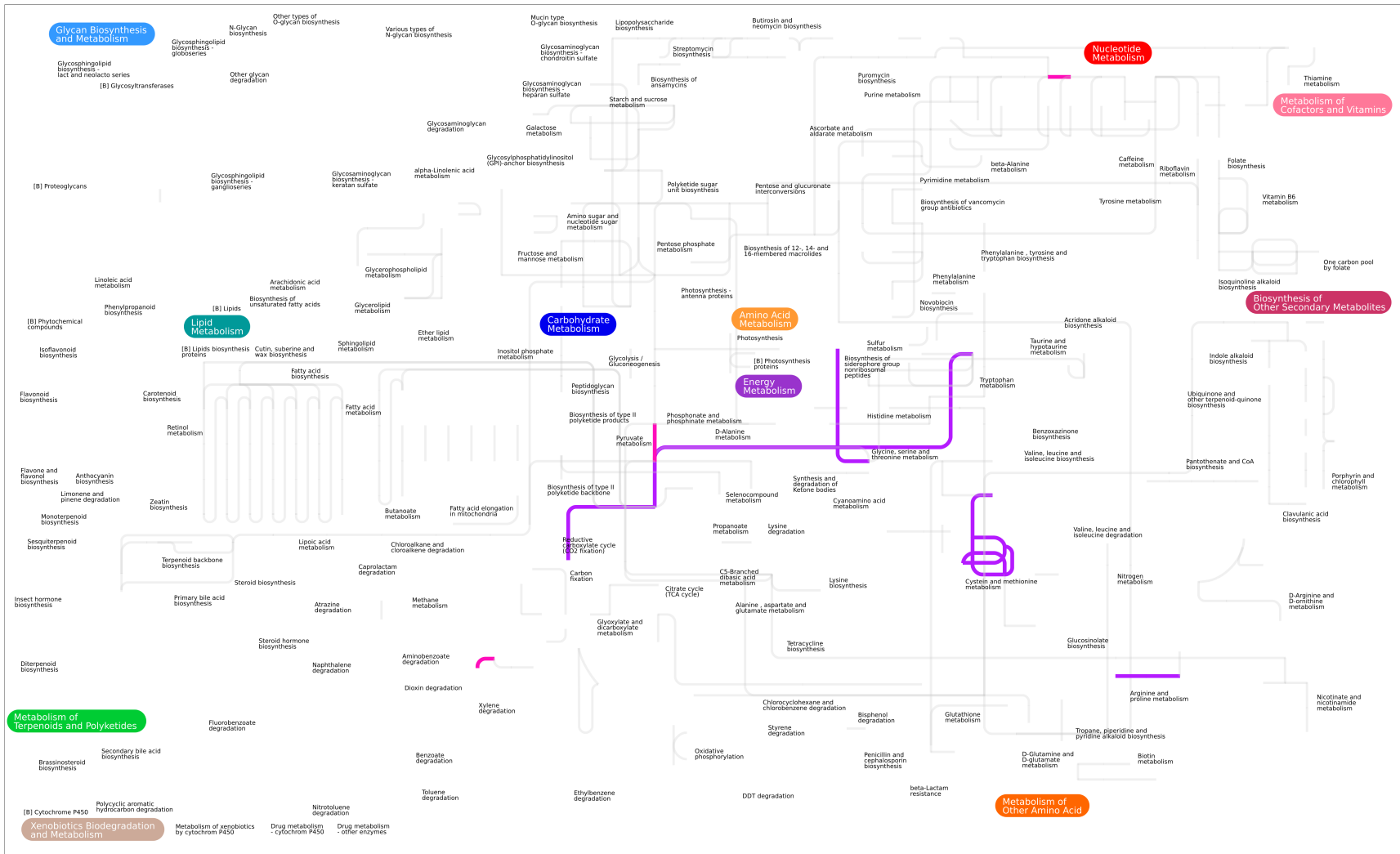


**Figure 10.** *F. nucleatum* metabolic pathway map of genes regulated oppositely; repressed in *S. sanguinis* and induced in *P. gingivalis* (purple), induced in *S. sanguinis* and repressed in *P. gingivalis* (pink).

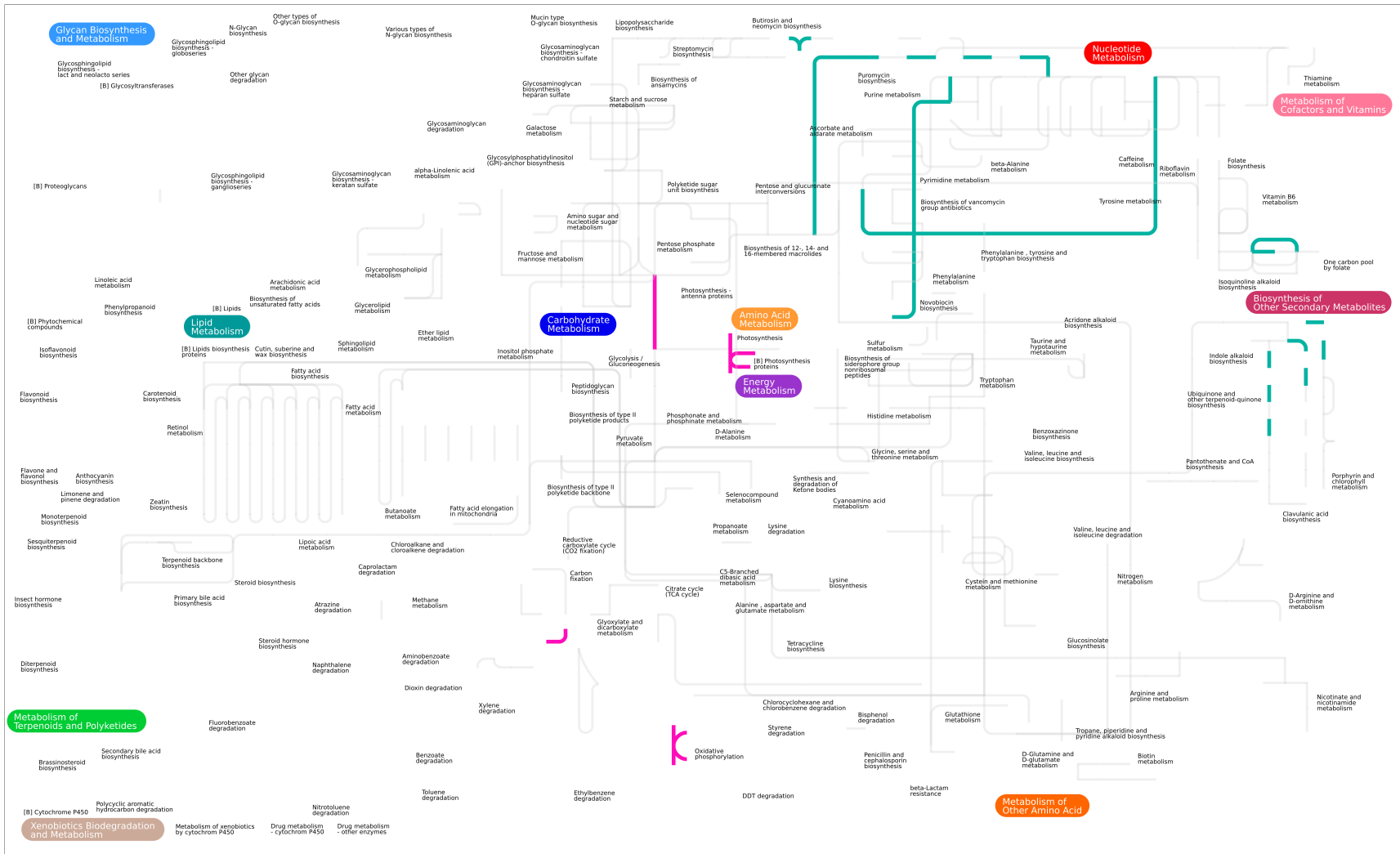


**Figure 11.** *F. nucleatum* metabolic pathway map of genes induced (teal) or repressed (pink) in the presence of *S. sanguinis* in a RadD-dependent manner.

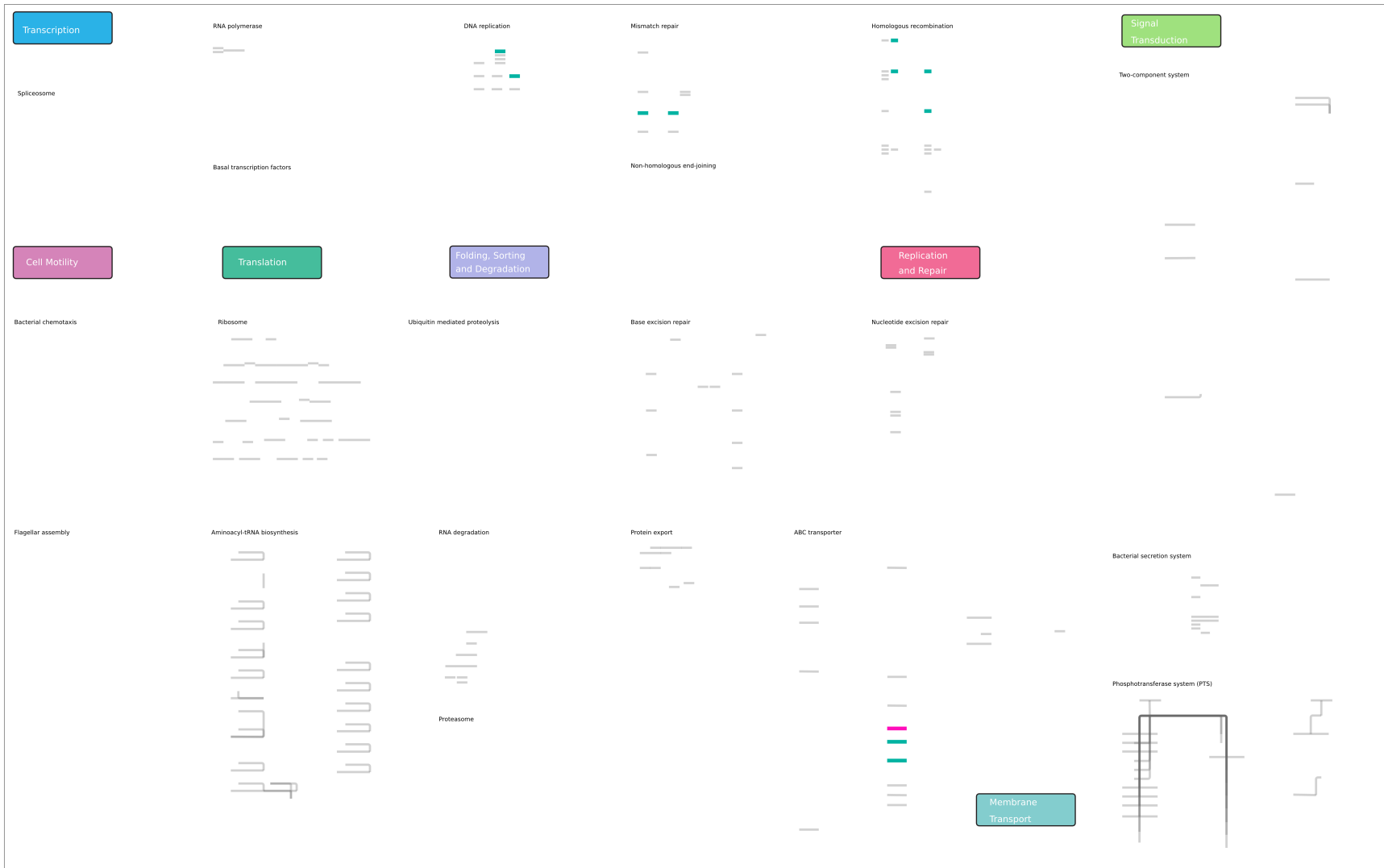


**Figure 12.** *F. nucleatum* regulatory pathway map of genes induced (teal) or repressed (pink) in the presence of *S. sanguinis* in a RadD-dependent manner.



\*p<0.05  
\*\*p<0.01

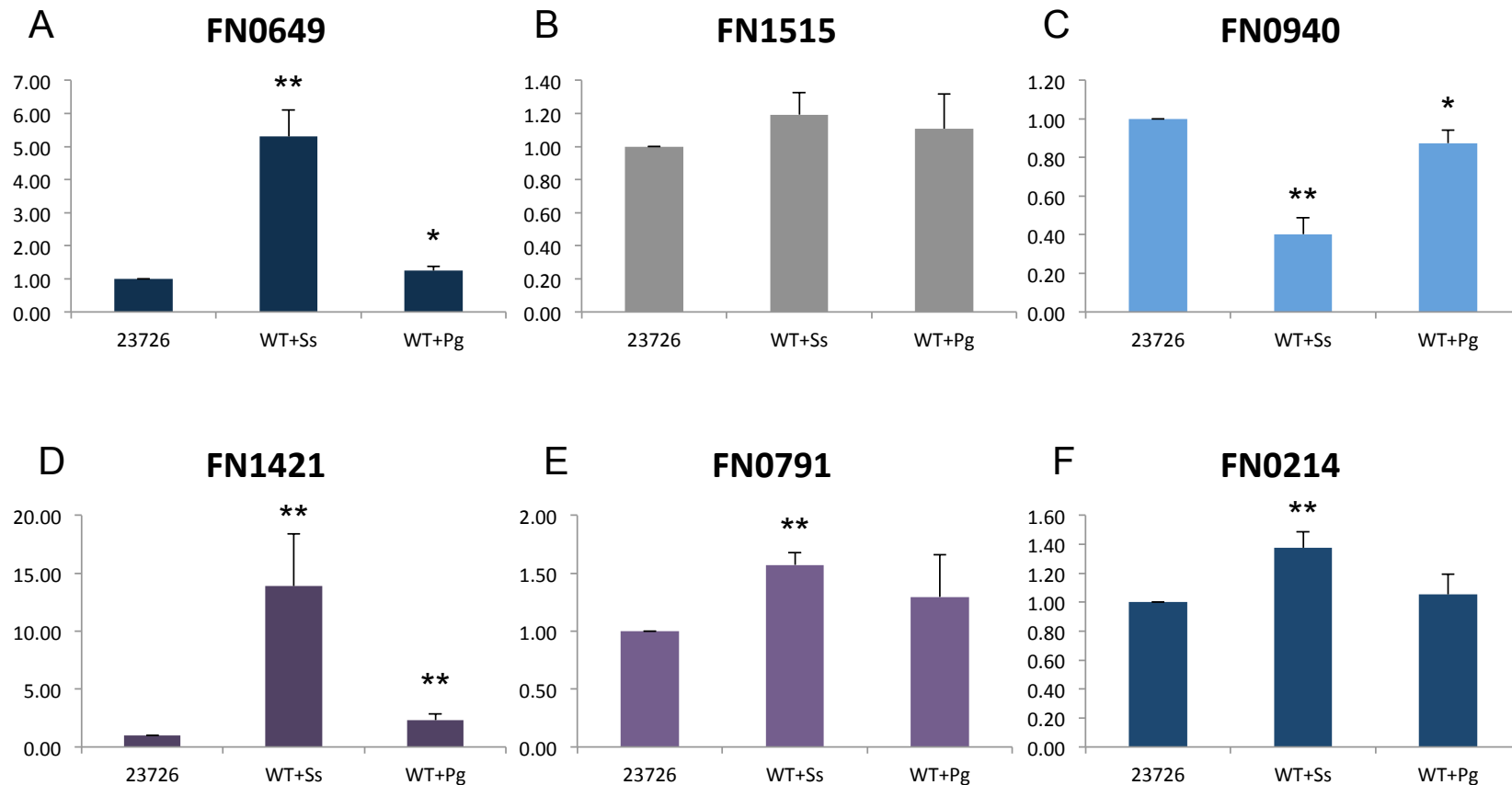


**Figure 14.** Gene expression comparison of selected genes relative to wild-type *F. nucleatum* alone in FnSs or FnPg. (A) Gene expression of homolog of FN0649. (B) Gene expression of homolog of FN0214, (C) Gene expression of homolog of FN0940, (D) Gene expression of homolog of FN0085, (E) Gene expression of homolog of FN0791, and (F) Gene expression of homolog of FN0272. Data represent the means and standard deviation of at least three independent experiments.

## References

1. Kolenbrander PE, London J. Adhere today, here tomorrow: oral bacterial adherence. *J Bacteriol.* 1993;175(11):3247-3252. <http://www.ncbi.nlm.nih.gov/pubmed/8501028>. Accessed July 18, 2016.
2. Bradshaw DJ, Marsh PD, Keith Watson G, Allison C. Role of *Fusobacterium nucleatum* and coaggregation in anaerobe survival in planktonic and biofilm oral microbial communities during aeration. *Infect Immun.* 1998;66(10):4729-4732.
3. Park J, Shokeen B, Haake S, Lux R. Characterization of *Fusobacterium nucleatum* ATCC 23726 Adhesins Involved in Strain-Specific Attachment to *Porphyromonas gingivalis*. *Int J Oral Sci.* 2016;(In Press).
4. Cisar JO, Kolenbrander PE, McIntire FC. Specificity of coaggregation reactions between human oral streptococci and strains of *Actinomyces viscosus* or *Actinomyces naeslundii*. *Infect Immun.* 1979;24(3):742-752. doi:0019-9567/79/06-0742/11\$02.00/0.
5. Kolenbrander PE, Palmer RJ, Periasamy S, Jakubovics NS. Oral multispecies biofilm development and the key role of cell-cell distance. *Nat Rev Microbiol.* 2010;8(7):471-480. doi:10.1038/nrmicro2381.
6. Kaplan CW, Lux R, Haake SK, Shi W. The *Fusobacterium nucleatum* outer membrane protein RadD is an arginine-inhibitable adhesin required for inter-species adherence and the structured architecture of multispecies biofilm. *Mol Microbiol.* 2009;71(1):35-47. doi:10.1111/j.1365-2958.2008.06503.x.
7. McHardy IH. Analysis of Interspecies Interactions of Periodontal Bacteria Using Microarrays. *ProQuest Diss Theses.* 2011:156. <http://search.proquest.com/docview/1022181168?accountid=14512>  
[http://ucelink.s.cdlib.org:8888/sfx\\_local?url\\_ver=Z39.88-2004&rft\\_val\\_fmt=info:ofi/fmt:kev:mtx:dissertation&genre=dissertations+&+theses&sid=ProQ:Dissertations+&+Theses+@+University+of+Ca](http://ucelink.s.cdlib.org:8888/sfx_local?url_ver=Z39.88-2004&rft_val_fmt=info:ofi/fmt:kev:mtx:dissertation&genre=dissertations+&+theses&sid=ProQ:Dissertations+&+Theses+@+University+of+Ca).
8. Simanian EJ. Determination of RadD-Dependent Gene Regulation in *Fusobacterium nucleatum* in Response to *Streptococcus sanguinis*. 2013. <http://escholarship.org/uc/item/7p46t0hv>.
9. Ellison C, Brun Y V, Karatan E, et al. Mechanosensing: a regulation sensation. *Curr Biol.* 2015;25(3):R113-R115. doi:10.1016/j.cub.2014.12.026.
10. Siryaporn A, Kuchma SL, O'Toole G a., Gitai Z. Surface attachment induces *Pseudomonas aeruginosa* virulence. *Proc Natl Acad Sci U S A.* 2014;111(47):16860-16865. doi:10.1073/pnas.1415712111.
11. Chawla A, Hirano T, Bainbridge BW, Demuth DR, Xie H, Lamont RJ. Community

- signalling between *Streptococcus gordonii* and *Porphyromonas gingivalis* is controlled by the transcriptional regulator CdhR. *Mol Microbiol.* 2010;78(6):1510-1522. doi:10.1111/j.1365-2958.2010.07420.x.
12. Xu L, Li H, Vuong C, et al. Role of the luxS Quorum-Sensing System in Biofilm Formation and Virulence of *Staphylococcus epidermidis* Role of the luxS Quorum-Sensing System in Biofilm Formation and Virulence of *Staphylococcus epidermidis*. *Infect Immun.* 2006;74(1):488-496. doi:10.1128/IAI.74.1.488.
  13. Lamont RJ, Hersey SG, Rosan B. Characterization of the adherence of *Porphyromonas gingivalis* to oral streptococci. *Oral Microbiol Immunol.* 1992;7(4):193-197. doi:10.1111/j.1399-302X.1992.tb00024.x.
  14. Kinder SA, Holt SC. Characterization of coaggregation between *Bacteroides gingivalis* T22 and *Fusobacterium nucleatum* T18. *Infect Immun.* 1989;57(11):3425-3433.
  15. Coykendall AL, Kaczmarek FS, Slots J. Genetic Heterogeneity in *Bacteroides asaccharolyticus* (Holdeman and Moore 1970) Finegold and Barnes 1977 (Approved Lists, 1980) and Proposal of *Bacteroides gingivalis* sp. nov. and *Bacteroides macacae* (Slots and Genco) comb. nov. *Int J Syst Bacteriol.* 1980;30(3):559-564. doi:10.1099/00207713-30-3-559.
  16. Guo L, McLean JS, Lux R, He X, Shi W. The well-coordinated linkage between acidogenicity and aciduricity via insoluble glucans on the surface of *Streptococcus mutans*. *Sci Rep.* 2015;5(November):18015. doi:10.1038/srep18015.
  17. McLean JS, Fansler SJ, Majors PD, et al. Identifying Low pH Active and Lactate-Utilizing Taxa within Oral Microbiome Communities from Healthy Children Using Stable Isotope Probing Techniques. Aziz RK, ed. *PLoS One.* 2012;7(3):e32219. doi:10.1371/journal.pone.0032219.
  18. Anders S, Huber W. Differential expression analysis for sequence count data. *Genome Biol.* 2010;11(10):R106. doi:10.1186/gb-2010-11-10-r106.
  19. McClure R, Balasubramanian D, Sun Y, et al. Computational analysis of bacterial RNA-Seq data. *Nucleic Acids Res.* 2013;41(14):e140. doi:10.1093/nar/gkt444.
  20. Yamada T, Letunic I, Okuda S, Kanehisa M, Bork P. iPath2.0: interactive pathway explorer. *Nucleic Acids Res.* 2011;39(Web Server issue):W412-W415. doi:10.1093/nar/gkr313.
  21. Tatusov RL, Galperin MY, Natale DA, Koonin E V. The COG database: a tool for genome-scale analysis of protein functions and evolution. *Nucleic Acids Res.* 2000;28(1):33-36.
  22. Kapatral V, Anderson I, Ivanova N, et al. Genome sequence and analysis of the

- oral bacterium *Fusobacterium nucleatum* strain ATCC 25586. *J Bacteriol.* 2005;184(7):2005-2018. doi:10.1128/JB.184.7.2005.
23. Ximénez-Fyvie L a, Haffajee a D, Socransky SS. Microbial composition of supra- and subgingival plaque in subjects with adult periodontitis. *J Clin Periodontol.* 2000;27(10):722-732. doi:doi:10.1034/j.1600-051x.2000.027010722.x.
  24. Noguchi N, Noiri Y, Narimatsu M, Ebisu S. Identification and localization of extraradicular biofilm-forming bacteria associated with refractory endodontic pathogens. *Appl Environ Microbiol.* 2005;71(12):8738-8743. doi:10.1128/AEM.71.12.8738-8743.2005.
  25. Han YW, Wang X. Mobile microbiome: oral bacteria in extra-oral infections and inflammation. *J Dent Res.* 2013;92(6):485-491. doi:10.1177/0022034513487559.
  26. Stones DH, Krachler AM. Dual function of a bacterial protein as an adhesin and extracellular effector of host GTPase signaling. *Small GTPases.* 2015;6(3):153-156. doi:10.1080/21541248.2015.1028609.
  27. Müller A, León-Kempis M del R, Dodson E, Wilson KS, Wilkinson AJ, Kelly DJ. A Bacterial Virulence Factor with a Dual Role as an Adhesin and a Solute-binding Protein: The Crystal Structure at 1.5 Å Resolution of the PEB1a Protein from the Food-borne Human Pathogen *Campylobacter jejuni*. *J Mol Biol.* 2007;372(1):160-171. doi:10.1016/j.jmb.2007.06.041.
  28. Karatan E, Watnick P. Signals, regulatory networks, and materials that build and break bacterial biofilms. *Microbiol Mol Biol Rev.* 2009;73(2):310-347. doi:10.1128/MMBR.00041-08.
  29. Bennett KW, Eley A. Fusobacteria : new taxonomy and related diseases. 1993;39:246-254.
  30. Roques CG, El kaddouri S, Barthet P, Duffort JF, Arellano M. Fusobacterium nucleatum involvement in adult periodontitis and possible modification of strain classification. *J Periodontol.* 2000;71(7):1144-1150. doi:10.1902/jop.2000.71.7.1144.
  31. Jorth P, Turner KH, Gumus P, Nizam N, Buduneli N, Whiteley M. Metatranscriptomics of the human oral microbiome during health and disease. *MBio.* 2014;5(2):e01012-e01014. doi:10.1128/mBio.01012-14.
  32. Evans DJ, Evans DG, Takemura T, et al. Characterization of a Helicobacter pylori neutrophil-activating protein. *Infect Immun.* 1995;63(6):2213-2220. doi:10.1016/S0378-1097(01)00174-4.
  33. Becker MR, Paster BJ, Leys EJ, et al. Molecular analysis of bacterial species associated with childhood caries. *J Clin Microbiol.* 2002;40(3):1001-1009.

doi:10.1128/JCM.40.3.1001.

34. Bodet C, Chandad F, Grenier D. Potentiel pathogénique de *Porphyromonas gingivalis*, *Treponema denticola* et *Tannerella forsythia*, le complexe bactérien rouge associé à la parodontite. *Pathol Biol.* 2007;55(3-4):154-162. doi:10.1016/j.patbio.2006.07.045.
35. Hajishengallis G, Lamont RJ. Breaking bad: manipulation of the host response by *Porphyromonas gingivalis*. *Eur J Immunol.* 2014;44(2):328-338. doi:10.1002/eji.201344202.
36. Smyer JR, Jeter RM. *Salmonella typhimurium*\*. *Strain.* 1989:26-32.
37. Cooper RA, Kornberg HL. The mechanism of the phosphoenolpyruvate synthase reaction. *Biochim Biophys Acta - Gen Subj.* 1967;141(1):211-213. doi:10.1016/0304-4165(67)90269-3.
38. Bainbridge B, Verma RK, Eastman C, et al. Role of *Porphyromonas gingivalis* phosphoserine phosphatase enzyme SerB in inflammation, immune response, and induction of alveolar bone resorption in rats. *Infect Immun.* 2010;78(11):4560-4569. doi:10.1128/IAI.00703-10.
39. Garsin D. Ethanolamine Utilisation in Bacterial Pathogens: Roles and Regulation. *Nat Rev Microbiol.* 2010;8(4):290-295. doi:10.1038/nrmicro2334.Ethanolamine.
40. Garsin DA. Ethanolamine: A signal to commence a host-associated lifestyle? *MBio.* 2012;3(4):172-174. doi:10.1128/mBio.00172-12.
41. Metzger Z, Lin YY, Dimeo F, Ambrose WW, Trope M, Arnold RR. Synergistic Pathogenicity of *Porphyromonas gingivalis* and *Fusobacterium nucleatum* in the Mouse Subcutaneous Chamber Model. *J Endod.* 2009;35(1):86-94. doi:10.1016/j.joen.2008.10.015.
42. Tan KH, Seers CA, Dashper SG, et al. *Porphyromonas gingivalis* and *Treponema denticola* Exhibit Metabolic Symbioses. *PLoS Pathog.* 2014;10(3):134-144. doi:10.1371/JOURNAL.PPAT.1003955.
43. Kuboniwa M, Hendrickson EL, Xia Q, et al. Proteomics of *Porphyromonas gingivalis* within a model oral microbial community. *BMC Microbiol.* 2009;9:98. doi:10.1186/1471-2180-9-98.
44. Hendrickson EL, Wang T, Dickinson BC, et al. Proteomics of *Streptococcus gordonii* within a model developing oral microbial community. *BMC Microbiol.* 2012;12(1):211. doi:10.1186/1471-2180-12-211.
45. Hendrickson EL, Wang T, Beck DAC, et al. Proteomics of *Fusobacterium nucleatum* within a model developing oral microbial community.

*Microbiologyopen*. 2014;3(5):729-751. doi:10.1002/mbo3.204.

46. Kotrba P, Inui M, Yukawa H. REVIEW Bacterial Phosphotransferase System ( ITS ) in Carbohydrate Uptake and Control of Carbon Metabolism. 2001;92(6):502-517.

## **Conclusion**

*F. nucleatum* remains a prime organism for exhaustive investigation due to its involvement in periodontal health and disease<sup>86</sup> and implication in a number of invasive human infections.<sup>87,88</sup> The overarching hypothesis that inspired our studies is that the adhesins mediating the expansive ability of *F. nucleatum* to attach to other organisms<sup>44</sup> is key to understanding its role in influencing human health and disease. In this work, we describe the identification and characterization of fusobacterial adhesins involved in interspecies interactions and their role beyond a function as cellular appendices mediating physical binding.

We were successful at identifying a fusobacterial large outer membrane protein, Fap2, as an adhesin involved in attachment to *P. gingivalis* strains. Investigation of this adhesin resulted in its characterization as galactose inhibitable. We also determined a novel role for the major fusobacterial adhesin, RadD, shown previously to mediate attachment to streptococci.<sup>15</sup> Arginine-inhibitable RadD was shown in our studies to be involved in binding to *P. gingivalis* in a species-specific manner. One or more adhesins involved in the attachment of *F. nucleatum* to *P. gingivalis* ATCC 33277 remain to be identified.

Observing RadD involvement in interspecies interactions and knowing that bacterial genes in the same operon are often functionally related led us to investigate the operon encoding RadD. Deletion of the genes in the operon resulted in the discovery of FAD-I as a factor influencing the regulation of *radD* transcription. Phenotypic and transcriptional surveys of the mutant lacking *fad-I* resulted in the interesting finding that

there is enhanced binding leading to taller biofilms in the absence of FAD-I corresponding with increased transcription of *radD*, allowing us to conclude that FAD-I acts as a transcriptional repressor of *radD*. Regulation of *radD* was further observed to be contact-dependent with early oral colonizer, *S. gordonii* but not *P. gingivalis*, suggesting partner-specific regulation of *F. nucleatum*.

Previous evidence support coaggregation as a highly specific interaction mediated through bacterial adhesins.<sup>7,46,89</sup> Our studies show that interaction specificity also influences global transcriptional changes in *F. nucleatum*. Partner-specific transcriptional responses were observed when we surveyed the fusobacterial transcriptome, suggesting contact-dependent regulation in *F. nucleatum* that can be distinguished by the type of interacting partner and possible the adhesin involved in the interaction.

In conclusion, we have provided evidence for the important role of fusobacterial adhesins in interspecies interactions. There exist adhesins that have yet to be identified and further investigation of *F. nucleatum* are needed on all levels to help us better understand this organism.

## References

1. Signat B, Roques C, Poulet P, Duffaut D. Fusobacterium nucleatum in periodontal health and disease. *Curr Issues Mol Biol*. 2011;13(2):25-36. doi:10.3109/08910609409141355.
2. Afra K, Laupland K, Leal J, et al. Incidence, risk factors, and outcomes of Fusobacterium species bacteremia. *BMC Infect Dis*. 2013;13(1):264. doi:10.1186/1471-2334-13-264.
3. Han YW. Fusobacterium nucleatum: A commensal-turned pathogen. *Curr Opin Microbiol*. 2015;23:141-147. doi:10.1016/j.mib.2014.11.013.
4. Kolenbrander PE, London J. Adhere today, here tomorrow: oral bacterial adherence. *J Bacteriol*. 1993;175(11):3247-3252. <http://www.ncbi.nlm.nih.gov/pubmed/8501028>. Accessed July 18, 2016.
5. Kaplan CW, Lux R, Haake SK, Shi W. The Fusobacterium nucleatum outer membrane protein RadD is an arginine-inhibitable adhesin required for inter-species adherence and the structured architecture of multispecies biofilm. *Mol Microbiol*. 2009;71(1):35-47. doi:10.1111/j.1365-2958.2008.06503.x.
6. Cisar JO, Kolenbrander PE, McIntire FC. Specificity of coaggregation reactions between human oral streptococci and strains of Actinomyces viscosus or Actinomyces naeslundii. *Infect Immun*. 1979;24(3):742-752. doi:0019-9567/79/06-0742/11\$02.00/0.
7. Park J, Shokeen B, Haake S, Lux R. Characterization of Fusobacterium nucleatum ATCC 23726 Adhesins Involved in Strain-Specific Attachment to Porphyromonas gingivalis. *Int J Oral Sci*. 2016;(In Press).
8. Kolenbrander PE, Inouye Y, Holdeman L V. New Actinomyces and Streptococcus coaggregation groups among human oral isolates from the same site. *Infect Immun*. 1983;41(2):501-506.